Alma Mater Studiorum – Università di Bologna
in cotutela con Università di Strasburgo

DOTTORATO DI RICERCA IN

Scienze e Tecnologie Agrarie, Ambientali e Alimentari
(Agricultural, Environmental and Food Science and Technology)

Ciclo XXIX

Settore Concorsuale: 07/D1

Settore Scientifico Disciplinare: AGR/12

RNA/RNA interactions involved in the regulation of Benyviridae viral cycle

Presentata da: Dott. Dall'Ara Mattia

Coordinatore Dottorato

Prof. Dinelli Giovanni

Supervisore

Dott. Ratti Claudio

Supervisore

Prof. Gilmer David

Esame finale anno 2018

Index

General Introduction

1. *Benyviridae* family: taxa characteristics

Benyviridae family belongs to group IV of the Baltimore classification [1], together with viruses possessing single-stranded positive-sense RNA genome (ssRNA (+)) that replicate through ssRNA(-) intermediates. The family possesses one single genus, *Benyvirus*, which includes four plant viral species: the type member *Beet necrotic yellow vein virus* (BNYVV), *beet soil-borne mosaic virus* (BSBMV), *burdock mottle virus* (BdMV) and *rice stripe necrosis virus* (RSNV) [2].

Initially assigned to *Tobamovirus* genus because of the virion morphology, BNYVV was included in the *Furovirus* genus characterized by the multipartite RNA genome species transmitted by fungal vectors [3]. *Furovirus* genus was then redefined in *Furovirus*, *Pomovirus*, *Pecluvirus*, *Hordeivirus* genera and *Benyvirus* genus [4] later added in the newborn *Benyviridae* family [2]. This new classification was based on the following taxa criteria: vector of transmission; number of open reading frame (ORF) encoding replicase subunits; presence or absence 3' end poly-A and presence or absence of triple gene block (TGB), a gene module involved in the cell-to-cell and long-distance movement in the host.

As the above mentioned genera, Benyviruses are non-enveloped rigid rod-shaped particles with helical symmetry, an axial channel and a diameter of about 20 nm (Figure 1). Depending on the genomic RNA encapsidated, virion lengths could reach 390 nm representing the longest rod-shaped particle ever observed within plant viruses [5]. Genome is split in up to five RNAs that, unlike the RNAs of other multipartite rod-shaped plant viruses, have a capped 5' end and a polyadenylated 3' end tail [2]. Longest RNA (RNA1) is monocistronic having one large ORF. This RNA encodes for a replication-associated polyprotein that undergoes an autocatalytic clivage. This characteristic is a second criteria distinguishing *Benyvirus* genus from other genera whose species carry two ORFs encoding multiple replication-associated proteins [5]. Finally similarly to Pomoviruses and

Pecluviruses, Benyviruses are characterized by their cell-to-cell movement function relying on a TGB and their host transmission mediated by protozoa vectors [4].

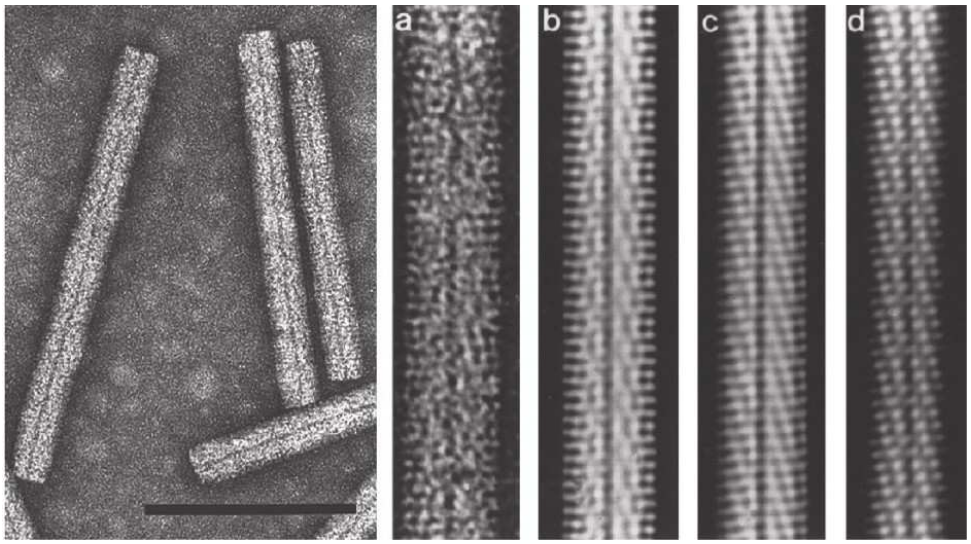

Figure 1 Negative contrast-stained BNYVV viral particles observed in transmission electron microscopy (a) and computer-filtered micrographs (b, c, d). Right-handed helix has a pitch of 2.6 nm and an axial repeat of four turns, involving 49 protein subunits [6]. One subunit covers four nucleotides (ibid). Bar represents 100 nm (modified from Gilmer and Ratti [2]).

2. Beet necrotic yellow vein virus

2.1 Types and Strains

BNYVV is a multipartite virus having up to five genomic RNAs required to complete its viral cycle in a natural context. Each RNA is separately encapsidated in independent particles. Viral isolates typically contain four particle species of 390, 265, 100 and 85 nm length. The presence of a fifth RNA species is described in European and Asian isolates giving a supplementary particle with a size ranging from 65 to 80 nm in length [7]. The five distinct encapsidated RNAs have been described and named RNA1 (6.8 kb), RNA2 (4.7 kb), RNA3 (1.8 kb), RNA4 (1.5 kb) and RNA5 (1.45 kb) [2]. Recent phylogenetic analyses based on CP, p25 and p31 nucleotide sequences [8,9] organized BNYVV isolates in A-I, A-II, A-III and B distinct types and in more than 10 strains [7].

Type and strain characteristics, such as CP, p25, and p31 clusters, presence or absence of RNA5 and geographical distribution are presented in table 1.

Type	Strain	Cluster CP	Cluster p25	Cluster p31	RNA5	Geographical distribution
A-I	China-H	A or B	I	I	+	China, Japan, UK
A-I	China-Y	A or B	I	I	+	China
A-II	P type	A	II	II	+	France, Kazakhstan, UK, Iran
A-II	Japan-D	A	II	II	+	Japan
A-II	Japan-O	A	II	I or II	+	Japan
A-II	China- B	A or B	II	II	+	China, Germany
A-II	China-L	B	II	I	+	China
A-III	Italian A type	A	I	III	-	Europe, USA, Middle East
B	China-X	A	III	I or III	+	China
B	B type	B	III	IV	-	Germany, France, Belgium, Austria, Switzerland, Czech Republic, China

Table 1 BNYVV types and derived strains. Groupings represents clusters derived from nucleotide sequence phylogenetic analyses of CP (A and B), p25 (I–III), and p31 (I–IV). + or – indicates presence of absence of RNA5 in the strain (modified from Tamada et al [7])

2.2 Vector transmission

BNYVV is persistently transmitted by the protozoan *Polymyxa betae* [10], a root obligate parasite of different plant species mainly belonging to *Chenopodiaceae* family. Four biological forms characterize the protozoan life cycle (Figure 2):

- Resting spores (sporosori) are able to remain viable and viruliferous in the soil for years. They germinate in the presence of host exudates together with suitable condition of temperature, pH and humidity [11].
- Primary biflagellate zoospores resulted from sporosori germination represent the main biological form of dissemination within *P. betae* life cycle. They reach and encyst in a rootlet cell in which their cytoplasmic content is injected through a tubular structure (Rohr) containing a dagger-like body (Stachel) [10]. BNYVV transmission in the host is thought to take place with the cytoplasmic fusion between zoospore and rootlet cell [11].
- Multinucleated plasmodium derived from the sporangial phase after several cycles of mitotic nuclear division [10].

- Zoosporangium, resulted from maturation of plasmodium, leads the production of secondary zoospores that can infect new roots once released in the rhizosphere. Multinucleate plasmodium can also maturate as sporogenic stage forming clusters of sporosori then released in to the soil with the senescence of infected plant rootlets [11]. Factors determining the sporangial or sporogenic cycle are still unknown since the two phases apparently overlap [10]. BNYVV acquisition by an aviruliferous vector seems to occur at the plasmodial level with a still unknown mechanism that determine the invagination of the plasmodial membrane around viral particles facilitated by trans-membrane motifs of minor capsid protein [12].

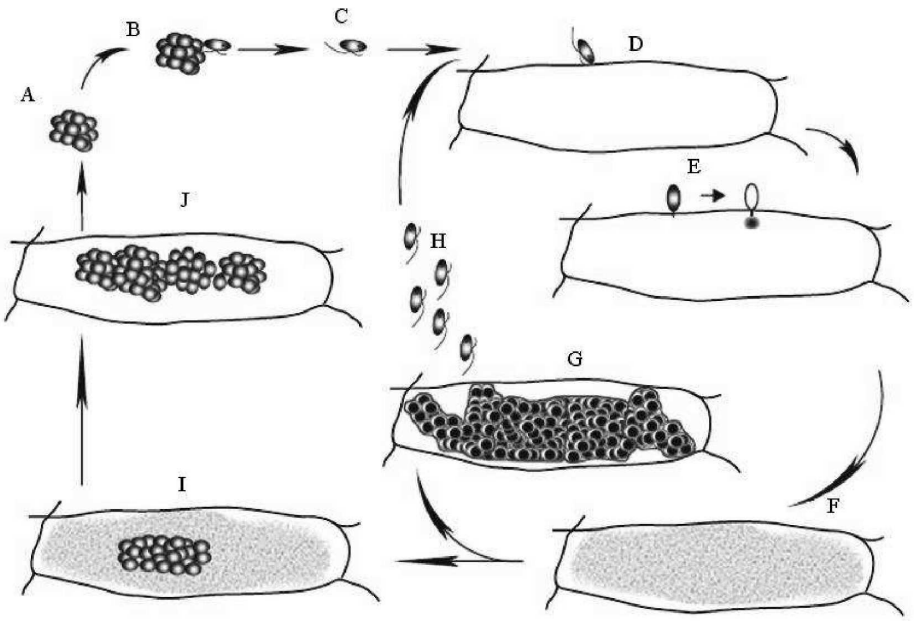

Figure 2 Representation of *P. betae* life cycle: Sporosori (A); Primary zoospore germination and movement in the rhizosphere thanks to its two whiplash flagella (B, C); Cell rootlet infection consisting in the cyst formation and cytoplasmic transfer from zoospore to the host cell (D, E); Multinucleate plasmodium formation (F); Zoosporangium evolves from sporangial plasmodium (G) and release secondary zoospore in the extracellular medium (H); Sporosori cluster (I), from sporogenic plasmodium, are released in the soil after rootlet senescence (J). (modified from Peltier et al [11]).

2.3 BNYVV host range

The natural host range of BNYVV is very narrow and limited to species from *Beta* genus, such as *B. vulgaris* and *B. macrocarpa,* or *Spinacea* genus such as *S. oleracea.* Initially thought to infect only species belonging to *Chenopodiaceae* family, relatively recently, BNYVV has been suggested

to have a wider host range since together with *P. betae* it has been detected in 29 different plant species grown in naturally infested soils, including *Amaranthaceae, Asteraceae, Brassicaceae, Caryophyllaceae, Papaveraceae, Poaceae and Urticaceae* [13]. However, detection analyses have been conducted with multiplex RT-PCR on root tissues (ibid) not considering a possible contamination by viruliferous *P. betae* spores. Further experiments of BNYVV infectivity are therefore necessary to confirm and validate such important host range extension.

2.4 Rhizomania

Rhizomania is the most important transmitted soil-borne disease affecting the sugar beet (*Beta vulgaris* var. s*accharifera*). In the early seventies, BNYVV has been identified as the causal agent of the disease[14] previously described by Canova in Padan Plain (Italy) as an abnormal proliferation of lateral rootlets with consequently reduction of the tap root weight and browning of the vascular system (Figure 3) [15,16]. BNYVV infection in sugar beet is mainly restricted to the root apparatus but sometimes extend as a systemic spread in leaves, causing vein necrosis and yellowing, symptoms that were used for naming the virus [14,16].

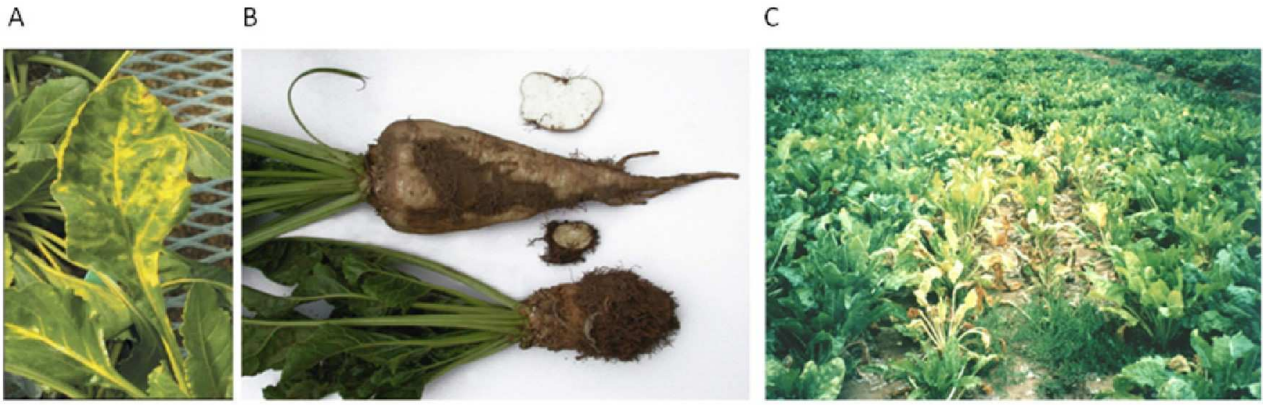

Figure 3 Rhizomania symptoms: systemic leaf necrosis and yellowing (A); diseased plant (bottom) shows abnormal proliferation of lateral rootlets with a consequent size reduction and necrosis of the tap root compared to healthy plant (top) (B); symptoms on field (C) (modified from Delbianco[17])

2.5 Genomic organization: RNA1 and RNA2 essential combination and accessory RNAs

Among the five BNYVV genomic RNAs, RNA1 is essential for the replication while RNA2 ensures the functions of encapsidation, cell-to-cell movement and RNA silencing suppression. While RNA3, RNA4 and RNA5 behave as accessory species for local infection or long distance infection in *S. oleracea* or *N. benthamiana,* these viral RNAs play important, distinct and dedicated roles in the pathogenicity and the transmission of the virus within the natural host [18,19] (Figure 4). For this reason these small genomic RNA species become accessory on laboratory hosts and could be used as viral vectors of expression in the presence of RNA1 and RNA2 helper combination [20,21].

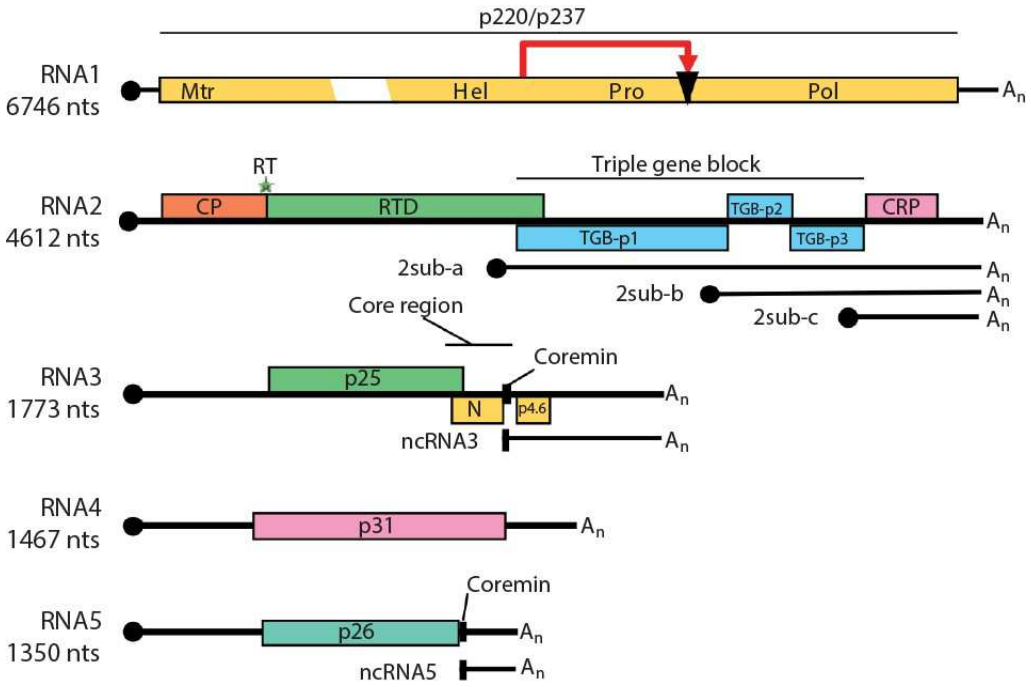

Figure 4 BNYVV genome organization and translational strategy. Genomic RNAs have a 5' end cap (black circle) and a 3' end polyA tail (An). RNA1 encodes a polyprotein that undergoes a self-cleavage (red arrow and black triangle). Methyltransferase (Mtr), helicase (Hel), protease (Pro) and RNA dependent RNA polymerase (Pol) are different domain identified on the polyprotein. RNA2 encodes for coat protein (CP) and for RT which expression depends on the suppressible UAG stop codon translational read trough (green star). CP and read-through domain (RTD) constitute RT protein. Via subgenomic RNA (sub) RNA2 encodes three triple gene block proteins (TGB-p1, TGB-p2, TGB-p3) and p14 a cysteine-rich protein (CRP) also known as the viral suppressor of RNA silencing. RNA3 encodes the p25 protein and possesses other two ORF which products N and p4.6 proteins were never detected. RNA4 encodes the p31 and RNA5 the p26. Noncoding (nc) RNA3 and ncRNA5 are produced by exoribonuclease activity [22]. The conserved coremin motif present in the 'core region' of RNA3 and in RNA5 is necessary for long distance movement in *Beta* species.

BNYVV RNA1 is 6,746 nts long [23] and encodes all viral factors required for the RNA replication since this RNA species is able to self replicate if transfected without the other genomic components in *Chenopodium quinoa* protoplasts [24]. RNA1 has one unique ORF containing two possible start codon (AUG_{154} and AUG_{496}) encoding for two long polypeptides p237 and p220 [25] having both three distinct domains associated with viral replication: methyltransferase domain (MTR), NTP-binding/helicase domain (HEL) and RNA-dependent RNA-polymerase domain (RdRp) (ibid). Papain-like protease domain is located between HEL and RdRp and is responsible for the post-translational cleavage of the p237 and p220 into p150 and p66. The RNA1-encoded protein or the clivage products interact each other, in a still unknown stoichiometric ratio, to establish a functional replicase complex associated with the endoplasmic reticulum (ER) network [25–27]. Interestingly no major endoplasmic reticulum (ER) reorganization has been observed in infected cells suggesting that production of a huge viral factory is avoided by the virus [27] probably preventing a competition for the replication machinery between essential and shorter "non essential" RNAs.

Polycistronic RNA2 is 4,612 nts long and is characterized by having different translational strategies to express five ORFs encoding six different proteins[28]. Coat protein of 21 kDa (CP) is expressed directly by genomic RNA2 starting from its AUG_{145} start codon [29]. An UAG_{709} stop codon is suppressed once in ten times by a read-through translation mechanism to produce the minor capsid protein p75 (RT) (ibid). Localized at one extremity of each viral particle, RT is required for the nucleation process that probably takes place in the cytoplasmic side of the outer mitochondrial membrane [30]. Furthermore, alanine scanning mutagenesis of this protein identified a C-terminal half motif (KTER) essential for the transmission of viral particles by *P. betae* vector [31].

The four other ORFs are translated from three subgenomic RNAs (sgRNAs) which sequences are collinear to the 3' half end of RNA2. These sgRNAs bring ORF2, ORF3 and ORF4, encoding TGB proteins (p42, p13 and p15), and the ORF5, required for the production of p14 closer to the 5'

terminus to allow translation. P42 is translated from 2sub-a, p13 and p15 from 2sub-b while p14 from 2sub-c [32]. The p42 has a nucleic acid binding activity and sequence motifs characteristic of superfamily I DNA or RNA helicase including a P-loop ATP/GTP binding domain [33]. The p13 protein possesses a highly conserved hydrophilic motif flanked by two hydrophobic domains able to cross ER and plasma membranes while p15, translated by a ribosomal leaking scanning of p13 start codon appears mainly hydrophobic [34]. BNYVV RNAs move cell-to-cell through plasmodesmata in a CP independent manner, an hordei-like mechanism requiring only the three TGB proteins [32,35]: The p42 proteins cooperatively interact with viral RNAs thanks to their N-terminal domain and form ribonucleoprotein complexes (RNP) delivered by the integral membrane proteins p13 and p15 to plasmodesmata following the ER network [35–37]. Hordei-like TGB proteins accumulate during infection with conserved TGB1/TGB2/TGB3 ratios of approximately 100:10:1 [38] . Such relative ratios are not determined for BNYVV but could presumably be similar since the unregulated expression of BNYVV TGB proteins inhibits cell-to-cell movement [39].

The 3'end proximal ORF5 encodes a C-4 zinc finger cysteine-rich protein of 14 kDa (p14). This protein is the viral suppressor of RNA silencing (VSR) and localizes both in the cytoplasm and the nucleolus [40]. The p14 VSR activity is mainly cytoplasmic and has been associated with reduced accumulation of secondary small interfering (si) RNAs derived from endogenous RNA-dependent RNA-polymerase 6 (RDR6) pathway [40,41]. Affecting silencing transitivity of plant RNAi, p14 counteracts the restriction of systemic spread of BNYVV genomic components, playing a crucial role in the long-distance movement of the virus [40,41].

Furthermore p14 acts synergically with a viral noncoding RNA produced from genomic RNA3 (ncRNA3) for the viral long distance movement in *B. macrocarpa* and in *Nicotiana benthamiana* infected with a BNYVV expressing an hypomorphe VSR. Together, these data suggest a link between silencing suppression and viral spread [40,41].

RNA3 is 1,774 nts long [42] and is involved in the viral long-distance movement in *Beta* species [18] as well as in the manifestation of rhizomania symptoms in *B. vulgaris* [43,44] . RNA3 contains three different ORF, encoding a protein of 25 kDa and two other proteins never detected in natural context (N and p4.6) [27]. The p25 protein localizes in the nuclear and cytoplasmic compartment independently of other viral factors [45], thanks to a N-terminal nuclear localization signal ($_{57}$KRIRFR$_{62}$) and a C-terminal nuclear export sequence ($_{169}$VYMVCLVNTV$_{178}$) [45,46]. P25 is an avirulence protein [47] and has been suggested to represent the pathogenic determinant for the rhizomania disease since transgenic *Arabidopsis thaliana* lines constitutively expressing the protein, display a root-branching phenotype, express high levels of auxin and low amounts of jasmonic acid derivatives [48]. Nuclear import and export motifs, together with a zinc finger domain, suggest that p25 could acts as a transcriptional factor. Such hypothesis has been corroborated in yeast one hybrid experiments in which the Gal4 or LexA DNA-binding domain-fusion with p25 is able to promote the transcription of the reporter genes. The domain responsible for transcription activation is constituted by p25 residues 103 to 146 [49]. Systemic spread in *Beta* species do not rely on p25 expression but on the strictly connection between "coremin" motif (located within the "core" domain) and the accumulation of ncRNA3 [18,22,50]. A 5′-3′ exoribonuclease processing of RNA3 stalls on a highly structured sequence involving the "coremin" motif and lead to the accumulation of ncRNA3 *in vivo* with a probable saturation of the exoribonuclease with consequences on the RNA silencing machinery [22,41]. As stated above, this could explain the synergy observed between the VSR and the accumulation of the ncRNA3 species [40,41].

Monocistronic RNA4 is 1,467 nts long [42] and encodes a cytosolic protein of 31 kDa [51] involved in the aggravation of foliar symptoms and, together with p75, in the vector transmission [52]. Experiments in *N. benthamiana* demonstrated a role of the p31 protein in a root specific suppression of RNA silencing [52]. Such behavior still needs to be confirmed in *Beta* species.

RNA5 is 1,350 nts long and encodes a protein of 26 kDa which functional properties resemble those of the RNA3-encoded p25 protein [53,54]. As p25, p26 protein localizes both in the cytosol and nucleus and strongly activates transcription in yeast one hybrid system [55]. Transcriptional activation domain is located in the first 17 amino acid residues of the protein and is not related to the necrosis symptoms on *C. quinoa*, suggesting a probable avirulence behavior of p26 on such host [55,56]. When present, RNA5 increases symptomatology on *B. vulgaris* roots [57] and provokes necrotic lesions on *C. quinoa* leaves. As RNA3, RNA5 possesses the coremin sequence, produces a noncoding RNA (ncRNA5) which is able to complement an absence of RNA3 required for the long distance movement on *B. macrocarpa* [58].

3. Ins and Outs of Multipartite Positive-Strand RNA Plant Viruses: Packaging versus Systemic Spread

A Review published by:

Mattia Dall'Ara, Claudio Ratti, Salah E. Bouzoubaa and David Gilmer

Viruses **2016**, *8*, 228; doi:10.3390/v8080228 www.mdpi.com/journal/viruses

viruses

MDPI

Review

Ins and Outs of Multipartite Positive-Strand RNA Plant Viruses: Packaging versus Systemic Spread

Mattia Dall'Ara [1,2], Claudio Ratti [2,*], Salah E. Bouzoubaa [1] and David Gilmer [1,*]

[1] Institut de Biologie Moléculaire des Plantes, Integrative Virology, CNRS UPR2367, Université de Strasbourg, 12 rue du Général Zimmer, 67084 Strasbourg, France; mattia.dallara5@unibo.it (M.D'A.); salah.bouzoubaa@ibmp-cnrs.unistra.fr (S.E.B.)

[2] Dipartimento di Scienze Agrarie, Area Patologia Vegetale, Università di Bologna, Viale Fanin 40, 40127 Bologna, Italy

* Correspondence: claudio.ratti@unibo.it (C.R.); gilmer@unistra.fr (D.G.); Tel.: +39-051-2096733 (C.R.); +33-367-155362 (D.G.)

Academic Editor: Eric O. Freed

Received: 31 May 2016; Accepted: 9 August 2016; Published: 18 August 2016

Abstract: Viruses possessing a non-segmented genome require a specific recognition of their nucleic acid to ensure its protection in a capsid. A similar feature exists for viruses having a segmented genome, usually consisting of viral genomic segments joined together into one viral entity. While this appears as a rule for animal viruses, the majority of segmented plant viruses package their genomic segments individually. To ensure a productive infection, all viral particles and thereby all segments have to be present in the same cell. Progression of the virus within the plant requires as well a concerted genome preservation to avoid loss of function. In this review, we will discuss the "life aspects" of chosen phytoviruses and argue for the existence of RNA-RNA interactions that drive the preservation of viral genome integrity while the virus progresses in the plant.

Keywords: phytovirus; segmented genome; genome integrity; systemic movement; RNA-RNA interaction

1. Introduction

Preserving genome integrity is a key challenge for any organism, and viruses with an RNA-based genome are not excluded from this basic rule. Obligate parasites that have a monopartite genome mainly face recombination events that draw viral evolution. While viruses with segmented genomes also encounter similar evolutionary traits, another constraint applies to the maintenance of genome integrity. Indeed, all genomic segments should be available within the same cell and be transmitted from one cell or one organism to another. To do so, all genomic components must be packaged within the same viral particle. This is well exemplified by *Orthomyxoviridae* members where all genomic negative-stranded ribonucleoprotein (RNP) complexes are selectively assembled together within one enveloped viral particle [1], or *Bunyaviridae* [2] where all three segments are maintained together within the envelope. Similar examples can be drawn for double-stranded RNA viruses such as *Reoviridae* or the well-known *Cystoviridae* pseudomonas phage Ø6 that possesses three genomic double-stranded (ds)RNA segments within the same viral structure [3].

Viruses that possess a positive-stranded RNA genome are found in genera that infect bacteria (e.g., *Leviviridae* enterobacteria phage Qß), animals and insects (e.g., *Picornavirales* enterovirus C—namely poliovirus—and cricket paralysis virus) and also plants (e.g., *Virgaviridae*, tobacco mosaic virus). To date, distinguishing features of (+)-strand RNA viruses that infect bacteria, animals or insects reside in the nature of the viral genome that is limited to either one single-stranded (ss)RNA molecule or two genomic RNAs packaged within a unique icosahedral capsid (e.g., *Nodaviridae*, flock house virus). However, (+)-strand RNA phytoviruses with segmented genomes range between

two to five positive-strand RNA molecules and such so-called multipartite viruses possess either an icosahedral (sometimes bacilliform) or helical shape. A large majority of these phytoviruses have distinctive features compared to the aforementioned animal (+)-strand RNA viruses, as each segment can be individually packaged as ribonucleoprotein complexes within a helical structure. Icosahedral phytoviruses with a segmented positive-sense RNA genome either package single segment species in each capsid or a combination of segments within the limits of physical size constraints. A.L.N. Rao has reviewed mechanisms driving genome packaging of spherical plant RNA viruses [4] while Solovyev and Makarov recently focused on plant viruses with helical capsids [5].

The question about the requirement for the long distance movement of the 'virus' of either virion (packaged RNA) or RNP complex is still open and it appears closely linked to the ability of the viral RNAs to be "packaged." Such infection of vascular tissues is not as uniform as those of mesophyll cells where phytoviruses usually begin their journey by moving cell to cell (for review see [6]). Several boundaries constituted by the bundle sheath (BS) of V or IV class veins (for vein classification, refer to [7]) followed by the vascular parenchyma (VP) have to be passed by the viral material in order to reach companion cells (CCs) and follow the photoassimilates flow of the sieve elements (SEs). To finish the journey, the reverse route passing through class III veins to access CC and then mesophyll cells has to be pursued to start moving cell-to-cell in the distant tissues (Figure 1).

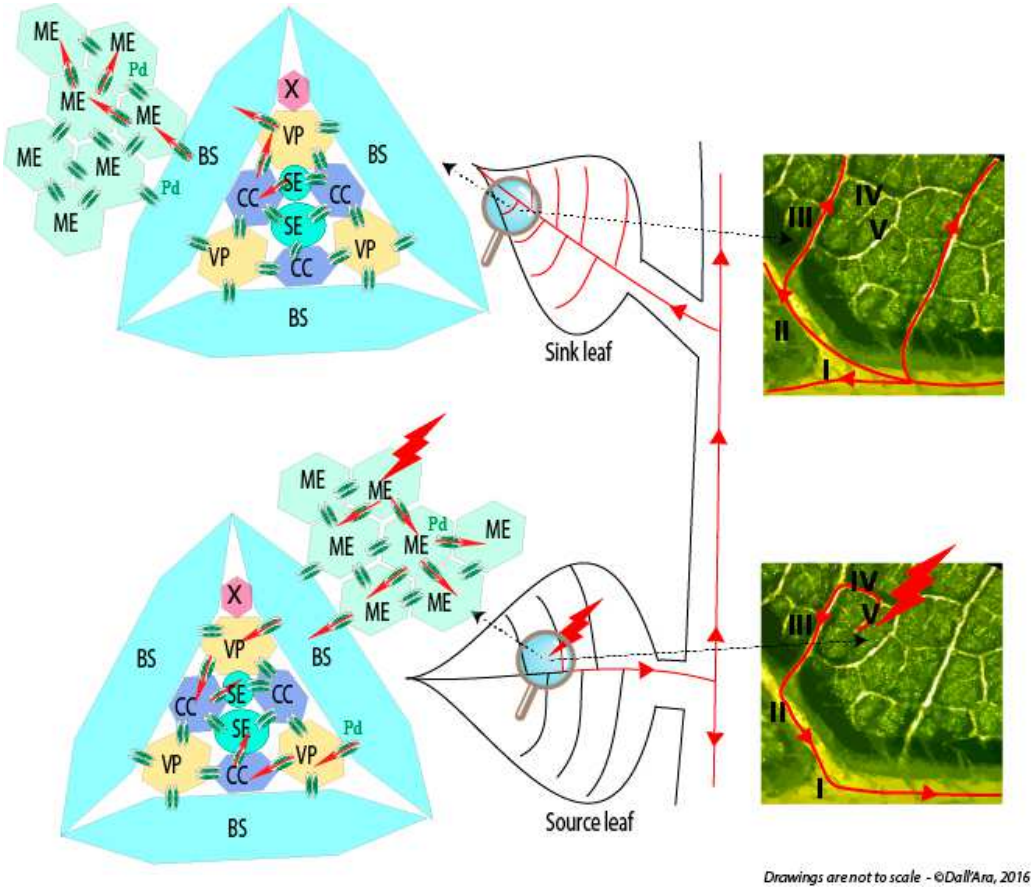

Figure 1. Schematic representation of the initial infection (red thunderbolt) and its progression (red lines and arrows) within a source leaf of an infected plant. Infectious material passes through plasmodesmata (Pd, double green ovals) from mesophyll (ME), bundle sheath (BS), vascular parenchyma (VP) to companion cells (CC) to access sieve elements (SE) and reach the distant tissues. A reverse route occurs in the upper leaves (sink leaf) or roots (not represented). Right panels show leaf venation and illustrate viral phloem loading and unloading through minor and major veins of source and sink leaves. X, Xyleme; I−V: vein classes.

Whatever the structural shape adopted for plant multipartite RNA viruses, their genomic segments are separated by distinct capsids. This situation raises concerns about the preservation of the viral genome integrity that requires all RNA segments to move from one cell to a neighbor or distant cell in the plant (Figure 1). This ensures the setup of a novel infection site where all viral genes need to be expressed. Here, up to three-decade old as well as new literature describing packaging, cell-to-cell and vascular movement of plant icosahedral and helical viruses has been reviewed to bring into the light our conceptual view of the nature of the systemic moving of viral material in the infected plant. Without addressing details about the RNA expression and replication mechanisms, we propose to distinguish between virions acting as storage of infectious material, ready for transmission, and moving material constituted of RNP complexes containing all RNA segments of the multipartite genome. These RNP complexes involving RNA-RNA interactions act as drivers for the "in planta" viral cycle and appear as the adequate entities for genome preservation, particularly in the long-distance journey of the virus. While this concept appears "insignificant" for monopartite RNA viruses, multipartite viruses need to preserve the expression of their entire genome in the targeted cells. After the description of chosen monopartite phytoviruses, we review and discuss the situation of multipartite RNA viruses and focus on their need to preserve the expression of their entire genome in the targeted cells. A model for benyviruses has been illustrated to present our hypotheses.

2. Lessons from Turnip Crinkle Virus, Satellite Tobacco Mosaic Virus, Groundnut Rosette Virus and Tobacco Mosaic Virus: Monopartite RNA Genomes

For some viral species, icosahedral shells are able to assemble in virus-like particles where the genome, usually dsDNA, is incorporated using energy-dependent nanomachines, extensively studied for bacterioviruses T4, P22 or Ø29. The latter uses a non-coding RNA hexamer for DNA entry. Recent insights about the genomic encapsidation of the positive-strand RNA genome of bacterioviruses MS2 revealed the importance of coat protein (CP) dimer interactions, with an estimated number of 60 hairpin RNA structures distributed around the RNA genome (packaging signals), leading to induced-fit RNA-viral protein interactions rather than electrostatic interactions. In this sense, genomic MS2 RNA constitutes a scaffold for assembly initiated or terminated by the assembly protein, following a Hamiltonian path [8–10].

2.1. Positive-Strand RNA Packaging into Icosahedral Units

2.1.1. Autonomous Turnip Crinkle Virus

Turnip crinkle virus (TCV) from the *Tombusviridae* family is structured by an association of 180 copies of a 38 kDa CP. Its crystallographic structure resembles the tomato bushy stunt virus. TCV viral particles can be dissociated at elevated pH where RNA is attached to six CP subunits that permit reassembly in vitro [11]. Mapping protein-RNA interactions revealed the interaction between CP and two RNA domains. A 15 base-pair (bp) long hairpin structure has been identified within the replicase gene and a 28 nucleotide (nt) bulged hairpin loop is present within a 186 nt essential element within the CP coding sequence. Viral encapsidation was also shown to be dependent on the length of the viral RNA [12], suggesting the requirement of a separation between 5′ (replicase gene) and 3′ (CP gene) CP-interacting sequences, suggesting a bipartite packaging signal for this monopartite RNA viral genome. TCV CP is dispensable for the viral cell-to-cell movement but essential for the systemic spread [13] as this protein acts as a suppressor of RNA silencing [14,15].

2.1.2. Helper Virus Replication-Dependent Satellite Tobacco Mosaic Virus

Satellite tobacco mosaic virus (STMV) is an icosahedral $T = 1$ virus with a small genomic RNA. Atomic structure revealed 30 stem-loop RNA structures, each associated with a two-fold symmetry axis [16]. Interestingly, the RNA secondary structure of STMV analyzed in solution [17] does not correspond to the structure predicted in the $T = 1$ capsid. This discrepancy indicates a selection of the RNA genome into an icosahedral structure following a Hamiltonian pathway as described for MS2

bacteriophage [10]. The existence of multiple RNA folding structures of the genome could account for distinct functions tightly regulating viral protein expression and regulated by viral proteins. This satellite virus requires a helper virus (HV) for its replication. Interestingly, HV replicating STMV belong to helical viruses such as tobacco mosaic virus (TMV) [18]. A systemic movement of both the satellite virus spherical particle and HV helical entities would require a mechanism able to recognize both structural entities. However, drawing hypotheses about possible interactions between satellite RNA and HV RNA could explain a satellite RNA transport by an HV RNP moving complex.

2.1.3. Umbraviruses Replicate Autonomously but Are Packaged in *Trans*

Groundnut rosette virus (GRV) belongs to the *Umbravirus* genus and does not form conventional virions. Indeed, this species does not encode coat proteins. GRV possesses a monopartite genome encoding proteins necessary for its autonomous replication and movement within the plant. Its genome encapsidation occurs during mixed infection with an HV that belongs to the *Luteoviridae* family, specifically transmitted by aphids and only in the presence of a satellite RNA required for the selective encapsidation of GRV [19]. In a host plant, GRV is able to replicate on its own and infect the entire host while the helper luteovirus remains restricted to the phloem. GRV movement is provided by the expression of the open reading frame (ORF) 3 product and recruits fibrillarin to ensure the formation of an RNP complex essential for its systemic spread [20]. This example illustrates the systemic movement of a viral entity without viral shell formation.

2.2. Positive-Strand RNA Packaging into Helical Units: Lessons from Tobacco Mosaic Virus

The reconstruction of TMV from purified CP and viral RNA [21] set up the fundamental basis for understanding rod-shaped and flexuous helicoidal viruses that has been recently reviewed elsewhere [5]. Upon the recognition of an RNA signature on the viral genome, CP nucleates and cooperatively recruits further copies of structural proteins to cover the entire genome with a first coverage of the 5′ domain followed by the protection of the 3′ terminus. Conversely, uncoating of TMV is thought to occur in the cell by a partial disassembly of the CP subunits at the 5′ termini of viral RNA (Ω region) leading to ribosomal scanning and uncoating while the first ORFs are translated. The encoded proteins produce the replicase complex that recognizes the 3′ partially uncoated domain and starts the synthesis of the viral complementary strand and simultaneously removes remaining CP-associated subunits. This ensures a proper recognition of internal promoters required for the subgenomic RNA synthesis and left-ended terminal promoter required for positive-strand synthesis. While subgenomic RNAs (sgRNAs) are produced, expression of the movement protein (MP), required for the efficient transport of viral material from the infected cell to neighboring cells, and CP expression finalize the progression of the viral cycle. TMV CP assembles spontaneously without any cellular factors. TMV genome recognition and encapsidation require both the formation of a 34 to 38 CP subunit disk (namely protohelix or two-ring disk) and the presence of an origin of assembly (OA) on the viral RNA. This leads to the rapid encapsidation (~6 min) of the ~6.4 kb RNA with 2130 copies of the CP subunits. TMV-OA is constituted by three stem loops, with stem loop 1 playing an essential function for the initiation of nucleation, together with a repetition of G residues every three nucleotides within an unpaired region [22]. Importantly, this property led to the engineering of a viral Lego® for nanotechnologies. The combination of genetically modified CP subunits, sometimes together with wild-type CP (both expressed in *Escherichia coli*) with RNAs containing TMV-OA, led to the construction of nanostructures displaying new chemical reactivity, owing to their usage as nanomaterials [23].

Reverse genetics using a full-length infectious clone of TMV demonstrated that the CP is not required for cell-to-cell movement but is needed for the efficient systemic infection of hosts such as *Nicotiana benthamiana (N. benthamiana)* [24]. Hence, TMV particles would thereby constitute stable mechanically transmissible entities between sessile hosts whereas RNP complexes containing the CP could represent the moving material within the host. This is illustrated by the description of TMV RNPs isolated from infected *N. tabacum* cv. Samsun plants [25]. Such RNPs differ from virions by their

higher buoyant density and contain TMV genomic RNA, polypeptides of 17.5 kDa (TMV CP), 31 kDa (possibly TMV MP), 37 kDa and 39 kDa. Purified RNAs from these RNPs retained the ability to be encapsidated in vitro [25].

The progression of TMV infection within mesophyll cells is well characterized and occurs thanks to the transport of uncoated viral RNAs and MP RNP complex. However, little is known about the nature of the infectious material that permits viral vascular movement. Disruption of the OA by point mutations that preserve functional CP abolishes TMV systemic movement, suggesting that virions represent the long-distance entities [26]. Nevertheless, experimental results outlined below suggest that the hypothesis of TMV virion as the moving material may have to be reconsidered.

As stated above, in the absence of CP synthesis, TMV is able to move cell-to-cell to access VP but fails to enter CC, suggesting a requirement of the CP to cross the VP/CC boundary [27]. The TMV CP seems to play a central role in the passage of the infectious material through vascular tissues. However, the formation of viral particles does not appear to be a prerequisite because several mutants (insertion or deletion) that affect the RNA binding region of the CP are still able to move long distance, albeit with sometimes delayed kinetics [28]. The crossing of each specific boundary between different cell types seems to require different strategies that could involve dedicated viral factors.

Masked strain M-TMV shows a delayed systemic spread as compared to the virulent strain U1-TMV. However, comparable replication levels and cell-to-cell movement efficiency in mesophyll cells is described for the inoculated leaves [29]. The delayed systemic movement behavior is attributed to an eight-amino acid mutation in the 126 kDa protein, formerly acting as an RNA silencing suppressor, and hence in the 183 kDa replication protein. Immunohistochemical analysis of class V veins of infected leaves revealed a deficient viral accumulation in the VP and, consequently CC cells, for viruses carrying the p126 mutation [30]. The different behavior of the two strains is maintained in class III veins and mesophyll tissues of non-inoculated leaves even if the number of infected CCs is comparable, suggesting that wild-type p126 is required for BS/VP and CC/VP boundary crossings [30]. It is not known if p126 acts alone or as part of a vRNP complex [30]; however, viral replication complexes constituted of p126, MP and viral RNA are reported to move between cells [31].

Although RNA stabilization by encapsidation may be a prerequisite for TMV to enter VP and CCs, it is not necessary in the SE where no RNase activity was detected in exudates [32–34]. Furthermore, the absence of translation could reinforce the hypothesis of a viral RNP complex as the form of transport, because its correct conformation should not be disrupted by the scanning activity of ribosomes. Replacement of the TMV CP by GRV Orf3 leads to systemic movement of the recombinant viral RNA without the formation of virions [35]. The Orf3 product interacts with TMV RNA to form helical-structured filamentous RNP complexes lacking the uniform rod-shaped viral particles [36].

Other indirect experiments permit speculation about the possibility of MP to be included as a constituent of the viral entity that moves long distance. In tobacco plants with a reduced synthesis of pectin methylesterase in vascular tissue, a cell-wall enzyme which interacts with MP [37], TMV is able to load in the SE but cannot be unloaded in non-inoculated leaves [38]. Beyond the CP, the MP is required for TMV cell-to-cell and long-distance movement that could involve two independent mechanisms. Gain and loss-of-function experiments support such a hypothesis. TMV does not systemically infect vanilla orchid. The related *Tobamovirus* odontoglossum ringspot virus protein (ORSV) is able to infect such a host but is unable to move long distance in tobacco [39]. The replacement of TMV MP by ORSV MP permits chimeric TMV to systemically infect vanilla orchid and restrains the infection to local lesions in tobacco plants [39]. The host-range determinant of ORSV resides in the eleven C-terminal amino acids of the MP. The deletion of this domain restores the ability of the chimera to provoke a systemic infection on tobacco and prevents the spread in orchids [39].

3. Multipartite RNA Genomes

3.1. Positive-Strand RNA Packaging into Icosahedral Units

3.1.1. Dianthovirus: Bipartite Genome

Red clover necrotic mosaic virus (RCNMV) belongs to the *Dianthovirus* genus and *Tombusviridae* family. This icosahedral virus possesses a bipartite positive-sense single-stranded RNA genome. RNA1 codes for the proteins involved in replication and also for CP subunits through a sgRNA [40–44]. RNA2 is monocistronic and codes for the MP, a multifunctional protein implicated in suppression of RNA silencing, in cell-to-cell and long-distance movement of the virus [45–47]. Although RNA1 replicates alone, it is not able to produce the sgRNA or CP subunits in the absence of RNA2 [48–51]. A kissing interaction has been found between RNA2 and RNA1. This 8-base pairing occurs between the trans-activating TA element, present in the RNA2 MP ORF and the TA-binding site (TABS) present in sgRNA promoter on the RNA1. The heterodimerization is essential for the production of sgRNA [51], whose production is regulated by RNA2. This interaction is also required for the RNA1-RNA2 packaging [48], because no OA is present on RNA1. Besides these biological roles, the kissing interaction within the OA allowed the engineering of virus-like particles able to efficiently encapsidate nanoparticles or Quantum Dots [52]. Therefore, the particularity of RCNMV is, on the one hand, the encapsidation of the RNA heterodimer in the same particle and, on the other hand, the packaging of multiple copies of RNA2 that could fit in tailored viral shells [53].

While the CP is not required for cell-to-cell movement, it is considered necessary for the systemic spread of RCNMV [54]. However, some experiments performed in *N. benthamiana* revealed that RNA1 and RNA2 could move long distance in the absence of the CP and thus without the formation of virions [42]. Although this property appears to depend on the host plant and temperature, it does illustrate again that systemic movement as an RNP complex is possible. Whatever the precise mechanism of its systemic movement, this bipartite viral genome provides direct evidence for the regulation of the viral cycle via the RNA-RNA interaction of distinct viral RNA species.

3.1.2. Brome Mosaic Virus: Tripartite Genome

All three components of the tripartite genome of brome mosaic virus (BMV) (~8.2 kbp) are essential for viral replication and for systemic infection of plants. The RNAs are encapsidated separately in 28 nm particles with $T = 3$ quasi-icosahedral symmetry [55]. RNA1 and 2 are packaged separately, whereas RNA3 is co-packaged with sgRNA (namely RNA4) into a third particle [4]. A ~200 nt conserved 3′ tRNA-like structure (TLS) with determinants for tyrosylation is present on all genomic RNAs and acts as a nucleating element (NE) of CP subunits. This NE is required for the packaging of viral RNA3 and RNA4 [56] but not for RNA1 and 2 packaging [57]. Conserved 3′ untranslated regions (UTRs) appeared to contain additional elements promoting encapsidation and distribution of the RNAs in three indistinguishable particles. The RNA3 encapsidation is dependent on a 187 nt long packaging element (PE) that resides within the MP coding sequence [58]. Besides, RNA3 and 4 packaging was found to be dependent on the replication and on a possible interaction between RNA3 PE and RNA4 NE domains [59]. In wheat germ extracts, pre-swollen particles render viral RNAs available for direct protein synthesis [60], suggesting a co-translational disassembly that has been observed for other spherical viruses such as alfalfa mosaic virus, cowpea chlorotic mottle virus and southern bean mosaic virus [61]. During the course of the viral replication cycle, viral RNAs and proteins allow new viral particles to accumulate. This morphogenesis takes place around replication factories: the co-localization of BMV replicase, CP and viral RNAs could thus control packaging specificity [62,63]. Viral cell-to-cell movement is dependent on the expression of the 3a movement protein, whereas CP is dispensable in some natural or MP-mutated BMV isolates [64,65].

Packaging was thought to play an important role in long-distance movement of the virus in the plant. However, using *Agrobacterium tumefaciens*-mediated transient expression of BMV genomic RNAs in leaves of *N. benthamiana*, Gopinath and Kao demonstrated that viral RNAs can also move long

distance independently, without the presence of the viral CP [66], probably forming RNP complexes with cellular factors. When produced alone, BMV RNA3 is able to move long distance without the assistance of any viral proteins, while RNA1 and RNA2 both need the MP for systemic movement [66]. This allowed the reconstruction of the entire functional genome in distant tissues of the plant, a requisite for the successful infection of the host. Taken together, these data suggest that the preservation of genome integrity during long-distance movement appears to be mediated by means of a complex in which BMV RNA3 together with MP could play a fundamental role. This led to the hypothesis that viral RNAs interact, in the same cell or in the same environment such as vascular tissues, during the transit of RNA/RNP species. Another aspect of a systemic movement mechanism can be drawn as a result of this experiment. One could argue that in plant, interconnected cells could exchange viral proteins involved in the amplification or in the movement of the viral RNAs that could reach distant cells. In this situation, the proteins or the RNAs will then act in *trans*. To access distant cells, *trans* acting proteins or viral messenger RNAs will be needed in huge amount. Taking these requirements into consideration, only segmented DNA viruses—such as geminiviruses or nanoviruses (circular ssDNA genome) that express mRNA thanks to their stabilized replicative dsDNA segments—can fulfill such a constitutive expression. These viral DNAs ensure a continuous expression of proteins in different tissues, and viral products could move from one cell to another as proteins, mRNAs or both. In the case of BMV described above, the use of agroinfection allowed the continuous production of infectious viral RNAs from cDNAs. This situation recapitulates what could happen for segmented DNA phytoviruses described above.

Recent advances using RNA sequencing (RNAseq) analyses demonstrated the role of TLS structures in the systemic transport of mRNAs containing such structural motifs [67]. The presence of such TLS on BMV RNAs (and TMV as well) may explain why these RNAs could move on their own. Some multipartite RNA viruses such as the benyviruses described below do not possess 3′ TLS and thus will require the presence of a dedicated highly structured motif within each segment to fulfill the movement of each genomic RNA. However, one should take into account that RNA amplification of multipartite RNA viruses depends at least on the expression of the replication machinery and a viral suppressor of RNA silencing. Segregated segments will not be autonomous for amplification and their expression will be transient and not sufficient to promote the production of viral protein or to allow a stabilization of yet non-replicated RNA segments. Therefore, these RNAs will face the RNA decay or could induce cell death if they are expressed. Furthermore, if we assume the movement of viral proteins between communicating cells, this will require the presence of a sequence signal for each protein species for their intercellular transport. A study quantifying the degree of symplastic continuity between plant cells revealed that mobility of non-targeted proteins is strongly dependent on their molecular weight, on the developmental stages and the growth conditions [68]. Thus, if these hypotheses could not be completely excluded, they are difficult to conceive for plant multipartite RNA viruses, particularly for those possessing a helical shape.

3.2. Positive-Strand RNA Packaging into Helical Particle Units

If TLS motifs and/or signal peptides could drive the systemic movement of RNP complexes, the hypothesis of an RNP involving RNA-RNA network nucleating genomic segments and driven by few viral proteins appears easier to draw. To highlight our thoughts and findings, we present our views applied to the benyvirus biology and then extend our approach to pomoviruses.

3.2.1. Benyviruses: Up to Five Genomic RNAs

The *Benyviridae* family is composed of the *Benyvirus* genus of four viral species, namely, beet necrotic yellow vein virus (BNYVV), beet soil-borne mosaic virus (BSBMV), burdock mottle virus and rice stripe necrosis virus, the latter two species having a bipartite genome [69]. Benyviruses are rod-shaped virions of variable length with a constant diameter ranging from 18 to 20 nm. The particle length depends on the genomic RNA individually packaged. Among this family, BNYVV is the most studied species together with BSBMV. These two viruses share a similar genome organization, segment

number, host range and transmission vector. Serologically distant, one species is able to amplify and package genomic RNA segments of the other in laboratory conditions [69]. This indicates the presence of conserved promoter structural elements at the extremities of the genomic RNAs, the ability of subgenomic promoter recognition by the replicase, as well as a possibility of RNA-RNA interactions allowing RNP complexes´ formation and function.

The OA for viral particle morphogenesis has only been studied on the RNA3 and RNA4 species. Preliminary experiments indicate the presence of *cis* acting sequences located in the first 300 and the last 70 nt of the RNA3 species [70]. Since the non coding RNA 3 (former sgRNA3) sequence coterminous with RNA3 is not encapsidated, the OA sequence was presumed to reside within the 5′ UTR of RNA3 [70]. Using a collection of deletion mutants, an encapsidation signal was identified between nt 181–207 [71,72]. The absence of sequence conservation between this RNA OA and other viral RNAs suggests that this domain could be involved in a particular and transient folding required for the packaging. Moreover, nothing is yet known about the possible existence of a bipartite motif that could involve the 3′ conserved UTRs since the RNA3-derived replicon vector (Rep3, constituted by the 5′ and 3′ UTRs of RNA3) is encapsidated [70,72]. The recognition of the viral OA by structural proteins differs from the one described for tobamoviruses (e.g., TMV). To ensure a correct encapsidation process, the minor structural protein needs to be expressed by a read-through bypass of the coat protein stop codon [73]. This 75 kDa coat protein-readthrough (CP-RT) protein is recovered from purified viral particles and has been visualized by transmission electron microscopy (TEM) after immunolabelling [74]. Mutants expressing the CP alone or missing the N-terminal part of the RT domain are deficient in packaging [75,76]. These data suggest a recognition of the viral OAs by the CP-RT domain followed by a cooperative recruitment of the CP subunit to ensure proper packaging [76]. If it exists, the specific subcellular localization of virion assembly is unknown. However, on the one hand, the encapsidation could be coupled to the replication process and thus be associated with the endoplasmic reticulum (ER) vicinity as the replication seems to occur on the ER (Figure 2, step 2) [77]. On the other hand, this packaging could also be transiently associated to mitochondria as virions surrounding the organelle structures have been observed [78]. Further work conducted on the CP-RT protein allowed the identification of a mitochondrial targeting sequence and a transmembrane domain on the minor structural protein [79].

In local host species such as *Chenopodium quinoa*, BNYVV produces local lesions within which each RNA species accumulates and encapsidates individually (Figure 2, step 1) [80]. Local lesion formation requires at least the presence of RNA1 and RNA2 to fulfill the housekeeping functions of replication, cell-to-cell movement and viral suppression of RNA silencing. The coat protein is dispensable for local infection [81].

In systemic hosts such as *Beta* species or *N. benthamiana*, local infection starts as in *Chenopodium quinoa* and then reaches the vasculature of the plant leading to the possible dissemination of the viral material in the entire plant as described in Figure 1. The differential accumulation of virion species in primary infected cells [80] argues against a dissemination of viral particles. On the one hand, taking into account the existence of an unidentified receptor for the virus, there is likelihood to saturate this entry gate with particles containing small genomic RNA species unable to replicate on their own. On the other hand, in a model lacking a receptor for the viral entry, even if still non-estimated, the probability for each segment to enter the same distant cell appears low. Similarly, non-orchestrated dissemination of a viral genomic segment to randomly distant cells will end up with the same conclusion: a low probability to reconstruct the entire viral genome. Our interrogations about the nature of moving material started with the following observations on BNYVV. All viral particles are structurally identical and only differ by their size, and all four (sometimes five) viral genomic RNAs are required to fulfill the entire cycle on the *Beta* species hosts [82–84]. However, RNA1 and RNA2 are sufficient for *N. benthamiana* systemic infection thanks to a replication machinery provided, as stated before, by RNA1 and to structural proteins together with the triple gene block (TGB) movement proteins (TGB1, -2 and -3) and post-transcriptional gene silencing suppressor (viral suppressors of RNA silencing, VSR) provided by RNA2 species [85,86] (Figure 2). In this host, RNA3

is dispensable, but when present it moves long distance and accentuates symptom severity [87]. Interestingly, in the presence of RNA1 + RNA2, the RNA3-derived viral expression vector Rep3 does not move long distance in *N. benthamiana* host. As Rep3 is encapsidated, we ruled out the thesis of virions as moving material and we formulated the hypothesis about the existence of RNA-RNA interactions allowing RNA segments to interact with one another to ensure a stabilization of an RNP complex for the long-distance movement of the viral genome in the plant. Such an RNP complex contains CP as this structural protein is required for systemic spread [81]. A reinvestigation of the properties of RT mutants´ behavior described previously [76] confirmed our thoughts. Indeed, in this article some BNYVV mutants unable to form virions are still able to infect plants systemically. Thus, the minimal mobile RNP complex requires RNA1 and RNA2-interacting species to ensure the expression of housekeeping genes. Because RNA2 drives the production of subgenomic RNAs collinearly with its 3′ extremity [88], we postulated that the interaction domain consists of a region present on RNA2 but not included in the sgRNAs sequence, lest 3′ RNA2 collinear sequences interfere with genomic RNA interaction. Therefore, we focused our attention on the first 2000 nt and identified a sequence able to interact with RNA1 species using electromobility shift assay performed on in vitro transcripts. A similar approach performed on RNA3 species revealed the existence of more than one domain involved in the interaction with RNA2 (Dall'Ara et al., in preparation). To confirm our approach and share our findings, we transposed our hypothesis onto potato mop top virus, a tripartite helical virus that does not require structural proteins for its long-distance movement. These findings are discussed below in regard to mutants described in the literature.

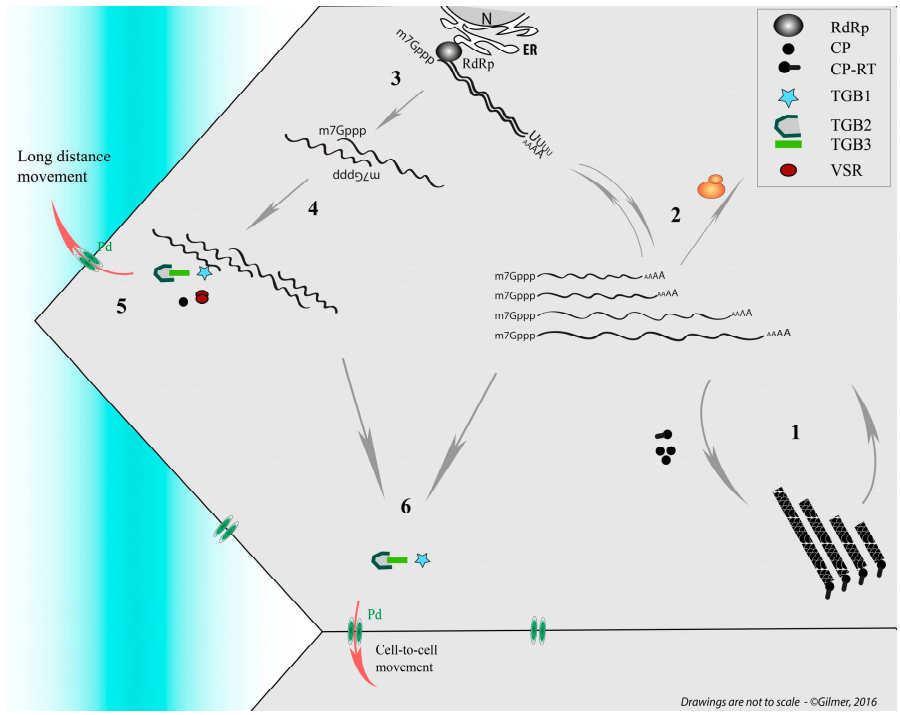

Figure 2. Simplified representation of replication cycle and movement of Beet necrotic yellow vein virus (BNYVV) used as model. The four genomic RNAs of the segmented helical virus (1) are expressed and amplified (2). On this scheme the RNA-RNA interaction network between genomic segments (3 and 4), stabilized by viral proteins, allows the preservation of genome integrity during long-distance movement (5) in the sieve elements (blue shaded). In particular the presence of the coat protein (CP) and the viral suppressors of RNA silencing (VSR) is necessary for their systemic movement. Vice versa the genomic RNAs can move cell to cell without the need of the CP expression but require triple gene block (TGB) movement proteins (6). ER: endoplasmic reticulum; CP-RT: coat protein-readthrough; N: Nucleus; RdRp: RNA-dependent RNA polymerase.

3.2.2. Potato Mop Top Virus: Tripartite, but Two Is Enough

Potato mop top virus (PMTV) belongs to the *Pomovirus* genus together with beet soil-borne virus, beet virus Q, and broad bean necrosis virus. PMTV is a helical rod-shaped virus with a diameter of 18–20 nm and variable lengths (~120 to ~290 nm) according to the genomic ssRNA being packaged [89]. The particles possess a fragile and partially uncoiled extremity [90]. The viral genome is segmented on three positive-sense RNAs. RNA1 allows the expression of two proteins involved in viral replication thanks to a read-through mechanism. RNA2 encodes for major (CP) and minor (CP-RT) structural proteins, the later produced by ribosomal read-through of the CP Amber stop codon. RNA3 possesses four different ORFs that encode for the triple gene block movement proteins (TGB1, TGB2 and TGB3) and one cysteine-rich protein of 8 kDa [89]. As described for BNYVV, minor structural protein is detected at one extremity of some particles. CP-RT is involved in the transmission by the *Spongospora subterranean* vector, because spontaneous deletions occur in isolates with disrupted transmission, particularly after serial mechanical inoculation [91,92]. However, this minor structural protein is dispensable for viral morphogenesis because deletions of the RT domain, or mutations that prevent read-through from occurring, accumulate viral particles [93]. The encapsidation of viral genomic RNAs is also dispensable for systemic spread because "no-protein" and "CP-RT only" RNA2 mutants move [93]. This particularity explains the systemic infection of *N. benthamiana* using a combination of transcripts corresponding to RNA1 and RNA3 [94] and thus demonstrates that PMTV long-distance movement occurs as an RNP complex. The RNA-binding domain constituted by the 84 N-terminal residues of the TGB1 movement protein ensures PTMV RNP complex long-distance movement and appears dispensable for cell-to-cell movement [95]. This domain ensures TGB1 nucleolar localization and its association to microtubules that could allow the recruitment of a cellular factor necessary for the vasculature entry of the RNPs [95]. This renders "PMTVΔRNA2" comparable to GRV, which uses ORF3 protein to recruit fibrillarin to form viral RNP complexes able to move long distance [96] (see Section 2.1.3).

With the reinterpretation of the literature describing the systemic movement of PMTV RNA2 deletion mutants [93], we pointed out an interesting property for the "CP-only" mutant. This viral RNA2 mutant is unable to move long distance in the presence of RNA1 and RNA3. A similar behavior appears for deletion mutants within the C-terminal part of the CP-RT sequence, leading the authors to conclude that a 140 amino acid CP-RT domain is specifically required for the systemic movement of RNA2. However, abolition of CP synthesis in these mutants restored the RNA2 species´ long-distance transport. Consequently, we postulate on the existence of a sequence acting as a "riboswitch" that could be regulated either by a CP interaction or by refolding during ribosomal translation. Such alternative structures could allow or prevent genomic RNA-RNA network interactions, required for long-distance transport or its recruitment as messenger RNA, respectively.

Taking into consideration our preliminary data accumulated on BNYVV, we checked if similar RNA-RNA interactions could exist, using the IntaRNA program (Freiburg RNA Tools) [97,98] and looking for heterologous RNA-RNA interactions between PMTV genomic RNAs (Sw isolate). We took into consideration the sequences that were preserved in natural and artificial RNA2 deletion mutants that were still able to move long distance [93,99]. We found a 20 nt long sequence (5′- ^{2760}UAGGGAAGAUGUCAGGUAAG^{2779} -3′), located within the CP-RT C-terminal coding sequence that could possibly interact with a sequence (5′- ^{2244}CUUGCCUGACGUCGAUCCUG^{2263} -3′) present in the RNA1 replicase sequence with a 2 nt bulge (underlined). In a model where genome integrity needs to be preserved during the systemic movement by the association of all genomic RNAs in a RNP complex, such 20 nt base pairing, with a predicted variation of the Gibbs free energy of −16.35 Kcal/mol, could participate in an RNA2-RNA1 specific interaction. We did not extend our computational analyses to the RNA3-RNA2 or RNA3-RNA1 interaction domains. However, taking into account the systemic infection mediated by RNA1 and RNA3, such domains should exist [100].

The advantage of a regulatory network involving RNA-RNA interactions eliminates the need for a viral protein dedicated to associate RNA species with a correct stoichiometry. At the beginning of a cell infection, translation and replication events are predominantly monopolizing viral RNAs

that switch between unstructured and structured forms. Thereby, RNA-RNA interactions could take place in *trans* and will guarantee the formation of RNP complexes dedicated to the long-distance movement thanks to the movement proteins produced via subgenomic RNAs. Late in the infection, the accumulation of structural protein would negatively regulate the RNA-RNA interaction, leading to the encapsidation of genomic RNA species ready for their acquisition by the vector thanks to the minor structural protein recognition [92]. As for BNYVV, experiments need to be performed to verify the existence of a "riboswitch" in order to validate or discard these hypotheses.

4. Multipartite Positive-Strand RNA Genomes Have to Preserve Their Genome Integrity

As previously mentioned, to maintain their viral genome as a functional unit, segmented positive-strand viruses require the presence of at least one of each viral RNA segment in the target cell. Such conditions require a high multiplicity of infection (MOI), especially for viruses with four or more genomic entities as demonstrated by theoretical studies [101]. Because the infection of different plant cell types and tissues does not occur as a uniform process, a multipartite phytovirus has to pass through constraints and to sustain other biological costs in order to maintain its genome integrity.

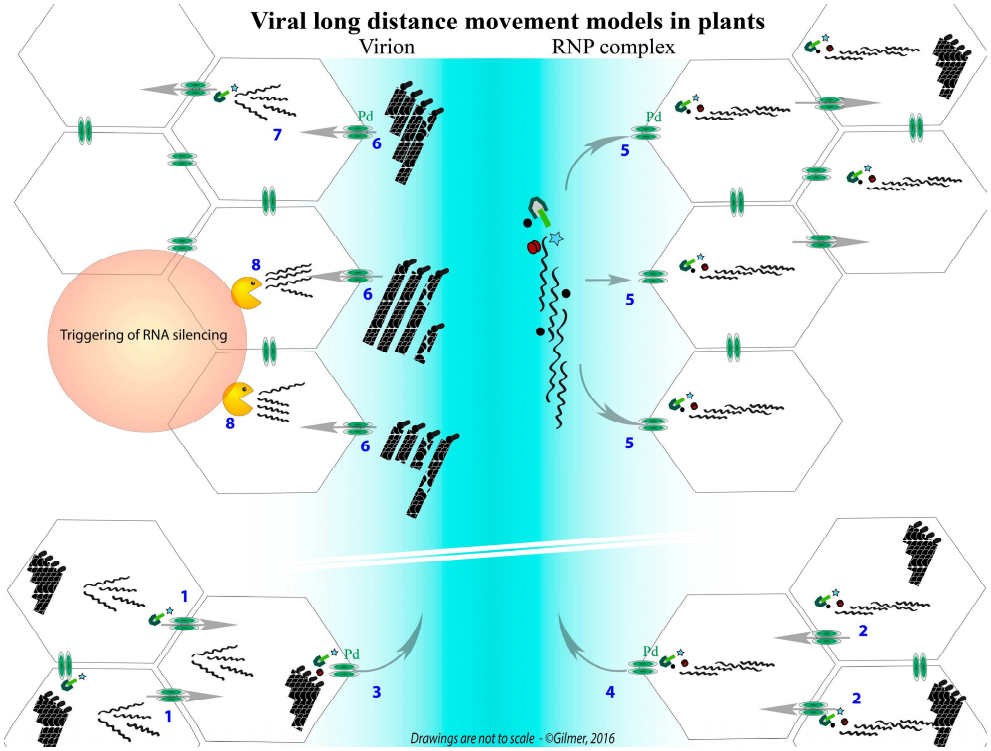

Figure 3. Confrontation of two models describing the long-distance movement of multipartite RNA viruses using the BNYVV as an example. The bottom of the graphic represents the progression of an initial infection of mesophyll cells, wherein the infection progresses thanks to the individual cell-to-cell movement of viral RNAs, driven by TGB movement proteins (1) or as ribonucleoprotein (RNP) complexes involving RNA-RNA network between genomic segments (2). In the sieve elements (blue), the virion (3) or the RNP complexes (4) are transported through plasmodesmata thanks to the viral proteins. RNP complexes, driving the export of the viral genomic RNA network, could provide each distant cell with an entire and fully functional genome (**5**). Virions (or single viral RNAs, not presented) are transported in the sieve elements and are randomly distributed in the distant cells (**6**). Only the combination providing one of each viral particle (or RNA) is able to initiate an infection that preserves the genome integrity (**7**). The particles (or RNA) entering cells without the entire genome are either deficient for replication (not shown) or unable to move from cell to cell and express the VSR, leading to the trigger of RNA silencing (**8**).

Viral cell-to-cell movement ensures the progression of the infection via plasmodesmata, the connection channels between plant cells (Figure 3, steps 1 and 2). In the phloem (a circulation fluid that provides nutrients to all parts of the plant), fluidic mechanic rules dominate. These physical constraints tend to separate small and large viral particles with two tendencies: the first will reduce the velocity of large entities in the fluid, due to increased contacts with the phloem capillary system, whereas small entities will be less affected. Because the phloem is not just a "tube" but consists of vascular elements (sieve elements) connected with companion cells (see Figure 1), viral entities are subject to a "gel filtration" separation. These two effects increase the risk of a loss of one viral component during the journey, compromising the integrity of the viral genome and, therefore, moderate and reduce the speed of systemic movement and infection that should occur in each "visited cell".

However, the viral genome must contend with RNA decay mechanisms whereby RNA species are translated or cleaved by the silencing machinery (Figure 3, step 8). Therefore, having its genomic components physically separated would increase the chance of essential viral segments being degraded, thus leading to a defective viral entity. Natural infections show that this is not the case, favoring our idea of a collective transport of genomic RNA species (Figure 3, steps 4 and 5). Hence, RNA-RNA interactions are not the only key elements. Various experiments indicate the involvement of structural protein(s), probably in the stabilization of the interactions, as well as non-structural proteins, such as movement proteins or viral suppressors of RNA silencing that counteract the cellular defenses in the distant cells.

5. Concluding Remarks: Lessons from Superinfection Exclusion Reports

We have reviewed published literature about distinct virus packaging and long-distance movement focusing on some data and arguments in favor of a viral transport as RNP complexes rather than virions. Describing BMV long-distance movement, it appears that the RNA3 species could as well be involved in RNA-RNA interactions with other viral species to nucleate the formation of a RNP complex as postulated for BNYVV and PMTV RNA1-RNA2 species. While one RNA species modulates the recruitment of other species, no information is yet available about the stoichiometry of the genomic components in the moving RNP complex. In order to safeguard genomic integrity, it could be postulated that more than one RNA species should be present to ensure, on the one hand, the expression of essential protein(s) in the distant cell and, on the other hand, the presence of replication-ready genomic components.

A notable example of preservation of viral genomic integrity is the superinfection exclusion (SIE) that exists among some phytoviruses and prevents some co-infections from occurring. Described for T-even bacteriophages, SIE consists on the inhibition of viral genome entry in the cytoplasm of an infected cell thanks to the expression of viral proteins [102]. In eukaryotes, viral mechanisms are also described for viruses that tend to deplete viral receptors from the infected cell as described for the human immunodeficiency virus (HIV) CD4 receptor internalization and proteolysis thanks to the expression of the Vpu protein [103]. A limited co-infection of distant tissues has been described in plants inoculated with two recombinant monopartite potyvirus variants (Tobacco etch virus) thanks to the use of fluorescent reporter proteins, suggesting as well the establishment of a limited access to the cell, with one variant excluding the other [104].

A similar observation was made in sugar beet infected with both BNYVV and BSBMV (two benyviruses). The infection of the plant with one virus limits the possible infection of the same plant with the second virus, if inoculated a few days later [105], suggesting a "SIE-like" mechanism for benyviruses. Using viral reporter RNAs from BSBMV and BNYVV RNA3 replicons, both packaged in *trans* during their amplification by BNYVV RNA1 + RNA2, we previously demonstrated that within local lesions, reporter RNA species exclude one another, leading to sectored lesions as shown in Figure 4 [106]. If such a process occurs on viral particles rather than on viral RNAs, then there will be a high probability for an exclusion of small entities (such as particles containing RNA3 or RNA4) in cells where RNA1 and RNA2 already started to be expressed and replicated. This property bolsters our hypothesis that specific RNA-RNA interactions preserve viral genome integrity during the viral

journey within an infected plant. While some plant species susceptible to local infection could resist the systemic spread of these multipartite viruses, it could be assumed that some cellular RNA could compete by interacting with the domains involved in this RNA-RNA network formation, but this is another story . . .

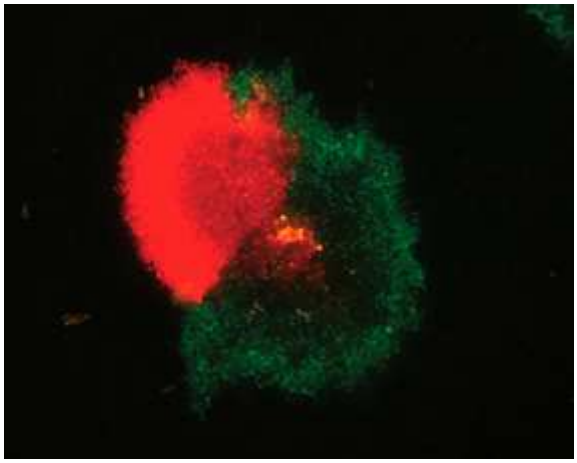

Figure 4. Fluorescence profile of a *C. quinoa* local lesion observed 7 days post infection after rub-inoculation of BNYVV RNA1 and RNA2 supplemented with a mixture of two replicons derived from BSBMV and BNYVV RNA3s, expressing monomeric red fluorescent protein (mRFP) and enhanced green fluorescent protein (EGFP), respectively. This image illustrates the existence of an exclusion mechanism for similar but distinct RNA species during the progression of the infection, with both replicons being able to be encapsidated by BNYVV CP (details are described in Ratti et al., 2009 [104]).

Acknowledgments: The authors are grateful to current and past members of their laboratories for constructive discussions and would like to acknowledge Todd Blevins for his help in language editing and the three reviewers for their constructive comments. Mattia Dall'Ara's work was supported by the Italian ministry PhD grant (048794-0000712558) and by Marco Polo and Da Vinci programs of mobility contribution, funded by the University of Bologna and the Italo-French University of Turin, respectively. The funders had no role in study design, data collection and analysis, decision to publish, or preparation of the manuscript.

Conflicts of Interest: All authors report no conflicts of interest.

References

1. Gerber, M.; Isel, C.; Moules, V.; Marquet, R. Selective packaging of the influenza A genome and consequences for genetic reassortment. *Trends Microbiol.* **2014**, *22*, 446–455. [CrossRef] [PubMed]
2. Guu, T.S.; Zheng, W.; Tao, Y.J. Bunyavirus: Structure and replication. *Adv. Exp. Med. Biol.* **2012**, *726*, 245–266.
3. Huiskonen, J.T.; de Haas, F.; Bubeck, D.; Bamford, D.H.; Fuller, S.D.; Butcher, S.J. Structure of the bacteriophage phi6 nucleocapsid suggests a mechanism for sequential RNA packaging. *Structure* **2006**, *14*, 1039–1048. [CrossRef] [PubMed]
4. Rao, A.L. Genome packaging by spherical plant RNA viruses. *Annu. Rev. Phytopathol.* **2006**, *44*, 61–87. [CrossRef] [PubMed]
5. Solovyev, A.G.; Makarov, V.V. Helical capsids of plant viruses: Architecture with structural lability. *J. Gen. Virol.* **2016**. [CrossRef] [PubMed]
6. Waigmann, E.; Ueki, S.; Trutnyeva, K.; Citovsky, V. The ins and outs of nondestructive cell-to-cell and systemic movement of plant viruses. *Crit. Rev. Plant Sci.* **2004**, *23*, 195–250. [CrossRef]
7. Roberts, A.G.; Cruz, S.S.; Roberts, I.M.; Prior, D.; Turgeon, R.; Oparka, K.J. Phloem unloading in sink leaves of *Nicotiana benthamiana*: Comparison of a fluorescent solute with a fluorescent virus. *Plant Cell* **1997**, *9*, 1381–1396. [CrossRef] [PubMed]

8. Dykeman, E.C.; Grayson, N.E.; Toropova, K.; Ranson, N.A.; Stockley, P.G.; Twarock, R. Simple rules for efficient assembly predict the layout of a packaged viral RNA. *J. Mol. Biol.* **2011**, *408*, 399–407. [CrossRef] [PubMed]
9. Dykeman, E.C.; Stockley, P.G.; Twarock, R. Building a viral capsid in the presence of genomic RNA. *Phys. Rev. E Stat. Nonlin Soft Matter Phys.* **2013**, *87*, 022717. [CrossRef] [PubMed]
10. Rolfsson, O.; Middleton, S.; Manfield, I.W.; White, S.J.; Fan, B.; Vaughan, R.; Ranson, N.A.; Dykeman, E.; Twarock, R.; Ford, J.; et al. Direct evidence for packaging signal-mediated assembly of bacteriophage MS2. *J. Mol. Biol.* **2016**, *428*, 431–448. [CrossRef] [PubMed]
11. Sorger, P.K.; Stockley, P.G.; Harrison, S.C. Structure and assembly of turnip crinkle virus. II. Mechanism of reassembly in vitro. *J. Mol. Biol.* **1986**, *191*, 639–658. [CrossRef]
12. Qu, F.; Morris, T.J. Encapsidation of turnip crinkle virus is defined by a specific packaging signal and RNA size. *J. Virol.* **1997**, *71*, 1428–1435. [PubMed]
13. Cohen, Y.; Gisel, A.; Zambryski, P.C. Cell-to-cell and systemic movement of recombinant green fluorescent protein-tagged turnip crinkle viruses. *Virology* **2000**, *273*, 258–266. [CrossRef] [PubMed]
14. Deleris, A.; Gallego-Bartolome, J.; Bao, J.; Kasschau, K.D.; Carrington, J.C.; Voinnet, O. Hierarchical action and inhibition of plant dicer-like proteins in antiviral defense. *Science* **2006**, *313*, 68–71. [CrossRef] [PubMed]
15. Qu, F.; Ren, T.; Morris, T.J. The coat protein of turnip crinkle virus suppresses posttranscriptional gene silencing at an early initiation step. *J. Virol.* **2003**, *77*, 511–522. [CrossRef] [PubMed]
16. Harvey, S.C.; Zeng, Y.; Heitsch, C.E. The icosahedral RNA virus as a grotto: Organizing the genome into stalagmites and stalactites. *J. Biol. Phys.* **2013**, *39*, 163–172. [CrossRef] [PubMed]
17. Archer, E.J.; Simpson, M.A.; Watts, N.J.; O'Kane, R.; Wang, B.; Erie, D.A.; McPherson, A.; Weeks, K.M. Long-range architecture in a viral RNA genome. *Biochemistry* **2013**, *52*, 3182–3190. [CrossRef] [PubMed]
18. Valverde, R.A.; Heick, J.A.; Dodds, J.A. Interactions between satellite tobacco mosaic virus, helper tobamovirus, and their hosts. *Phytopathology* **1991**, *81*, 99–104. [CrossRef]
19. Robinson, D.J.; Ryabov, E.V.; Raj, S.K.; Roberts, I.M.; Taliansky, M.E. Satellite RNA is essential for encapsidation of groundnut rosette umbravirus RNA by groundnut rosette assistor luteovirus coat protein. *Virology* **1999**, *254*, 105–114. [CrossRef] [PubMed]
20. Taliansky, M.E.; Robinson, D.J. Molecular biology of umbraviruses: Phantom warriors. *J. Gen. Virol.* **2003**, *84*, 1951–1960. [CrossRef] [PubMed]
21. Fraenkel-Conrat, H.; Williams, R.C. Reconstitution of active tobacco mosaic virus from its inactive protein and nucleic acid components. *Proc. Natl. Acad. Sci. USA* **1955**, *41*, 690–698. [CrossRef] [PubMed]
22. Turner, D.R.; Butler, P.J. Essential features of the assembly origin of tobacco mosaic virus RNA as studied by directed mutagenesis. *Nucleic Acids Res.* **1986**, *14*, 9229–9242. [CrossRef] [PubMed]
23. Liu, Z.; Qiao, J.; Niu, Z.; Wang, Q. Natural supramolecular building blocks: From virus coat proteins to viral nanoparticles. *Chem. Soc. Rev.* **2012**, *41*, 6178–6194. [CrossRef] [PubMed]
24. Guenoune-Gelbart, D.; Elbaum, M.; Sagi, G.; Levy, A.; Epel, B.L. Tobacco mosaic virus (TMV) replicase and movement protein function synergistically in facilitating TMV spread by lateral diffusion in the plasmodesmal desmotubule of *Nicotiana benthamiana*. *Mol. Plant Microbe Interact.* **2008**, *21*, 335–345. [CrossRef] [PubMed]
25. Dorokhov, Y.L.; Alexandrova, N.M.; Miroshnichenko, N.A.; Atabekov, J.G. Isolation and analysis of virus-specific ribonucleoprotein of tobacco mosaic virus-infected tobacco. *Virology* **1983**, *127*, 237–252. [CrossRef]
26. Saito, T.; Yamanaka, K.; Okada, Y. Long-distance movement and viral assembly of tobacco mosaic virus mutants. *Virology* **1990**, *176*, 329–336. [CrossRef]
27. Ding, X.; Shintaku, M.H.; Carter, S.A.; Nelson, R.S. Invasion of minor veins of tobacco leaves inoculated with tobacco mosaic virus mutants defective in phloem-dependent movement. *Proc. Natl. Acad. Sci. USA* **1996**, *93*, 11155–11160. [CrossRef] [PubMed]
28. Dawson, W.O.; Bubrick, P.; Grantham, G.L. Modifications of the tobacco mosaic virus coat protein gene affecting replication, movement and symptomatology. *Phytopathology* **1988**, *78*, 783–789. [CrossRef]
29. Nelson, R.S.; Li, G.; Hodgson, R.A.; Beachy, R.N.; Shintaku, M.H. Impeded phloem-dependent accumulation of the masked strain of tobacco mosaic virus. *Mol. Plant Microbe Interact.* **1993**, *6*, 45–54. [CrossRef]
30. Ding, X.S.; Shintaku, M.H.; Arnold, S.A.; Nelson, R.S. Accumulation of mild and severe strains of tobacco mosaic virus in minor veins of tobacco. *Mol. Plant Microbe Interact.* **1995**, *8*, 32–40. [CrossRef]

31. Heinlein, M. Plant virus replication and movement. *Virology* **2015**, *479–480*, 657–671. [CrossRef] [PubMed]
32. Doering-Saad, C.; Newbury, H.J.; Bale, J.S.; Pritchard, J. Use of aphid stylectomy and RT-PCR for the detection of transporter mRNAs in sieve elements. *J. Exp. Bot.* **2002**, *53*, 631–637. [CrossRef] [PubMed]
33. Kragler, F. Rna in the phloem: A crisis or a return on investment? *Plant Sci.* **2010**, *178*, 99–104. [CrossRef]
34. Sasaki, T.; Chino, M.; Hayashi, H.; Fujiwara, T. Detection of several mRNA species in rice phloem sap. *Plant Cell Physiol.* **1998**, *39*, 895–897. [CrossRef] [PubMed]
35. Ryabov, E.V.; Robinson, D.J.; Taliansky, M.E. A plant virus-encoded protein facilitates long-distance movement of heterologous viral RNA. *Proc. Natl. Acad. Sci. USA* **1999**, *96*, 1212–1217. [CrossRef] [PubMed]
36. Taliansky, M.; Roberts, I.M.; Kalinina, N.; Ryabov, E.V.; Raj, S.K.; Robinson, D.J.; Oparka, K.J. An umbraviral protein, involved in long-distance RNA movement, binds viral RNA and forms unique, protective ribonucleoprotein complexes. *J. Virol.* **2003**, *77*, 3031–3040. [CrossRef] [PubMed]
37. Chen, M.-H.; Sheng, J.; Hind, G.; Handa, A.K.; Citovsky, V. Interaction between the tobacco mosaic virus movement protein and host cell pectin methylesterases is required for viral cell-to-cell movement. *EMBO J.* **2000**, *19*, 913–920. [CrossRef] [PubMed]
38. Chen, M.-H.; Citovsky, V. Systemic movement of a tobamovirus requires host cell pectin methylesterase. *Plant J.* **2003**, *35*, 386–392. [CrossRef] [PubMed]
39. Fenczik, C.A.; Padgett, H.S.; Holt, C.A.; Casper, S.J.; Beachy, R.N. Mutational analysis of the movement protein of odontoglossum ringspot virus to identify a host-range determinant. *Mol. Plant Microbe Interact.* **1995**, *8*, 666–673. [CrossRef] [PubMed]
40. Kim, K.H.; Lommel, S.A. Identification and analysis of the site of -1 ribosomal frameshifting in red clover necrotic mosaic virus. *Virology* **1994**, *200*, 574–582. [CrossRef] [PubMed]
41. Osman, T.A.M.; Buck, K.W. Double-stranded RNAs isolated from plant tissue infected with red clover necrotic mosaic virus correspond to genomic and subgenomic single-stranded rRNA. *J. Gen. Virol.* **1990**, *71*, 945–948. [CrossRef]
42. Xiong, Z.; Kim, K.H.; Giesman-Cookmeyer, D.; Lommel, S.A. The roles of the red clover necrotic mosaic virus capsid and cell-to-cell movement proteins in systemic infection. *Virology* **1993**, *192*, 27–32. [CrossRef] [PubMed]
43. Xiong, Z.; Lommel, S.A. The complete nucleotide sequence and genome organization of red clover necrotic mosaic virus RNA-1. *Virology* **1989**, *171*, 543–554. [CrossRef]
44. Zavriev, S.K.; Hickey, C.M.; Lommel, S.A. Mapping of the red clover necrotic mosaic virus subgenomic RNA. *Virology* **1996**, *216*, 407–410. [CrossRef] [PubMed]
45. Lommel, S.A.; Weston-Fina, M.; Xiong, Z.; Lomonossoff, G.P. The nucleotide sequence and gene organization of red clover necrotic mosaic virus RNA-2. *Nucleic Acids Res.* **1988**, *16*, 8587–8602. [CrossRef] [PubMed]
46. Powers, J.G.; Sit, T.L.; Heinsohn, C.; George, C.G.; Kim, K.H.; Lommel, S.A. The red clover necrotic mosaic virus RNA-2 encoded movement protein is a second suppressor of RNA silencing. *Virology* **2008**, *381*, 277–286. [CrossRef] [PubMed]
47. Wang, H.L.; Wang, Y.; Giesman-Cookmeyer, D.; Lommel, S.A.; Lucas, W.J. Mutations in viral movement protein alter systemic infection and identify an intercellular barrier to entry into the phloem long-distance transport system. *Virology* **1998**, *245*, 75–89. [CrossRef] [PubMed]
48. Basnayake, V.R.; Sit, T.L.; Lommel, S.A. The red clover necrotic mosaic virus origin of assembly is delimited to the RNA-2 trans-activator. *Virology* **2009**, *384*, 169–178. [CrossRef] [PubMed]
49. Osman, T.A.M.; Buck, K.W. Replication of red clover necrotic mosaic virus RNA in cowpea protoplasts: RNA 1 replicates independently of RNA 2. *J. Gen. Virol.* **1987**, *68*, 289–296. [CrossRef]
50. Paje-Manalo, L.L.; Lommel, S.A. Independent replication of red clover necrotic mosaic virus RNA-1 in electroporated host and nonhost nicotiana species protoplasts. *Phytopathology* **1989**, *79*, 457–461. [CrossRef]
51. Sit, T.L.; Vaewhongs, A.A.; Lommel, S.A. RNA-mediated trans-activation of transcription from a viral RNA. *Science* **1998**, *281*, 829–832. [CrossRef] [PubMed]
52. Loo, L.; Guenther, R.H.; Basnayake, V.R.; Lommel, S.A.; Franzen, S. Controlled encapsidation of gold nanoparticles by a viral protein shell. *J. Am. Chem. Soc.* **2006**, *128*, 4502–4503. [CrossRef] [PubMed]
53. Basnayake, V.R.; Sit, T.L.; Lommel, S.A. The genomic RNA packaging scheme of red clover necrotic mosaic virus. *Virology* **2006**, *345*, 532–539. [CrossRef]

54. Vaewhongs, A.A.; Lommel, S.A. Virion formation is required for the long-distance movement of red clover necrotic mosaic virus in movement protein transgenic plants. *Virology* **1995**, *212*, 607–613. [CrossRef] [PubMed]
55. Lane, L.C. Bromoviruses. In *Handbook of Plant Virus Infections and Comparative Diagnosis*; Kurstak, E., Ed.; Elsevier/North Holland Biomedical Press: Amsterdam, The Netherlands, 1981; pp. 333–375.
56. Choi, Y.G.; Rao, A.L. Packaging of brome mosaic virus RNA3 is mediated through a bipartite signal. *J. Virol.* **2003**, *77*, 9750–9757. [CrossRef] [PubMed]
57. Annamalai, P.; Rao, A.L. In vivo packaging of brome mosaic virus RNA3, but not RNAs 1 and 2, is dependent on a cis-acting 3′ tRNA-like structure. *J. Virol.* **2007**, *81*, 173–181. [CrossRef] [PubMed]
58. Damayanti, T.A.; Tsukaguchi, S.; Mise, K.; Okuno, T. Cis-acting elements required for efficient packaging of brome mosaic virus RNA3 in barley protoplasts. *J. Virol.* **2003**, *77*, 9979–9986. [CrossRef] [PubMed]
59. Annamalai, P.; Rao, A.L. Packaging of brome mosaic virus subgenomic RNA is functionally coupled to replication-dependent transcription and translation of coat protein. *J. Virol.* **2006**, *80*, 10096–10108. [CrossRef] [PubMed]
60. Mandahar, C.L. Infection by and uncoating of virus particles. In *Multiplication of RNA Plant Viruses*; Mandahar, C.L., Ed.; Springer Netherlands: Dordrecht, The Netherlands, 2006; p. 339.
61. Brisco, M.; Hull, R.; Wilson, T.M. Swelling of isometric and of bacilliform plant virus nucleocapsids is required for virus-specific protein synthesis in vitro. *Virology* **1986**, *148*, 210–217. [CrossRef]
62. Seo, J.K.; Kwon, S.J.; Rao, A.L. A physical interaction between viral replicase and capsid protein is required for genome-packaging specificity in an RNA virus. *J. Virol.* **2012**, *86*, 6210–6221. [CrossRef] [PubMed]
63. Sztuba-Solinska, J.; Fanning, S.W.; Horn, J.R.; Bujarski, J.J. Mutations in the coat protein-binding cis-acting RNA motifs debilitate RNA recombination of brome mosaic virus. *Virus Res.* **2012**, *170*, 138–149. [CrossRef] [PubMed]
64. Sasaki, N.; Kaido, M.; Okuno, T.; Mise, K. Coat protein-independent cell-to-cell movement of bromoviruses expressing brome mosaic virus movement protein with an adaptation-related amino acid change in the central region. *Arch. Virol.* **2005**, *150*, 1231–1240. [CrossRef] [PubMed]
65. Takeda, A.; Nakamura, W.; Sasaki, N.; Goto, K.; Kaido, M.; Okuno, T.; Mise, K. Natural isolates of brome mosaic virus with the ability to move from cell to cell independently of coat protein. *J. Gen. Virol.* **2005**, *86*, 1201–1211. [CrossRef] [PubMed]
66. Gopinath, K.; Kao, C.C. Replication-independent long-distance trafficking by viral RNAs in *Nicotiana benthamiana*. *Plant Cell* **2007**, *19*, 1179–1191. [CrossRef] [PubMed]
67. Zhang, W.; Thieme, C.J.; Kollwig, G.; Apelt, F.; Yang, L.; Winter, N.; Andresen, N.; Walther, D.; Kragler, F. tRNA-related sequences trigger systemic mRNA transport in plants. *Plant Cell* **2016**, *28*, 1237–1249. [CrossRef] [PubMed]
68. Crawford, K.M.; Zambryski, P.C. Non-targeted and targeted protein movement through plasmodesmata in leaves in different developmental and physiological states. *Plant Physiol.* **2001**, *125*, 1802–1812. [CrossRef] [PubMed]
69. Gilmer, D.; Ratti, C. Benyvirus. In *Virus Taxonomy: Classification and Nomenclature of Viruses: Ninth Report of the International Committee on Taxonomy of Viruses*; King, A.M.Q., Adams, M.J., Carstens, E.B., Lefkowitz, E.J., Eds.; Elsevier: San Diego, CA, USA, 2012; pp. 1133–1138.
70. Jupin, I.; Richards, K.; Jonard, G.; Guilley, H.; Pleij, C.W. Mapping sequences required for productive replication of beet necrotic yellow vein virus RNA 3. *Virology* **1990**, *178*, 273–280. [CrossRef]
71. Gilmer, D.; Allmang, C.; Ehresmann, C.; Guilley, H.; Richards, K.; Jonard, G.; Ehresmann, B. The secondary structure of the 5′-noncoding region of beet necrotic yellow vein virus RNA 3: Evidence for a role in viral RNA replication. *Nucleic Acids Res.* **1993**, *21*, 1389–1395. [CrossRef] [PubMed]
72. Gilmer, D.; Richards, K.; Jonard, G.; Guilley, H. *Cis*-active sequences near the 5′-termini of beet necrotic yellow vein virus RNAs 3 and 4. *Virology* **1992**, *190*, 55–67. [CrossRef]
73. Ziegler, V.; Richards, K.; Guilley, H.; Jonard, G.; Putz, C. Cell-free translation of beet necrotic yellow vein virus: Readthrough of the coat protein cistron. *J. Gen. Virol.* **1985**, *66*, 2079–2087. [CrossRef]
74. Haeberle, A.M.; Stussi-Garaud, C.; Schmitt, C.; Garaud, J.C.; Richards, K.E.; Guilley, H.; Jonard, G. Detection by immunogold labelling of p75 readthrough protein near an extremity of beet necrotic yellow vein virus particles. *Arch. Virol.* **1994**, *134*, 195–203. [CrossRef] [PubMed]

75. Schmitt, C.; Balmori, E.; Jonard, G.; Richards, K.E.; Guilley, H. In vitro mutagenesis of biologically active transcripts of beet necrotic yellow vein virus RNA 2: Evidence that a domain of the 75-kda readthrough protein is important for efficient virus assembly. *Proc. Natl. Acad. Sci. USA* **1992**, *89*, 5715–5719. [CrossRef] [PubMed]
76. Tamada, T.; Schmitt, C.; Saito, M.; Guilley, H.; Richards, K.; Jonard, G. High resolution analysis of the readthrough domain of beet necrotic yellow vein virus readthrough protein: A KTER motif is important for efficient transmission of the virus by *Polymyxa betae*. *J. Gen. Virol.* **1996**, *77*, 1359–1367. [CrossRef] [PubMed]
77. Pakdel, A.; Mounier, C.; Klein, E.; Hleibieh, K.; Monsion, B.; Mutterer, J.; Erhardt, M.; Bouzoubaa, S.; Ratti, C.; Gilmer, D. On the interaction and localization of the beet necrotic yellow vein virus replicase. *Virus Res.* **2015**, *196*, 94–104. [CrossRef] [PubMed]
78. Erhardt, M.; Dunoyer, P.; Guilley, H.; Richards, K.; Jonard, G.; Bouzoubaa, S. Beet necrotic yellow vein virus particles localize to mitochondria during infection. *Virology* **2001**, *286*, 256–262. [CrossRef] [PubMed]
79. Valentin, C.; Dunoyer, P.; Vetter, G.; Schalk, C.; Dietrich, A.; Bouzoubaa, S. Molecular basis for mitochondrial localization of viral particles during beet necrotic yellow vein virus infection. *J. Virol.* **2005**, *79*, 9991–10002. [CrossRef] [PubMed]
80. Tamada, T.; Shirako, Y.; Abe, H.; Saito, M.; Kigushi, T.; Harada, T. Production and pathogenicity of isolates of beet necrotic yellow vein virus with different numbers of RNA components. *J. Gen. Virol.* **1989**, *70*, 3399–3409. [CrossRef]
81. Quillet, L.; Guilley, H.; Jonard, G.; Richards, K. In vitro synthesis of biologically active beet necrotic yellow vein virus RNA. *Virology* **1989**, *172*, 293–301. [PubMed]
82. Rahim, M.D.; Andika, I.B.; Han, C.; Kondo, H.; Tamada, T. RNA4-encoded p31 of beet necrotic yellow vein virus is involved in efficient vector transmission, symptom severity and silencing suppression in roots. *J. Gen. Virol.* **2007**, *88*, 1611–1619. [CrossRef] [PubMed]
83. Tamada, T.; Abe, H. Evidence that beet necrotic yellow vein virus RNA-4 is essential for transmission by the fungus *Polymyxa betae*. *J. Gen. Virol.* **1989**, *70*, 3391–3398. [CrossRef]
84. Tamada, T.; Uchino, H.; Kusume, T.; Saito, M. RNA 3 deletion mutants of beet necrotic yellow vein virus do not cause rhizomania disease in sugar beets. *Phytopathology* **1999**, *89*, 1000–1006. [CrossRef] [PubMed]
85. Andika, I.B.; Kondo, H.; Tamada, T. Evidence that RNA silencing-mediated resistance to beet necrotic yellow vein virus is less effective in roots than in leaves. *Mol. Plant Microbe Interact.* **2005**, *18*, 194–204. [CrossRef] [PubMed]
86. Chiba, S.; Hleibieh, K.; Delbianco, A.; Klein, E.; Ratti, C.; Ziegler-Graff, V.; Bouzoubaa, S.; Gilmer, D. The benyvirus RNA silencing suppressor is essential for long-distance movement, requires both zinc-finger and NoLS basic residues but not a nucleolar localization for its silencing-suppression activity. *Mol. Plant Microbe Interact.* **2013**, *26*, 168–181. [CrossRef] [PubMed]
87. Delbianco, A.; Lanzoni, C.; Klein, E.; Rubies Autonell, C.; Gilmer, D.; Ratti, C. Agroinoculation of beet necrotic yellow vein virus cDNA clones results in plant systemic infection and efficient *Polymyxa betae* transmission. *Mol. Plant Pathol.* **2013**, *14*, 422–428. [CrossRef] [PubMed]
88. Gilmer, D.; Bouzoubaa, S.; Hehn, A.; Guilley, H.; Richards, K.; Jonard, G. Efficient cell-to-cell movement of beet necrotic yellow vein virus requires 3′ proximal genes located on RNA 2. *Virology* **1992**, *189*, 40–47. [CrossRef]
89. Adams, M.J.; Heinze, C.; Jackson, A.O.; Kreuze, J.F.; Macfarlane, S.; Torrance, L. Family *Virgaviridae*. In *Virus Taxonomy: Classification and Nomenclature of Viruses: Ninth Report of the International Committee on Taxonomy of Viruses*; King, A.M.Q., Adams, M.J., Carstens, E.B., Lefkowitz, E.J., Eds.; Elsevier: San Diego, CA, USA, 2012; pp. 1139–1162.
90. Kassanis, B.; Woods, R.D.; White, R.F. Some properties of potato mop-top virus and its serological relationship to tobacco mosaic virus. *J. Gen. Virol.* **1972**, *14*, 123–132. [CrossRef]
91. Cowan, G.H.; Torrance, L.; Reavy, B. Detection of potato mop-top virus capsid readthrough protein in virus particles. *J. Gen. Virol.* **1997**, *78 Pt 7*, 1779–1783. [CrossRef] [PubMed]
92. Reavy, B.; Arif, M.; Cowan, G.H.; Torrance, L. Association of sequences in the coat protein/readthrough domain of potato mop-top virus with transmission by *Spongospora subterranea*. *J. Gen. Virol.* **1998**, *79 Pt 10*, 2343–2347. [CrossRef] [PubMed]

93. Torrance, L.; Lukhovitskaya, N.I.; Schepetilnikov, M.V.; Cowan, G.H.; Ziegler, A.; Savenkov, E.I. Unusual long-distance movement strategies of potato mop-top virus RNAs in *Nicotiana benthamiana*. *Mol. Plant Microbe Interact.* **2009**, *22*, 381–390. [CrossRef] [PubMed]
94. Savenkov, E.I.; Germundsson, A.; Zamyatnin, A.A., Jr.; Sandgren, M.; Valkonen, J.P.T. Potato mop-top virus: The coat protein-encoding RNA and the gene for cysteine-rich protein are dispensable for systemic virus movement in *Nicotiana benthamiana*. *J. Gen. Virol.* **2003**, *84*, 1001–1005. [CrossRef] [PubMed]
95. Wright, K.M.; Cowan, G.H.; Lukhovitskaya, N.I.; Tilsner, J.; Roberts, A.G.; Savenkov, E.I.; Torrance, L. The N-terminal domain of PMTV TGB1 movement protein is required for nucleolar localization, microtubule association, and long-distance movement. *Mol. Plant Microbe Interact.* **2010**, *23*, 1486–1497. [CrossRef] [PubMed]
96. Kim, S.H.; Macfarlane, S.; Kalinina, N.O.; Rakitina, D.V.; Ryabov, E.V.; Gillespie, T.; Haupt, S.; Brown, J.W.; Taliansky, M. Interaction of a plant virus-encoded protein with the major nucleolar protein fibrillarin is required for systemic virus infection. *Proc. Natl. Acad. Sci. USA* **2007**, *104*, 11115–11120. [CrossRef] [PubMed]
97. Busch, A.; Richter, A.S.; Backofen, R. Intarna: Efficient prediction of bacterial sRNA targets incorporating target site accessibility and seed regions. *Bioinformatics* **2008**, *24*, 2849–2856. [CrossRef] [PubMed]
98. Wright, P.R.; Georg, J.; Mann, M.; Sorescu, D.A.; Richter, A.S.; Lott, S.; Kleinkauf, R.; Hess, W.R.; Backofen, R. Coprarna and intarna: Predicting small RNA targets, networks and interaction domains. *Nucleic Acids Res.* **2014**, *42*, W119–W123. [CrossRef] [PubMed]
99. Sandgren, M.; Savenkov, E.I.; Valkonen, J.P. The readthrough region of potato mop-top virus (PMTV) coat protein encoding RNA, the second largest RNA of PMTV genome, undergoes structural changes in naturally infected and experimentally inoculated plants. *Arch. Virol.* **2001**, *146*, 467–477. [CrossRef] [PubMed]
100. Dall'Ara, M.; (University of Bologna, Bologna, Italy); Ratti, C.; (University of Bologna, Bologna, Italy); Bouzoubaa, S.E.; (University of Strasbourg, Strasbourg, France); Gilmer, D.; (University of Strasbourg, Strasbourg, France). Personal communication, 2016.
101. Iranzo, J.; Manrubia, S.C. Evolutionary dynamics of genome segmentation in multipartite viruses. *Proc. Biol. Sci.* **2012**, *279*, 3812–3819. [CrossRef] [PubMed]
102. Lu, M.J.; Henning, U. Superinfection exclusion by T-even-type coliphages. *Trends Microbiol.* **1994**, *2*, 137–139. [CrossRef]
103. Roy, N.; Pacini, G.; Berlioz-Torrent, C.; Janvier, K. Mechanisms underlying HIV-1 Vpu-mediated viral egress. *Front. Microbiol.* **2014**, *5*, 177. [CrossRef] [PubMed]
104. Tromas, N.; Zwart, M.P.; Lafforgue, G.; Elena, S.F. Within-host spatiotemporal dynamics of plant virus infection at the cellular level. *PLoS Genet.* **2014**, *10*, e1004186. [CrossRef] [PubMed]
105. Mahmood, T.; Rush, C. Evidence of cross-protection between beet soilborne mosaic virus and beet necrotic yellow vein virus in sugar beet. *Plant Dis.* **1999**, *83*, 521–526. [CrossRef]
106. Ratti, C.; Hleibieh, K.; Bianchi, L.; Schirmer, A.; Autonell, C.R.; Gilmer, D. Beet soil-borne mosaic virus RNA-3 is replicated and encapsidated in the presence of BNYVV RNA-1 and -2 and allows long distance movement in *Beta macrocarpa*. *Virology* **2009**, *385*, 392–399. [CrossRef] [PubMed]

4. Aim of the study

The aim of this study is to investigate fundamental aspects of *Benyviridae* lifestyle related to its multipartite structure. I proposed to evaluate and validate some aspects of a proposed model involving RNA/RNA interactions regulating the viral cycle and a conservation of genomic integrity during the viral spread in the host. In this model, a specific network of RNA/RNA interactions is suspected to determine the recognition and mobilization of each genomic RNA in a modular RNP complex that represents the mobile infectious unit for BNYVV spread in the plant [59].

In Chapter I, I explored one of the main benefits of having a split genome: the capacity for BNYVV to adapt to different infection conditions by the differential accumulation of its genomic segments. For this purpose, I optimized and validated a dual step Digital droplets (dd) RT-PCR protocol to verify if BNYVV stabilizes the ratio between its genomic RNAs in set-point genomic formulas. These experiments were conducted in different infected hosts (*C. quinoa*, *S. oleracea* and *B. macrocarpa*) and organs (leaves and roots), comparing total and encapsidated genomic RNAs, the latter corresponding to the transmissible form of the virus.

To date, the viral movement across the plant is described as an uncoordinated trafficking of particles or RNP complexes [60]. However, the differential accumulation of BNYVV vRNAs within the infected tissues could require unsustainable costs to preserve viral genomic integrity, ensuring in each infected cell the presence of a complete set of viral segments. This lead to the formulation of two opposed hypotheses:

1. BNYVV segments may not necessarily be present “all together” in each infected cells and RNA replication and stabilization are ensured by the trafficking of viral protein that takes advantage of the symplastic continuity.
2. A specific mechanism guarantees the coordinated movement of each segment as infective units.

To assess one or the other hypothesis, in Chapter II, I reported the experiments performed to test for a simultaneous presence of the four genomic BNYVV RNAs within each infected cell. For this purpose, I optimized a protocol of Real-Time RT-PCR on single protoplast isolated from systemically infected *S. oleracea*.

Finally, in Chapter III, I searched for the existence of RNA1 and RNA2 interactions that would explain the long distance movement of these essential RNAs. Indeed, RNA1 and RNA2 are sufficient for productive infection in the entire plant and therefore represent a minimal efficient RNP complex stabilized by their interaction. *In silico* and *in vitro* experiments have been exploited to establish if any interaction occurs and determine the domains in the interactions. The biological relevance of the interactions has been tested by reverse genetic experiments.

4. References

1. Baltimore, D. Expression of animal virus genomes. *Bacteriol. Rev.* **1971**, *35*, 235–241.

2. Gilmer, D.; Ratti, C.; ICTV Report Consortium ICTV Virus Taxonomy Profile: Benyviridae. *J. Gen. Virol.* **2017**, *98*, 1571–1572, doi:10.1099/jgv.0.000864.

3. Koenig, R.; Lesemann, D. E. Beet necrotic yellow vein virus. In *Encyclopedia of Microbiology, (4 Volume Set)*; Elsevier, 2000; pp. 422–429 ISBN 9780080548487.

4. Torrance, L.; Mayo, M. A. Proposed re-classification of furoviruses. *Arch. Virol.* **1997**, *142*, 435–439.

5. Lapierre, H.; Signoret, P. A. Viruses and virus diseases of Poaceae (Gramineae). *Viruses virus Dis. Poaceae (Gramineae).* **2004**.

6. Steven, A. C.; Trus, B. L.; Putz, C.; Wurtz, M. The molecular organization of beet necrotic yellow vein virus. *Virology* **1981**, *113*, 428–438, doi:10.1016/0042-6822(81)90172-0.

7. Tamada, T.; Kondo, H.; Chiba, S. Genetic Diversity of Beet Necrotic Yellow Vein Virus. In *Rhizomania*; Springer International Publishing: Cham, 2016; pp. 109–131.

8. Chiba, S.; Kondo, H.; Miyanishi, M.; Andika, I. B.; Han, C.; Tamada, T. The Evolutionary History of Beet necrotic yellow vein virus Deduced from Genetic Variation , Geographical Origin and Spread , and the Breaking of Host Resistance. *Mol. Plant-Microbe Interact.* **2011**, *24*, 207–218, doi:10.1094/MPMI-10-10-0241.

9. Schirmer, A.; Link, D.; Cognat, V.; Moury, B.; Beuve, M.; Meunier, A.; Bragard, C.; Gilmer, D.; Lemaire, O. Phylogenetic analysis of isolates of Beet necrotic yellow vein virus collected worldwide. *J. Gen. Virol.* **2005**, *86*, 2897–2911, doi:10.1099/vir.0.81167-0.

10. Tamada, T.; Asher, M. J. C. The Plasmodiophorid Protist Polymyxa betae. In *Rhizomania*; Springer International Publishing: Cham, 2016; pp. 135–153.

11. Peltier, C.; Hleibieh, K.; Thiel, H.; Klein, E.; Bragard, C.; Gimer, D. Molecular Biology of the Beet necrotic yellow vein virus. *Plant Viruses* **2008**, *2*, 14–24.

12. Adams, M. J.; Antoniw, J. F.; Mullins, J. G. Plant virus transmission by plasmodiophorid fungi is associated with distinctive transmembrane regions of virus-encoded proteins. *Arch. Virol.* **2001**, *146*, 1139–53.

13. Legrève, A.; Schmit, J. F.; Bragard, C.; Maraite, H. The role and climate and alternative hosts in the epidemiology of rhizomania. In *Sixth Symposium of the International Working Group on Plant Viruses with Fungal Vectors*; Bologna, 2005; pp. 129–132.

14. Tamada, T.; Baba, T. Beet Necrotic Yellow Vein Virus from Rizomania-Affected Sugar Beet in Japan. *Japanese J. Phytopathol.* **1973**, *39*, 325–332_1, doi:10.3186/jjphytopath.39.325.

15. Canova, A. Appunti di patologia della barbabietola. *Inf. Fitopatol.* **1959**, *9*, 390–396.

16. Mcgrann, G. R. D.; Grimmer, M. K.; Mutasa-Göttgens, E. S.; Stevens, M. Progress towards the understanding and control of sugar beet rhizomania disease. *Mol. Plant Pathol.* **2009**, *10*, 129–141, doi:10.1111/j.1364-3703.2008.00514.x.

17. Delbianco, A. Molecular mechanisms involved in the pathogenesis of beet soil-borne viruses, University of Strasbourg, 2013.

18. Lauber, E.; Guilley, H.; Tamada, T.; Richards, K. E.; Jonard, G. Vascular movement of beet necrotic yellow vein virus in Beta macrocarpa is probably dependent on an RNA 3 sequence domain rather than a gene product. *J. Gen. Virol.* **1998**, *79*, 385–393, doi:10.1099/0022-

1317-79-2-385.

19. Andika, I. B.; Kondo, H.; Tamada, T. Evidence That RNA Silencing-Mediated Resistance to *Beet necrotic yellow vein virus* Is Less Effective in Roots Than in Leaves. *Mol. Plant-Microbe Interact.* **2005**, *18*, 194–204, doi:10.1094/MPMI-18-0194.

20. Schmidlin, L.; Link, D.; Mutterer, J.; Guilley, H.; Gilmer, D. Use of a Beet necrotic yellow vein virus RNA-5-derived replicon as a new tool for gene expression. *J. Gen. Virol.* **2005**, *86*, 463–467, doi:10.1099/vir.0.80720-0.

21. Guilley, H.; Bortolamiol, G.; Jonard, G.; Bouzoubaa, S.; Ziegler-Graff, V. Rapid screening of RNA silencing suppressors by using a recombinant virus derived from beet necrotic yellow vein virus. *J. Gen. Virol.* **2009**, *90*, 2536–2541, doi:10.1099/vir.0.011213-0.

22. Flobinus, A.; Chevigny, N.; Charley, P.; Seissler, T.; Klein, E.; Bleykasten-Grosshans, C.; Ratti, C.; Bouzoubaa, S.; Wilusz, J.; Gilmer, D. Beet Necrotic Yellow Vein Virus Noncoding RNA Production Depends on a 5′→3′ Xrn Exoribonuclease Activity. *Viruses* **2018**, *10*, 137, doi:10.3390/v10030137.

23. Bouzoubaa, S.; Quillet, L.; Guilley, H. Nucleotide sequence of beet necrotic yellow vein virus RNA-1. *J. Gen. Virol.* **1987**, *68*, 615–626, doi:10.1099/0022-1317-68-3-615.

24. Bouzoubaa, S.; Scheidecker, D. Infection of protoplasts with beet necrotic yellow vein virus RNA. *Proc. First Symp. Int. Work. Gr. Plant Viruses with Fungal Vectors, Braunschweig, Ger.* **1990**, 45–48.

25. Hehn, A.; Fritsch, C.; Richards, K. E.; Guilley, H.; Jonard, G. Evidence for in vitro and in vivo autocatalytic processing of the primary translation product of beet necrotic yellow vein virus RNA 1 by a papain-like proteinase. *Arch. Virol.* **1997**, *142*, 1051–8.

26. Pakdel, A.; Mounier, C.; Klein, E.; Hleibieh, K.; Monsion, B.; Mutterer, J.; Erhardt, M.; Bouzoubaa, S.; Ratti, C.; Gilmer, D. On the interaction and localization of the beet necrotic yellow vein virus replicase. *Virus Res.* **2015**, *196*, 94–104, doi:10.1016/J.VIRUSRES.2014.11.001.

27. Gilmer, D. Molecular Biology and Replication of Beet Necrotic Yellow Vein Virus. In *Rhizomania*; Springer International Publishing: Cham, 2016; pp. 85–107.

28. Bouzoubaa, S.; Ziegler-Graff, V.; Beck, D.; Guilley, H.; Richards, K.; Jonard, G. Nucleotide Sequence of Beet Necrotic Yellow Vein Virus RNA-2. *J. Gen. Virol.* **1986**, *67*, 1689–1700, doi:10.1099/0022-1317-67-8-1689.

29. Ziegler-Graff, V.; Richards, K.; Guilley, H.; Jonard, G.; Putz, C. Cell-free Translation of Beet Necrotic Yellow Vein Virus: Readthrough of the Coat Protein Cistron. *J. Gen. Virol.* **1985**, *66*, 2079–2087, doi:10.1099/0022-1317-66-10-2079.

30. Erhardt, M.; Dunoyer, P.; Guilley, H.; Richards, K.; Jonard, G.; Bouzoubaa, S. Beet Necrotic Yellow Vein Virus Particles Localize to Mitochondria during Infection. *Virology* **2001**, *286*, 256–262, doi:10.1006/viro.2001.0931.

31. Tamada, T.; Schmitt, C.; Saito, M.; Guilley, H.; Richards, K.; Jonard, G. High resolution analysis of the readthrough domain of beet necrotic yellow vein virus readthrough protein: a KTER motif is important for efficient transmission of the virus by Polymyxa betae. *J. Gen. Virol.* **1996**, *77*, 1359–1367, doi:10.1099/0022-1317-77-7-1359.

32. Gilmer, D.; Bouzoubaa, S.; Hehn, A.; Guilley, H.; Richards, K.; Jonard, G. Efficient cell-to-cell movement of beet necrotic yellow vein virus requires 3′ proximal genes located on RNA 2. *Virology* **1992**, *189*, 40–47, doi:10.1016/0042-6822(92)90679-J.

33. Bleykasten, C.; Gilmer, D.; Guilley, H.; Richards, K. E.; Jonard, G. Beet necrotic yellow vein virus 42 kDa triple gene block protein binds nucleic acid in vitro. *J. Gen. Virol.* **1996**, *77*, 889–897, doi:10.1099/0022-1317-77-5-889.

34. Lauber, E.; Bleykasten-Grosshans, C.; Erhardt, M.; Bouzoubaa, S.; Jonard, G.; Richards, K. E.; Guilley, H. Cell-to-cell movement of beet necrotic yellow vein virus: I. Heterologous complementation experiments provide evidence for specific interactions among the triple gene block proteins. *Mol. plant-microbe Interact.* **1998**, *11*, 618–625.

35. Verchot-Lubicz, J.; Torrance, L.; Solovyev, A. G.; Morozov, S. Y.; Jackson, A. O.; Gilmer, D. Varied movement strategies employed by triple gene block-encoding viruses. *Mol. plant-microbe Interact.* **2010**, *23*, 1231–1247, doi:10.1094/MPMI-04-10-0086.

36. Erhardt, M.; Vetter, G.; Gilmer, D.; Bouzoubaa, S.; Richards, K.; Jonard, G.; Guilley, H. Subcellular localization of the Triple Gene Block movement proteins of Beet necrotic yellow vein virus by electron microscopy. *Virology* **2005**, *340*, 155–166,

doi:10.1016/J.VIROL.2005.06.012.

37. Erhardt, M.; Morant, M.; Ritzenthaler, C.; Stussi-Garaud, C.; Guilley, H.; Richards, K.; Jonard, G.; Bouzoubaa, S.; Gilmer, D. P42 movement protein of Beet necrotic yellow vein virus is targeted by the movement proteins P13 and P15 to punctate bodies associated with plasmodesmata. *Mol. Plant-Microbe Interact.* **2000**, *13*, 520–528, doi:10.1094/MPMI.2000.13.5.520.

38. Jackson, A. O.; Lim, H.-S.; Bragg, J.; Ganesan, U.; Lee, M. Y. Hordeivirus Replication, Movement, and Pathogenesis. *Annu. Rev. Phytopathol.* **2009**, *47*, 385–422, doi:10.1146/annurev-phyto-080508-081733.

39. Bleykasten-Grosshans, C.; Guilley, H.; Bouzoubaa, S.; Richards, K. E.; Jonard, G. Independent Expression of the First Two Triple Gene Block Proteins of Beet Necrotic Yellow Vein Virus Complements Virus Defective in the Corresponding Gene but Expression of the Third Protein Inhibits Viral Cell-to-Cell Movement. *Mol. Plant-Microbe Interact.* **1997**, *10*, 240–246, doi:10.1094/MPMI.1997.10.2.240.

40. Chiba, S.; Hleibieh, K.; Delbianco, A.; Klein, E.; Ratti, C.; Ziegler-Graff, V.; Bouzoubaa, S.; Gilmer, D. The benyvirus RNA silencing suppressor is essential for long-distance movement, requires both zinc-finger and NoLS basic residues but not a nucleolar localization for its silencing-suppression activity. *Mol. Plant-Microbe Interact.* **2013**, *26*, 168–181, doi:10.1094/MPMI-06-12-0142-R.

41. Flobinus, A.; Hleibieh, K.; Klein, E.; Ratti, C.; Bouzoubaa, S.; Gilmer, D. A Viral Noncoding RNA Complements a Weakened Viral RNA Silencing Suppressor and Promotes Efficient Systemic Host Infection. *Viruses* **2016**, *8*, 272, doi:10.3390/v8100272.

42. Bouzoubaa, S.; Guilley, H.; Jonard, G. Nucleotide sequence analysis of RNA-3 and RNA-4 of beet necrotic yellow vein virus, isolates F2 and G1. *J. Gen. Virol.* **1985**, *66*, 1553–1564, doi:10.1099/0022-1317-66-7-1553.

43. Koenig, R.; Jarausch, W.; Li, Y.; Commandeur, U.; Burgermeister, W.; Gehrke Luddecke, M. P. Effect of recombinant beet necrotic yellow vein virus with different RNA compositions on mechanically inoculated sugarbeets. *J. Gen. Virol.* **1991**, *72*, 2243–2246, doi:10.1099/0022-1317-72-9-2243.

44. Jupin, I.; Guilley, H.; Richards, K. E.; Jonard, G. Two proteins encoded by beet necrotic yellow vein virus RNA 3 influence symptom phenotype on leaves. *EMBO J.* **1992**, *11*, 479–488, doi:10.1002/J.1460-2075.1992.TB05078.X.

45. Vetter, G.; Hily, J.-M.; Klein, E.; Schmidlin, L.; Haas, M.; Merkle, T.; Gilmer, D. Nucleo-cytoplasmic shuttling of the beet necrotic yellow vein virus RNA-3-encoded p25 protein. *J. Gen. Virol.* **2004**, *85*, 2459–2469, doi:10.1099/vir.0.80142-0.

46. Haeberle, A. M.; Stussi-Garaud, C. In situ localization of the non-structural protein P25 encoded by beet necrotic yellow vein virus RNA 3. *J. Gen. Virol.* **1995**, *76*, 643–650, doi:10.1099/0022-1317-76-3-643.

47. Chiba, S.; Miyanishi, M.; Andika, I. B.; Kondo, H.; Tamada, T. Identification of amino acids of the beet necrotic yellow vein virus p25 protein required for induction of the resistance response in leaves of Beta vulgaris plants. *J. Gen. Virol.* **2008**, *89*, 1314–1323, doi:10.1099/vir.0.83624-0.

48. Peltier, C.; Schmidlin, L.; Klein, E.; Taconnat, L.; Prinsen, E.; Erhardt, M.; Heintz, D.; Weyens, G.; Lefebvre, M.; Renou, J.-P.; Gilmer, D. Expression of the Beet necrotic yellow vein virus p25 protein induces hormonal changes and a root branching phenotype in Arabidopsis thaliana. *Transgenic Res.* **2011**, *20*, 443–466, doi:10.1007/s11248-010-9424-3.

49. Klein, E.; Link, D.; Schirmer, A.; Erhardt, M.; Gilmer, D. Sequence variation within Beet necrotic yellow vein virus p25 protein influences its oligomerization and isolate pathogenicity on Tetragonia expansa. *Virus Res.* **2007**, *126*, 53–61, doi:10.1016/j.virusres.2006.12.019.

50. Ratti, C.; Hleibieh, K.; Bianchi, L.; Schirmer, A.; Autonell, C. R.; Gilmer, D. Beet soil-borne mosaic virus RNA-3 is replicated and encapsidated in the presence of BNYVV RNA-1 and -2 and allows long distance movement in Beta macrocarpa. *Virology* **2009**, *385*, 392–399, doi:10.1016/j.virol.2008.12.013.

51. Niesbach-Klösgen, U.; Guilley, H.; Jonard, G.; Richards, K. Immunodetection in Vivo of beet necrotic yellow vein virus-encoded proteins. *Virology* **1990**, *178*, 52–61, doi:10.1016/0042-6822(90)90378-5.

52. Rahim, M. D.; Andika, I. B.; Han, C.; Kondo, H.; Tamada, T. RNA4-encoded p31 of beet

necrotic yellow vein virus is involved in efficient vector transmission, symptom severity and silencing suppresion in roots. *J. Gen. Virol.* **2007**, *88*, 1611–1619, doi:10.1099/vir.0.82720-0.

53. Kiguchi, T.; Saito, M.; Tamada, T. Nucleotide sequence analysis of RNA-5 of five isolates of beet necrotic yellow vein virus and the identity of a deletion mutant. *J. Gen. Virol.* **1996**, *77*, 575–580, doi:10.1099/0022-1317-77-4-575.

54. Koenig, R.; Haeberlé, A.-M.; Commandeur, U. Detection and Characterization of a Distinct Type of Beet Necrotic Yellow Vein Virus RNA 5 in a Sugarbeet Growing Area in Europe. *Arch. Virol.* **1997**, *142*, 1499–1504, doi:10.1007/s007050050176.

55. Link, D.; Schmidlin, L.; Schirmer, A.; Klein, E.; Erhardt, M.; Geldreich, A.; Lemaire, O.; Gilmer, D. Functional characterization of the Beet necrotic yellow vein virus RNA-5-encoded p26 protein: Evidence for structural pathgenicity determinants. *J. Gen. Virol.* **2005**, *86*, 2115–2125, doi:10.1099/vir.0.80937-0.

56. Covelli, L.; Klein, E.; Gilmer, D. The first 17 amino acids of the beet necrotic yellow vein virus RNA-5-encoded p26 protein are sufficient to activate transcription in a yeast one-hybrid system. *Arch. Virol.* **2009**, *154*, 347–351, doi:10.1007/s00705-008-0306-4.

57. Tamada, T.; Kusume, T.; Uchino, H.; Kiguchi, T.; Saito, M. Evidence that beet necrotic yellow vein virus RNS-5 is involved in symptom development of sugar-beet roots. *Proc. Third Symp. Int. Work. Gr. Plant Viruses with Fungal Vectors, West Park Conf. Centre, Dundee, Scotland, 6-7 August, 1996* 1996, 49–52.

58. Peltier, C.; Klein, E.; Hleibieh, K.; D'Alonzo, M.; Hammann, P.; Bouzoubaa, S.; Ratti, C.; Gilmer, D. Beet necrotic yellow vein virus subgenomic RNA3 is a cleavage product leading to stable non-coding RNA required for long-distance movement. *J. Gen. Virol.* **2012**, *93*, 1093–1102, doi:10.1099/vir.0.039685-0.

59. Dall'Ara, M.; Ratti, C.; Bouzoubaa, S.; Gilmer, D. Ins and Outs of Multipartite Positive-Strand RNA Plant Viruses: Packaging versus Systemic Spread. *Viruses* **2016**, *8*, 228, doi:10.3390/v8080228.

60. Niehl, A.; Heinlein, M. Cellular pathways for viral transport through plasmodesmata. *Protoplasma* **2011**, *248*, 75–99, doi:10.1007/s00709-010-0246-1.

Chapter I

Differential accumulation of BNYVV genomic RNAs during host infection

1. Introduction: benefits for multipartitism

Genomic segmentation of the hereditary material into multiple segments is a common feature for cellular organisms. Despite the heterogeneous distribution of genome types and hosts such as bacteria, animals, plants and fungi, segmentation feature is found in about 13% of all viral genera where genomes are split in two or more segments [1]. Virus infecting animal, bacteria and fungi prevalently co-package their complete set of genomic segments in a single virion or enveloped entity (described as segmented viruses), while plant viruses predominantly adopt the multipartite strategy, separating genomic segments into independent particles [1]. Furthermore 13 out of 20 plant viral families possess species with multipartite genomic organization making multipartitism a noticeable characteristic of plant viruses (ibid). This brought scientists to investigate the possible benefits for multipartite viruses and host specialization. Having small sized segments rather than one large genomic nucleic acid could represent the main advantage since replication of shorter genomes is, in theory, faster and present a higher fidelity rate [2,3]. However, competition experiments in cell culture between monopartite and "spontaneous bipartite form" of *foot and mouth disease virus* [4] evidenced fitness advantages for the segmented variant. This fitness was linked to the higher particle thermal stability rather than a faster kinetics of RNA synthesis. Moreover, a sufficiently high multiplicity of infection (MOI) in transmission was seen as a requirement for persistence [5]. Split genomes in complementary modules could also confer to co-infecting similar viruses, a reassortment capacity, that led to the selection of chimerical progeny with potential fitness advantages [6]. Segment exchanges represents also supplementary ways to counteract the effect of deleterious mutations [7].

If the above mentioned benefits are still under argumentation [8] and referred as well to segmented viruses, two recent studies on multipartite viruses have shown that, during host infection, relative frequencies of encapsidated genomic fragments converge to a set point genomic formulas

(SGF)[9,10]. The distinct particles accumulate differentially, with some segments more abundant than others. The resulted ratio seems to be adaptive to the infected host suggesting that partition have evolved to regulate gene expression in different contexts. Viruses selected for these studies were the nanoviridae *faba bean necrotic stunt virus* (FBNSV) [9] and the bromoviridae *alfalfa mosaic virus* (AMV) [10]. Both viruses are transmitted by animal vector (aphid) like 60% of multipartite virus genera [1], but represent two different model of multipartitism. With eight circular single stranded DNAs (ssDNAs), FBNSV has the largest number of genomic segments among multipartite plant viruses but such genome type is common only within 9% of multipartite genera [1] (Table 1). On the contrary, AMV possesses a tripartite positive sense single stranded RNA (ssRNA (+)) genome; an organization conserved within 74% of plant multipartite genera (ibid). However, bromoviridae genome organization is characterized by the distribution of essential housekeeping genes among all three segments and has no equivalent with other multipartite plant viruses except for *Hordeivirus* and *Pomovirus* (*Virgaviridae*) [1]. Interestingly, *Potato mop top virus*, the type member of Pomoviruses, is able to move cell to cell and long distance in *Nicotiana benthamiana* plants in the absence of the genomic RNA segment encoding structural proteins (major and minor CP) [11]. Multipartite plant viruses with a ssRNA(+) genome mainly present the segregation of housekeeping genes in two essential segments and, when present, extra segments carry so-called “unessential” genes linked to host or vector related functions usually needed to optimize the infection [1]. The *beet necrotic yellow vein virus* (BNYVV), which belongs to the *Benyviridae* family, is a representative member of this group of viruses and has the highest number of genomic RNAs organized in two essential segments and up to three accessory RNAs (Figure 4 in general introduction). RNA1 encodes the viral replicase, while RNA2 directs the synthesis of the major and minor capsid proteins (CP an p75) of the rod-shaped particles. Thanks to the synthesis of sub-genomic RNAs, the proteins required for the cell-to-cell movement (triple gene block, TGB) and the suppression of host posttranscriptional gene silencing (p14) are produced. The RNA3 species is involved in the long-distance movement and encodes the pathogenic determinant of the

Rhizomania disease on sugar beet (p25) while RNA4 is involved, together with the encapsidation process, in the efficiency of virus transmission by the soil-borne vector *Polymyxa betae*. When present, the RNA5 is responsible of the symptoms worsening [12].

Family (multipartite genera/total)	Genome type	Capsid	Segments
***Nanoviridae* (3/3)**	Circular ssDNA	Icosahedral	6_8
***Geminiviridae* (1/9)**	Circular ssDNA	Twinned icosahedral	2 or 1 and satellite
***Luteoviridae* (1/3)**	ssRNA (+)	Icosahedral	2
***Secoviridae* (6/9)**	ssRNA (+)	Icosahedral	2
***Tombusviridae* (2/16)**	ssRNA (+)	Icosahedral	2
***Benyviridae* (1/1)**	ssRNA (+)	rod-shaped	2,4_5
***Virgaviridae* (6/7)**	ssRNA (+)	rod-shaped	2_3
***Bromoviridae* (6/6)**	ssRNA (+)	Icosahedral and bacilliform	3
***Closteroviridae* (1/3)**	ssRNA (+)	filamentous	2
***Potyviridae* (5/8)**	ssRNA (+)	filamentous	2
Ourmiavirus, Idaeovirus, Cilevirus, Jingmenvirus	ssRNA (+)	filamentous	2_4
***Ophioviridae* (1/1)**	ssRNA(-)	filamentous	3_4
***Rhabdoviridae* (2/18)**	ssRNA(-)	bullet-shaped and bacilliform	2
Tenuivirus	ssRNA(-)	rod-shaped	4_6
***Partitiviridae* (5/5)**	dsRNA	Icosahedral	2_3

Table 1: List of multipartite phytoviruses among viral families. The number of multipartite genera within total genera members is indicated as well as the nature of the genome, the viral morphology and the number of segments. *Benyviridae* family regroups bipartite species or species having four or five genomic RNAs. List has been drown up with information taken from Lucía-Sanz and Manrubia [1].

Study of the gene copy number variation in a host dependent manner is a newborn aspect for the biology of multipartite viruses and has been investigated for BNYVV. The relative abundance of BNYVV RNAs has been calculated in different plant organs (leaves and roots) of hosts of different genera (*Chenopodium quinoa*, *Spinacea oleracea* and *Beta macrocarpa*) verifying if and how the virus stabilizes the ratio between its genomic segments in a host specific genomic formula (GF). Besides having a different genomic organization and capsid structure when compared to AMV and FBNSV (Table 1), BNYVV possesses different biological proprieties since it is a soil-borne virus transmitted by protozoa. AMV and FBNSV are aphid transmitted viruses and during aphid feeding, these viruses are guaranteed for important viral loads in sieve elements, thanks to the high vector population density and repeated inoculations events. This ensures a maintenance of a viral reservoir and a high MOI required to initiate cell to cell movement in the host from different companion cells

(CCs) [8]. Conversely, BNYVV initial infection occurs after protozoan transmission at a singular cell level. The cytoplasmic fusion between a target rootlet cell and the viruliferous zoospore [13] theoretically permits viral transmission from vector to host with reduced levels of MOI. From such kind of initial infection, the viral amplification takes place and gains adjacent cells before vascular spread of the infectious material in distant tissues. As stated above, GF could be dependent on host and organ and has never been studied for *Benyviridae* family.

In order to calculate the relative accumulation of BNYVV genomic segments in leaves and roots of *C. quinoa*, *S. oleracea* and *B. macrocarpa* a protocol of dual step Droplets digital (dd) RT-PCR has been optimized and validated.

2. Droplet digital (dd) PCR

Digital droplet (dd) PCR is a recently developed innovative technology that allows a precise quantification of target nucleic acids in a sample [14]. Using the same operating principle of conventional PCR methods of specific DNA target amplification, ddPCR differs from standard quantitative (q) PCR for the quantification method of nucleic acids. qPCR analyzes the amplification reaction in real time, following an increase of a fluorescence signal associated to the number of amplicons produced after each PCR cycle. Using standards and calibration curves, qPCR permits the determination of "gene" copy numbers. Similarly, ddPCR uses fluorescence to measure amplicon accumulations, but does not rely on standard curves. PCR reactions are analyzed at end-point within up to 20,000 of 1 nl water-in-oil droplet partitions acting as separated reactions. Therefore in theory, single nucleic acid molecules are dispersed in droplets following a Poisson distribution. The presence of a target nucleic acid gives rise to a single positive amplification event confined in the droplet (high amplitude fluorescence droplet). The ratio between positive and total events is used to determine exactly the copy number of target molecules in a sample (Figure 1). Raw results are statistically corrected after Poisson distribution analyses that calculate the

probability to have one or more molecule target in each positive droplet. Compared to qPCR, ddPCR present obvious advantages and is a reliable method for the absolute quantification of DNA targets in a sample. The direct and absolute counting of target DNA copies per input sample makes dispensable the use of standard curves or endogenous controls. Furthermore, end-point analyses render the method less susceptible to inhibitors that impact qPCR amplification curve by increasing the threshold cycle (CT) [15]. Finally, ddPCR sensitivity is increased for low target DNA quantities represented by a lower coefficient of variation compared to qPCR [16,17].

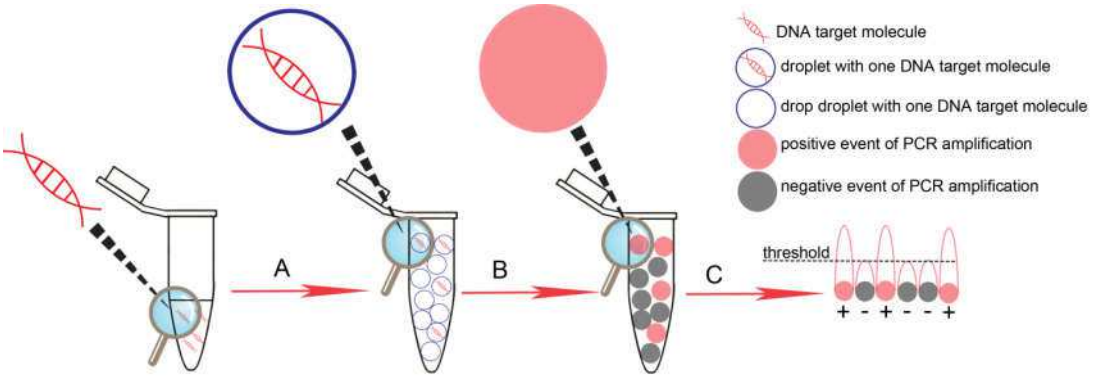

Figure 1 Schematic representation of ddPCR workflow**.** Sample DNA together with ddPCR reaction mix is partitioned by a droplet Generator (QX200™ Bio-Rad) into ~20,000 droplets (A). Template PCR amplification takes place in all droplets through a standard thermocycler (B). Droplet end-point fluorescence is detected in two channels (FAM or HEX) using a droplet reader (QX200™ Bio-Rad) (C). Raw data are analyzed using QuantaSoft software (Bio-Rad) using thresholds lines set manually according to fluorescence amplitude of negative controls. The software assigns a binomial value (positive or negative) for each droplet fluorescence amplitude. Ratio between positive and total droplets and statistical correction according to Poisson distribution, give the number of DNA molecules in the sample.

3. Validation of dual step ddRT-PCR protocol for the absolute quantification of BNYVV genomic RNAs

One of the main constrain of using retro-transcriptase (RT) reaction for a RNA quantification assay is the optimization of the synthesis of a single copy of cDNA for each target RNA molecule. Complex RNA secondary structure or insufficient level of downstream RNase H activity could compromise the equimolar RNA/cDNA conversion leading to misestimate the RNA template copy number. RNA targets and reagent mix partitioning in different droplets makes such aspects

negligible in one step ddRT-PCR where each reaction event effectively assigns one unequivocal fluorescent amplitude for each molecule target. However, since RNA retro-transcription must precede cDNA droplet partitioning to prevent the conversion and the amplification of BNYVV viral complementary RNAs issued from replication intermediates, optimization and validation of the first step of a dual step ddRT-PCR is mandatory. For this reason, standard BNYVV B-type genomic RNAs have been produced and quantified.

3.1 BNYVV Standard production

Standard B type BNYVV RNAs have been produced *in vitro* by run-off transcription of the full length linearized T7 cDNA clone pB214 (RNA2), pB35 (RNA3) and pB45 (RNA4) as described previously [18,19]. Since pB15 (RNA1) [19] run-off transcription produces significant amount of incomplete RNAs due to premature T7 polymerase stops, the last 2,991 nucleotides, have been amplified using 3755F and 6746R specific RNA1 primer (table 2) and GoTaq® Long PCR Master Mix (Promega) and cloned in pGEM®-T Easy Vector (Promega). The resulting *Hin*dIII-linearized plasmid has been *in vitro* transcribed. All enzymatic reactions have been carried out according to manufacturer's protocol. After DNA removal with RQ1 RNase-Free DNase (Promega), RNAs have been purified by phenol/chloroform extraction and NH_4OAc/EtOH precipitation prior analysis by agarose gel electrophoresis and quantification by Qubit™ 3.0 fluorometer (ThermoFisherScientific). Molecular concentration of each transcript has been determined using online calculator tool (www.end-memo.com/bio/dnacopynum.php) and four standard serial dilutions ($4x10^4$; $2x10^4$; $2x10^3$; $2x10^2$ molecules) have been prepared. The combination of all transcripts were mixed with 1ng of a total RNAs extracted from *S. oleracea*, *B. macrocarpa* or *C. quinoa* healthy plants.

RNA	PRIMERS	TAQ-MAN PROBES
1	**3755F**(CGGAAGAACTCGAAAGAAGG) **6746R** (TTTTTTTTTTTTTTATATCAATATACTG)	
1	**3946F** (TGGTTTCACAAGGAGATGTCGTT) **4024R** (TCTGCACAATCAAAGGCATCA)	3944 FAM-TTTTGGACATAGCACGTGTGGAAAACGATA
2	**662F** (TGGACCCGGGATAAATTTGA) **734R** (CGGGTGGACTGGTTCTACCTT)	653 HEX-ACCGGTTCAAATTACCATGGACACCTGTT
3	**54F** (ATATGTGAGGACGCTAGCCTGTT) **172R** (TGAAACGATGGAGTCACTATGCTT)	84 FAM- CTGACCGACCAAATCCAAGCGAGCTTAAT
4	**415F** (TCCTCCTTTGATACGTCATGAAGA) **490R** (CAATGGGCCAATCTCAATCC)	445 HEX-TGATTGTACTGCTAGGATGGTGCA

Table 2 Primers and probes used to amplify and detect BNYVV RNAs. Primers used to clone the 3' portion of BNYVV RNA1 in pGEM®-T Easy Vector (3755F and 6746R) and used for ddRT-PCR experiments are incluced.

3.2 Comparison between one step and dual step ddRT-PCR for the absolute quantification of standards

To quantify BNYVV genomic RNAs, primer and TaqMan probes (labeled with FAM and HEX fluorophores, Table 2) were designed using Primer Express Software v2.0 (Applied Biosystems) avoiding targeting of subgenomic RNA2 and noncoding RNA3 species. Primer specificity was successfully validated by performing dual step ddRT-PCR assays using standard dilutions with or without the specific BNYVV RNA targets as templates. 2 µl of each standard solution template were mixed with 3µl of the following reverse transcriptase mixture:

- 1 µl M-MLV 5X Reverse Transcriptase Reaction Buffer (Promega)
- 0.3 µl dNTPs (10 mM each)
- 0.2 µl M-MLV RT (200U/µl) (Promega)
- 0.5 µl BNYVV Reverse Primer (20 µM)
- 1 µl DNase/RNase free water

Reverse transcription reaction was carried out at 42°C for 1 h prior to the enzyme inactivation at 90°C for 5 min.

To 5 µl of each reverse transcriptase reaction, 15 µl of the following ddPCR mixture was added:

- 10 µl 2x ddPCR Supermix for Probes (Bio-Rad)
- 0.5 µl BNYVV Forward Primer (20 µM)
- 1 µl BNYVV FAM or HEX probe (4 µM)
- 3.5 µl DNase/RNase free water

The ddPCR reactions were carried out after droplet generation. Thermal cycling conditions are described in Table 3.

Step	Cycles	Temperature	Time
Polymerase activation	1	95° C	10 min
Denaturation	40	95° C	30 s
Annealing/Extension		62° C	1 min
Enzyme inactivation	1	95° C	10 min
Holding	1	4°C	∞

Table 3 Thermal cycling conditions used for one step ddRT-PCR reactions. Ramp rate was adjusted to 2°C/sec

Accuracy of dual step ddRT-PCR reactions was tested comparing copy numbers resulting from previous assays, to copy numbers obtained by one step ddRT-PCR using the same standard templates. The latter reaction was performed by mixing 2 µl of each standard solution template with 18 µl of the following ddRT-PCR mixture:

- 5 µl 4x One-Step RT-ddPCR Advanced kit for Probes (Bio-Rad)
- 2 µl Reverse transcriptase 20 U/µl (Bio-Rad)
- 1 µl DTT 300 mM
- 0.5 µl BNYVV Forward Primer (20 µM)
- 0.5 µl BNYVV Reverse Primer (20 µM)
- 1 µl BNYVV FAM or HEX probe (4 µM)
- 8 µl DNase/RNase free water

Thermal cycling conditions are described in Table 4.

Step	Cycles	Temperature	Time
Reverse transcription	1	42° C	30 min
Polymerase activation	1	95° C	10 min
Denaturation	40	95° C	30 s
Annealing/Extension		62° C	1 min
Enzyme inactivation	1	95° C	10 min
Holding	1	4°C	∞

Table 4 Thermal cycling conditions of one step ddRT-PCR. Ramp rate is adjusted to 2°C/sec

Data analysis was interpolated in two dimensions scatter plots for each BNYVV RNA having in ordinate axis one step ddRT-PCR and in abscissa axis dual step ddRT-PCR absolute quantifications

of RNA standards serial dilutions quantified by Qubit™ 3.0 . As shown in figure 2, best fit lines were linear ($R^2 > 0.99$) over standard range covering three order of magnitude with slopes ranging from 0.952 to 0.980 indicating a low error rate when one step ddRT-PCR absolute RNA quantification is compared with that of dual step ddRT-PCR. Relevant copy number underestimations (RNA1 and RNA2) comparing to Qubit quantification have been associated to the RNA degradation rate of "non-certified" standard used. Taken together these data indicate that retro-transcriptase events in dual step ddRT-PCR gave equimolar RNA/cDNA conversion for BNYVV RNAs.

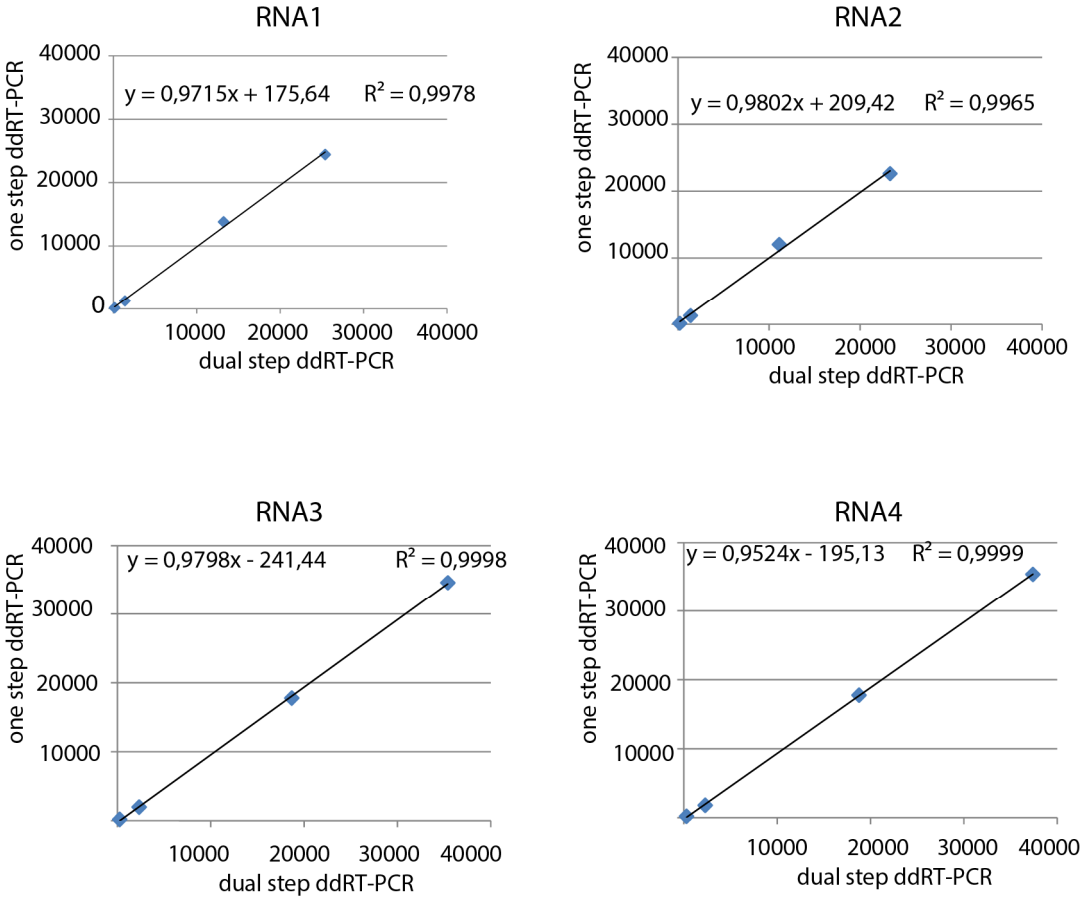

Figure 2 Scatter plots having in ordinate axis one step ddRT-PCR and in abscissa dual step ddRT-PCR absolute RNA quantifications of standard serial dilutions quantified by Qubit™ 3.0. For each BNYVV RNAs, absolute quantification scatter plot is reported as well as best fit lines and R^2 values.

3.3 Optimization of dual step ddRT-PCR for the quantification of BNYVV RNA1 to 4

Duplex dual step ddRT-PCR reactions for the RNA1 and RNA2 or RNA3 and RNA4 simultaneous absolute quantifications have been optimized. The following mixtures of retro-transcriptase and

ddPCR reactions have been conducted using the same thermal cycling condition described for single dual step ddRT-PCR:

Retro-transcriptase mixture:

- 1 µl M-MLV 5X Reverse Transcriptase Reaction Buffer (Promega)
- 0.3 µl dNTPs (10 mM each)
- 0.2 µl M-MLV RT (200U/µl) (Promega)
- 0.5 µl BNYVV1 or BNYVV3 Reverse Primer (20µM)
- 0.5 µl BNYVV2 or BNYVV4 Reverse Primer (20µM)
- 0.5 µl DNase/RNase free water
- 2 µl standard solution template

ddPCR mixture:

- 10 µl 2x ddPCR Supermix for Probes (Bio-Rad)
- 0.5 µl BNYVV1 or BNYVV3 Forward Primer (20µM)
- 0.5 µl BNYVV2 or BNYVV4 Forward Primer (20µM)
- 1 µl BNYVV1 or BNYVV3 FAM probe (4µM)
- 1 µl BNYVV2 or BNYVV4 HEX probe (4µM)
- 2 µl DNase/RNase free water

Recorded FAM and HEX fluorescence amplitudes of corresponding probes have been reported in a scatter plot where negative and positive droplets are distributed into four distinct groups: negative, FAM-positive, HEX-positive and positive droplets for both channels FAM and HEX. Results obtained from duplex RNA1 and RNA2 reaction shown clearly distinct and analyzable groups, while a non specific HEX signal from RNA3 FAM probe, prevents discrimination between the negative droplets and HEX positive droplets in RNA3 and RNA4 duplex reaction (Figure 3). For this reason absolute quantification of BNYVV RNA3 and RNA4 have been carried out using two independent reaction of dual step ddRT-PCR allowing a clear differentiation between negative and FAM or HEX positive droplets (Figure 4).

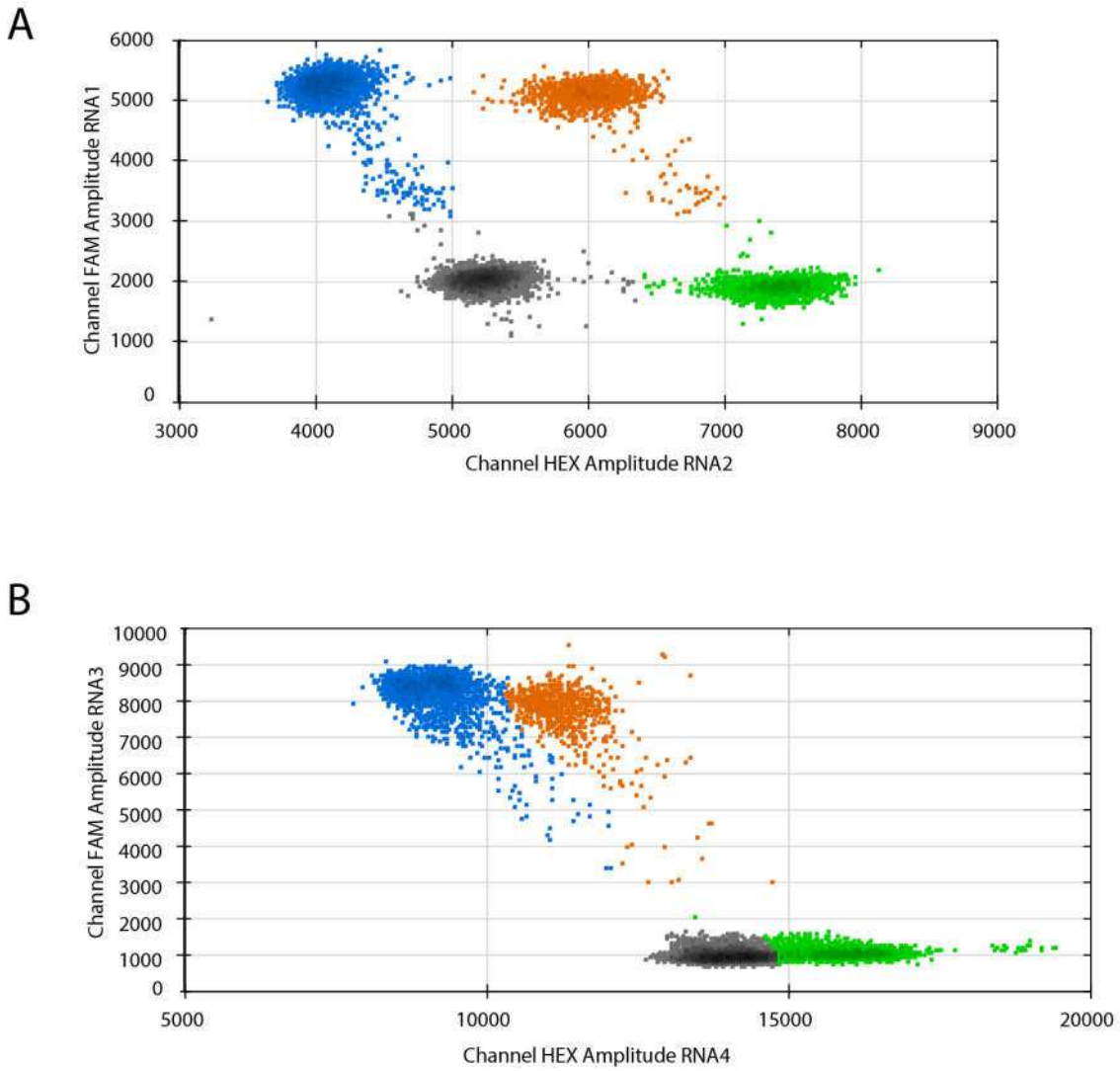

Figure 3 Duplex dual step dd-RTPCR scatter plots for the simultaneous quantification of BNYVV RNA1 and RNA2 (A) or RNA3 and RNA4 (B). Ordinate and abscissa axis report FAM and HEX amplitude signal respectively. Each dot represents one droplets reaction and colors define the kind of positivity assigned. Black dots represent negative reactions, blue dots positive reaction for RNA targeted by FAM probes, green dots positive reaction for RNA targeted by HEX probes and orange dots are positive reactions for both target RNAs. Duplex RNA1 and RNA2 reaction dots forms four distinct and clearly analyzable groups, while unspecific HEX signals from RNA3 FAM probe, prevent discrimination between the negative droplets and HEX positive droplets in RNA3 and RNA4 duplex reaction.

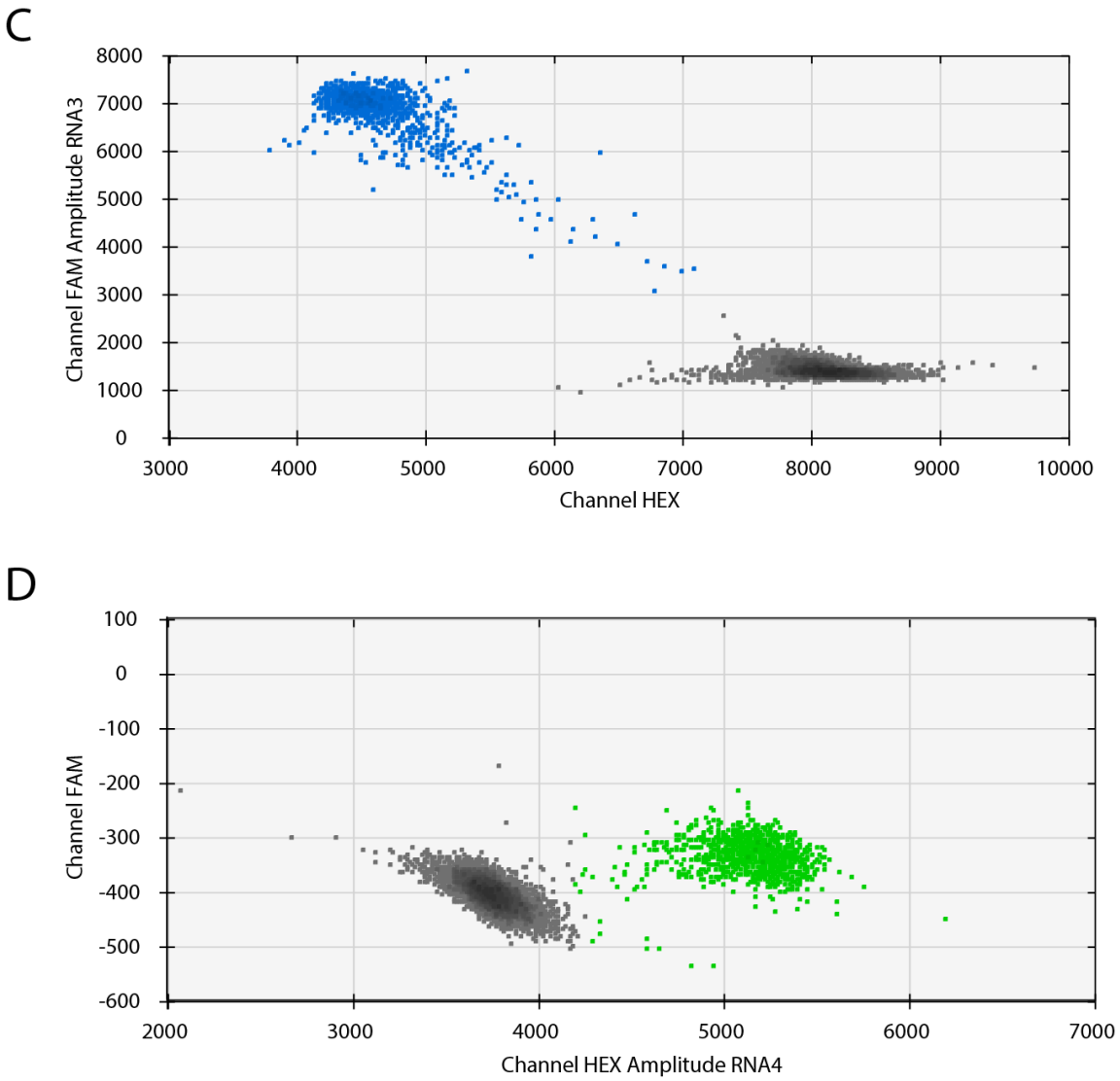

Figure 4 Dual step dd-RTPCR scatter plots for the quantification of BNYVV RNA3 (A) and RNA4 (B). Dots representing positive amplification reaction of RNA3 (blue) and RNA4 (green) cluster in groups sufficiently distinguishable from groups of negative droplets (black dots).

3.4 Host species and virus inoculation

B. macrocarpa, S. *oleracea* cv. Viking and *C. quinoa* have been chosen as experimental host. *B. macrocarpa* and *S. oleracea* have been infected by agro-infiltration with four agrobacteria, each containing one of the four plasmid allowing *in vivo* expression of infectious B type BNYVV RNA as described previously [20]. Mixture of bacterial suspension adjusted to OD_{600} = 0.3 in MA buffer (10 mM $MgCl_2$, 200 mM acetosyringone) have been syringe-inoculated on two true leaves of *B. macrocarpa* and *S. oleracea* seedlings. *C. quinoa* is not a susceptible host for agro- inoculation [21]

, therefore adult plant leaves were rub-inoculated with sap issued from a 3 day-old post inoculation (d.p.i.) agro-infected leaf of *S. oleracea.*

3.5 Total and encapsidated RNA extraction and preparation of samples for dual step ddRT-PCR

Two leaf discs (1 cm Ø) or root tissues (200 mg) have been collected from four infected *B. macrocarpa* and *S. oleracea* plants while four single local lesions have been selected from *C. quinoa* leaves. In particular, leaves and roots samples have been collected 3 weeks p.i. from symptomatic systemic *B. macrocarpa* and *S. oleracea* and 7 d.p.i. from *C. quinoa* inoculated leaves. Samples have been homogenized in 600µl of cold TM buffer (Tris 100mM, $MgCl_2$ 10mM, pH 7.5) and total RNA has been immediately purified by phenol/chloroform extraction and NaOAc/EtOH precipitation from half of the homogenate. Nuclease protected RNAs corresponding to encapsidated viral RNA has been purified following the Jupin et al. protocol [22], by extracting and precipitating the remaining homogenate after 1h of incubation at 37°C to allow vacuolar nuclease digestion of unprotected RNAs. Pellets have been resuspended in 50 µl of DNase/RNase free water and purified RNAs quantified with Qubit™ 3.0 fluorometer (ThermoFisherScientific). Dilutions were adjusted to analyze ~ 2 ng of *B. macrocarpa* and *S. oleracea* RNAs and ~ 0.4 ng of *C. quinoa* RNAs.

4. Results

RNA copy number for each segment has been converted into relative frequency by dividing its value with the sum of all quantified genomic RNAs of the sample (Figure 5). BNYVV GF in the different hosts and organs has been determined by dividing the mean of relative frequency for each segment by the mean of relative frequency of the less abundant RNA (RNA2). GF values have been rounded to the nearest tenth. One-way analysis of variance (ANOVA) has been used to compare the mean of frequency values of genomic RNAs within categories such as host type, organ type (leaves or roots) for each kind of RNA extraction protocol (total or encapsidated). Differences between

segment abundances were considered significant when P values were <0.05 (table 5). Furthermore, significant homogeneous group of segment accumulation have been considered using Tukey HSD pair tests (Figure 5) while significant difference in the frequency of the segments between the two types of RNA extraction have been evaluated using Student's t-test.

	LEAVES/LESIONS		ROOTS	
	Total RNA	Encapsidated RNA	Total RNA	Encapsidated RNA
B. macrocarpa	$F_{3,12}$ = 21.219; P = $4.3*e^{-5}$	$F_{3,12}$ = 45.613; P = $7.8*e^{-7}$	$F_{3,12}$ = 44.170; P = $9.26*e^{-7}$	$F_{3,12}$ = 5.000; P= 0.18
S. oleracea	$F_{3,12}$ = 44.773; P = $8,06e^{-7}$	$F_{3,12}$ = 17,180; P = $1,02*10^{-4}$	$F_{3,12}$ = 17,612; P = $1*10^{-4}$	$F_{3,12}$ = 39.985; P = $1,59e^{-6}$
C. quinoa	$F_{3,12}$ = 101.876; P = $8,38e^{-9}$	$F_{3,12}$ = 134,139; P = $1,70*e^{-9}$		

Table 5: one-way ANOVA analyses were performed to estimate the significant difference between relative frequency within total or encapsidated RNAs from *B. macrocarpa*, or *S. oleracea* leaves and roots and total or encapsidated RNA from *C. quinoa* local lesions. One Way ANOVA were determined by SPSS 15.0 software. F(x,y) correspond to the Fisher distribution where x and y refer to the degree of freedom between group and within group respectively.

As described for FBNSV and AMV [9,10] some genomic segments of the BNYVV appear less abundant than others independently from the organ and the host analyzed. RNA1 and RNA2 represent in most cases a homogeneous group with a mean of relative frequencies that range from ~0.04 to ~0.18 and from ~0.02 to ~0.1 respectively. RNA3 and RNA4 appear, in general, more abundant with mean of relative frequencies ranging from ~0.21 to ~0.57 and from ~0.21 to ~0.65 respectively. The significant variability observed between RNA3 and RNA4 accumulation is noticeable. These RNA species cluster in heterogeneous or homogeneous groups depending on the host, the organ analyzed and the RNA extraction (Figure 5). Significant difference between relative abundances of the same RNA in total and encapsidated RNA extraction have been founded in *S. oleracea* (RNA1 and RNA2 in leaves and RNA3 and RNA4 in roots) and in local lesions of *C. quinoa* (RNA1) but not in *B. macrocarpa* infected plants (Figure 5).

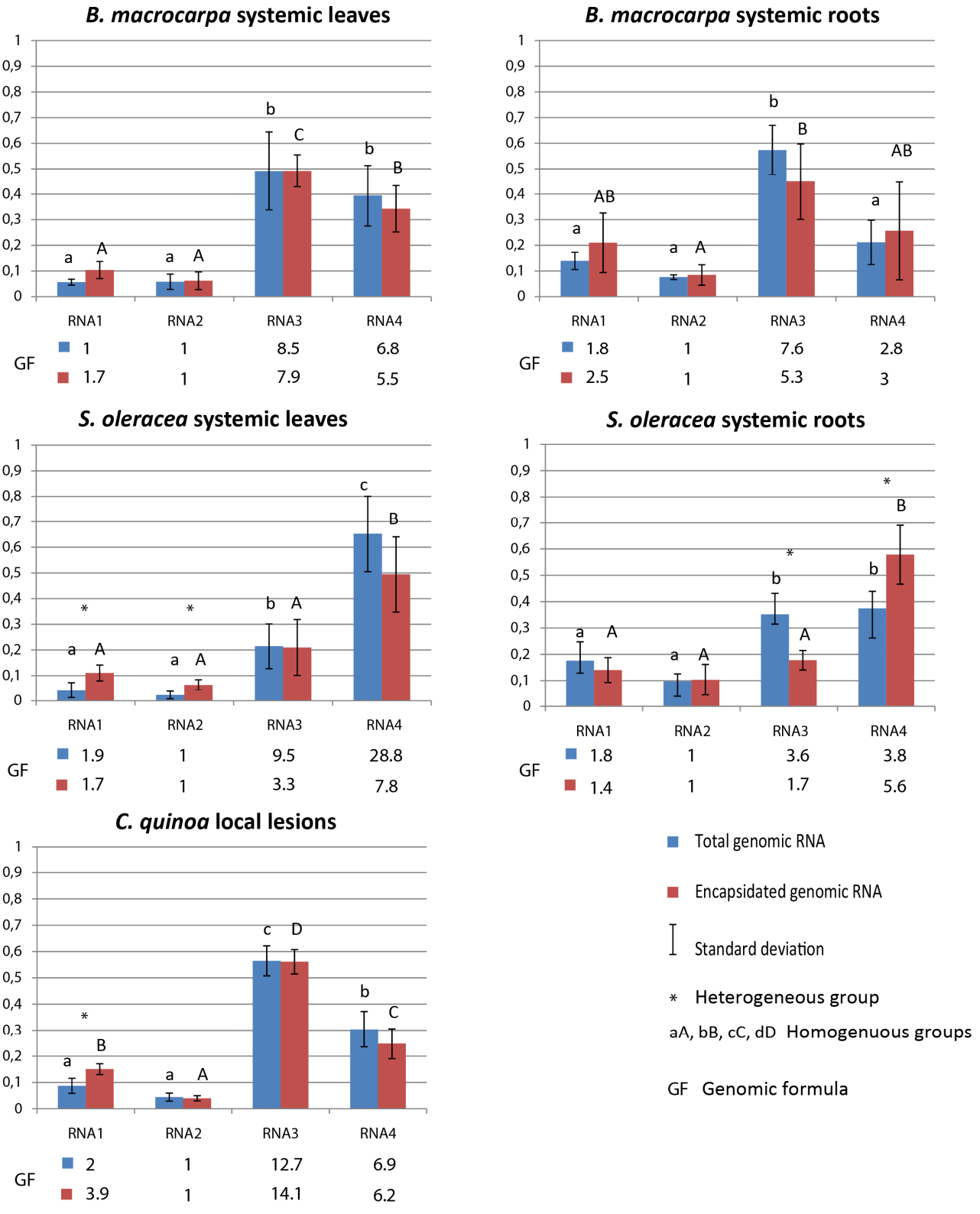

Figure 5 BNYVV genomic RNA relative frequencies evaluated in *B. macrocarpa* or *S. oleracea* leaves and roots or *C. quinoa* local lesions. Blue histograms represent the mean of relative frequencies calculated for total RNA extraction while red histograms represent the mean of frequencies for encapsidated genomic RNA. Bars represent standard deviation. Groups of homogeneity assessed by Tukey HSD pair tests are indicated by letter while significant differences between frequencies of the same RNA in total or encapsidated RNA extractions are indicated with asterisks and have been evaluated with Student's t-test. The genomic formula, calculated by dividing the mean of relative frequency for each segment by the mean of relative frequency of the less abundant RNA (RNA2) is reported under each histogram. One Way ANOVA and Student's t-test were calculated using SPSS 15.0 software

Student's t-test analyses were used to evaluate the variation of the mean of relative frequencies of each RNA species between leaves and roots of *B. macrocarpa* and *S. oleracea* (Figure 6). Interestingly, in both systemic hosts, significant differences were observed for total RNA species accumulation between leaves and roots while no significant variation were noticed for encapsidated RNA abundance between the two organs.

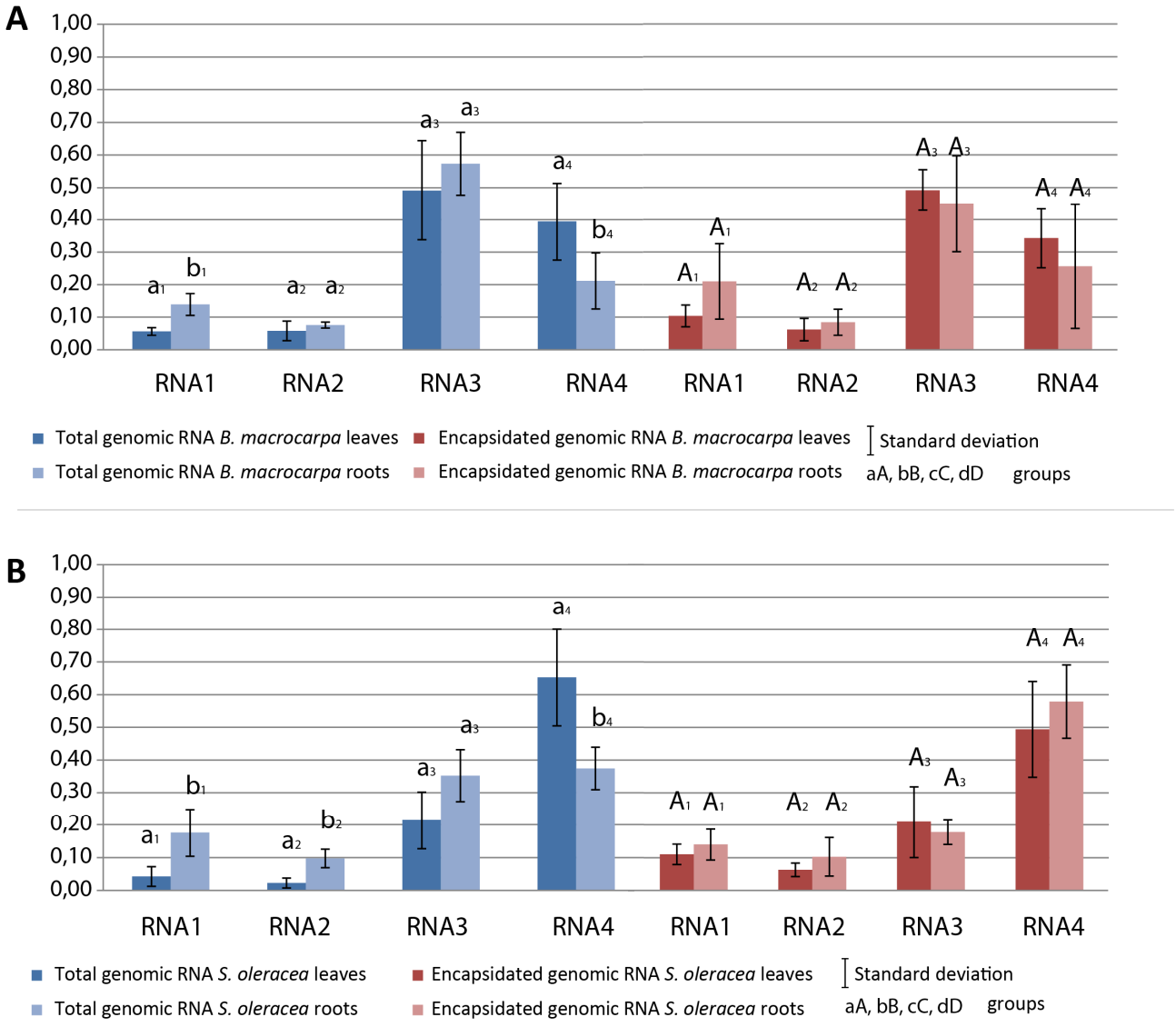

Figure 6 RNAs relative frequencies differ within different organs of the host. Comparison of the means of relative frequencies for each BNYVV RNAs calculated in systemically infected *B. macrocarpa* (A) or *S. oleracea* (B) leaves and roots. Significant differences in segment accumulation are indicated by letters and were assessed by Student's t-test. Error bars represent standard deviation. Student's t-test was determined using the SPSS 15.0 software.

Finally, Student's t-test and ANOVA one-way analysis have been applied to verify host type influence on the variation observed for each RNA in roots and leaves (Figure 7). In *B. macrocarpa*

and *S. oleracea* roots, RNA variation appears significant for RNA3 and RNA4 for both total and encapsidated RNA extractions. For leaves of the three hosts, independently of the RNA extraction protocol, RNA3 and RNA4 species appear to accumulate differentially in *S. oleracea* compared to *B. macrocarpa* and *C. quinoa* where each genomic RNA is represented by two homogenous groups of mean of relative frequencies (Figure 7).

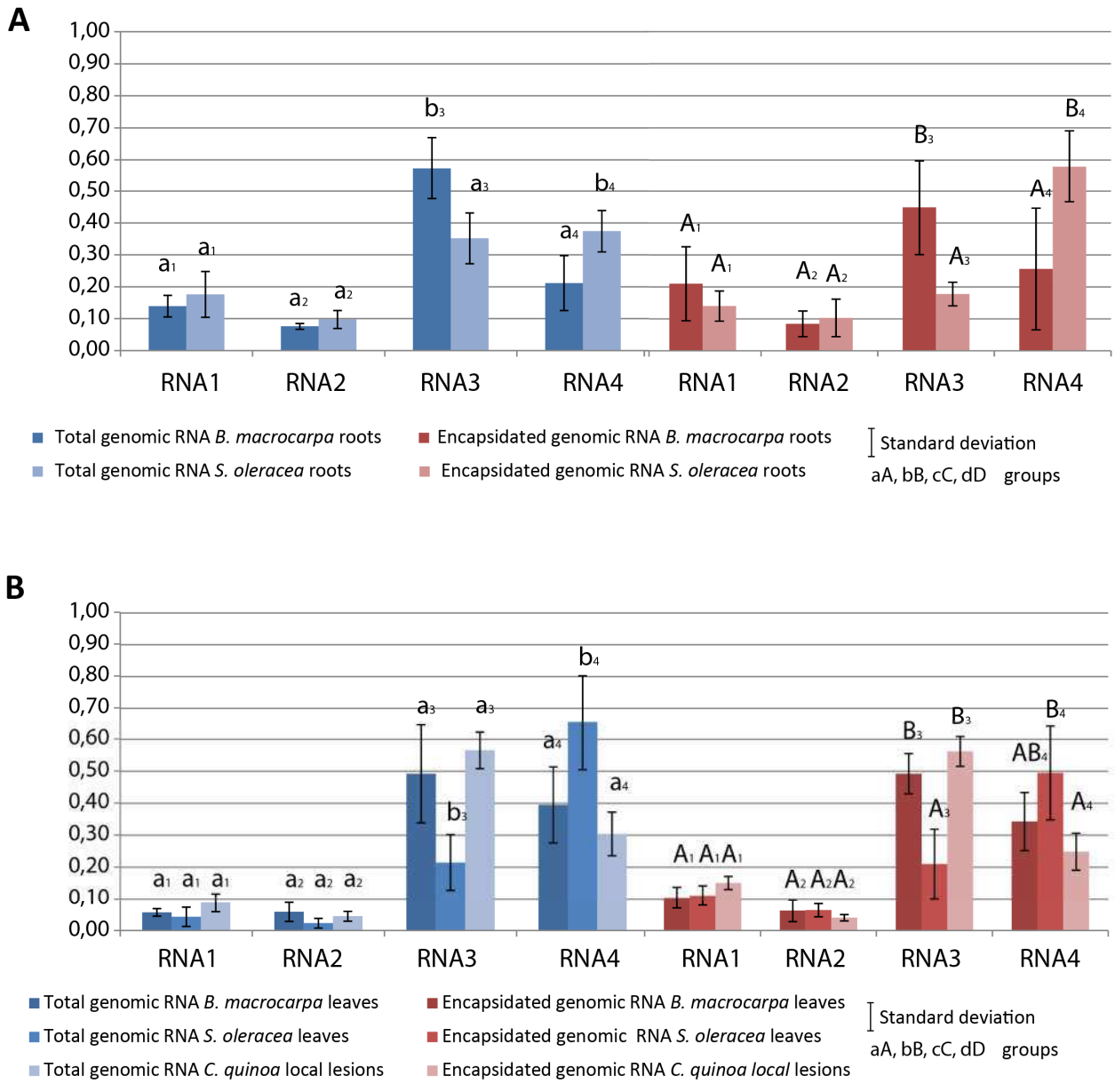

Figure 7 RNAs relative frequencies differ from one host to the other (A) Comparison of the calculated mean of relative frequencies of each BNYVV RNA in *B. macrocarpa* and *S. oleracea* roots. Significant differences in segment accumulation are indicated by letters and were assessed by Student's t-test. (B) The similar approach was applied for BNYVV RNA present in *B. macrocarpa*, *S. oleracea* and *C. quinoa* leaves. Groups of homogeneity indicated with letter have been assessed by Tukey HSD pair tests. Error bars indicate standard deviation. One Way ANOVA and Student's t-test were determined using the SPSS 15.0 software.

6. Discussion

The accumulation of BNYVV genomic RNAs has been compared in three hosts infected by the BNYVV. Host plant *C. quinoa* restricts BNYVV infection within the inoculated areas while *B. macrocarpa* and *S. oleracea* allow systemic BNYVV infection. However, while RNA3 is mandatory for BNYVV systemic infection in *B. macrocarpa*, the sole presence of RNA1 and RNA2 is sufficient for the virus to move long distance in *S. oleracea* [23]. It has been suggested that multipartite viruses adapt to different host or conditions by changing gene expression thanks to a gene copy number variation [9]. Such strategy has also been associated to monopartite viruses such as *Vaccinia virus* that responds to selection pressures experiments with the rapid amplification and duplication of K3L gene with a consequent expansion of the genome length [24]. Adaptive gene copy number variation is a common feature of prokaryote and animal parasites, other than of viruses. Among insect, „*Acyrthosiphon pisum* forms genetically distinct host-associated populations on multiple legume species thanks to copy number variation of up to 434 genes [25]. Furthermore resistance genes are commonly amplified by many bacteria as an adaptive response to antibiotic treatment [26,27]

If the variation of genomic segments relative abundance is a way for the rapid adaptation of the virus, the orchestration of gene expression often requires the maintenance of conserved stoichiometric ratios between particular genomic segments. AMV genomic formula is characterized by having fixed RNA1 and RNA2 stoichiometric coefficients (~1:3), and variable RNA3 coefficients that range from ~2 in *Nicotiana benthamiana* to ~16 in *Cucurbita pepo* [10]. In total RNA extractions, BNYVV RNA1 and RNA2 relative frequencies are low and comparable, and their stoichiometric rapport is mostly fixed to ~2:1. Conversely, RNA3 and RNA4 are more abundant and their ratio varies upon the host and the organ. RNA3 was found ~13 fold more

abundant than RNA2 in C. quinoa local lesions whereas RNA4 accumulated ~29 time more than RNA2 in *S. oleracea* leaves.

Such enhanced amplification of accessory RNAs represents an interesting aspect of gene copy number influence on gene expression regulation. BNYVV RNA3 species encodes the p25 protein, a pathogenic determinant described as an avirulence gene triggering resistance mechanisms [28,29]. The p25 protein expression is likely regulated during the different viral cycle steps in order to prevent its early expression and a resulting premature cell death. As soon as viral counter defenses are set, p25 expression could start to favors the viral infection progression. Regulation of p25 expression could be dependent on a mechanism that require a viral effector to trans-activate RNA3 translation. This protein is efficiently expressed in the viral context of systemic host infections as well as *C. quinoa* local lesions and poorly detected when translated *in vitro* from full length RNA3 or ectopically expressed in yeast or plant using Pol-II promoter driven expression vectors [30,31]. One could imagine a putative riboswitch motif present within the 450 nt-long 5' UTR of the RNA3 that allows such fine-tuned regulated p25 expression. Indeed, vectors producing 5' UTR truncated RNA3 allow the efficient p25 protein production [30,31]. Similarly, the 380 nt-long 5' UTR present on BNYVV RNA4 may as well contain such *cis* elements allowing a regulated p31 expression [30]. For these reasons a massive replication of ancillary RNAs is not correlated to the over expression of the encoded proteins but could be implicated in a mechanism that counteracts plant defense system. Increased amount of RNA3 and RNA4 could also lead to a saturation of the RNA silencing machinery protecting RNA1 and RNA2 from a degradation and consequently insuring the expression of the housekeeping genes. Such hypothesis should be corroborated by a quantitative analysis of BNYVV derived small interfering (si) RNAs during the infection expecting a prevalence of species derived from RNA3 and RNA4 rather than RNA1 and RNA2.

Quantification analyses of BNYVV genomic RNAs accumulation have been conducted choosing fixed BNYVV infection conditions: the inoculum consisted on identical concentrations agro-clones

and sampling has been performed on symptomatic tissues likely representing late stages of viral infection. However, the initial conditions of the infection may not constitute a determinant variable for the calculation of the genomic formula since the relative frequency variations in the inoculum do not produce significant variation in the analyzed tissues for AMV and FBNSV segments [9,10]. Conversely, quantifications performed on symptomatic tissues could average different snapshots of viral cycles steps, each characterized by specific gene expression and, probably, by specific relative frequencies between genomic RNAs. To explore how genomic formula changes during the infection, kinetic experiments of virus production in transfected protoplasts will be carried out. This will allow the study of the progression of the GF along a viral cycle initiated in a homogenous population of single cells, performing the renowned "single burst experiment" [32].

Comparative analyses of total or encapsidated BNYVV RNAs relative frequencies reveled that a correlation does not always occur in infected tissue of *C. quinoa* and *S. oleracea*. Such behavior has also been reported for AMV in *N. benthamiana* and was explained as an existing competition between RNAs during the encapsidation process [10]. When we compare the BNYVV RNAs relative frequencies in leaves and roots of *B. macrocarpa* or *S. oleracea* we observe that even without a clear correlation between segment relative frequencies within total RNAs, encapsidated RNA species accumulate as a host specific manner conserved in both organs. We could therefore speculate that the equilibrium between the replicative and expressed RNAs and the vector-transmitted encapsidated RNA species is regulated independently of the total amount of viral RNA species.

If on the one hand BNYVV RNAs encapsidation drives the viral transmission from host to vector and vice versa, on the other hand, during the host colonization, its biological importance is reduced and limited to the stabilization of genomic RNAs and to the shutdown of viral gene expression [30]. Moreover, non encapsidated viral RNAs represent the active form of the virus that drive viral expression and move within the host [33]. Knowing how such non encapsidated RNAs constitute

the moving genomic formula and how it is stabilized is essential to understand how the BNYVV and perhaps other multipartite plus-strand RNA viruses orchestrate viral infections. However, as no correlation between relative frequencies calculated in total and encapsidated RNA extractions was drawn, it appears difficult to determine the stoichiometric ratio between BNYVV non encapsidated RNAs. An optimization of the analysis is therefore required to distinguish between encapsidated and non encapsidated RNAs. On possibility would consist on the addition of purified virions of the BNYVV-closely related *beet soil borne mosaic virus* [21] in the homogenization TM buffer as a nuclease resistant reference genome. This will allow the normalization of total and encapsidated RNA extractions and then deduce the copy number of non encapsidated RNAs by a simple subtraction.

6. References

1. Lucía-Sanz, A.; Manrubia, S. Multipartite viruses: adaptive trick or evolutionary treat? *npj Syst. Biol. Appl.* **2017**, *3*, doi:10.1038/s41540-017-0035-y.

2. Nee, S. The evolution of multicompartmental genomes in viruses. *J. Mol. Evol.* **1987**, *25*, 277–281, doi:10.1007/BF02603110.

3. Iranzo, J.; Manrubia, S. C. Evolutionary dynamics of genome segmentation in multipartite viruses. *Proc. R. Soc. B Biol. Sci.* **2012**, *279*, 3812–3819, doi:10.1098/rspb.2012.1086.

4. García-Arriaza, J.; Manrubia, S. C.; Toja, M.; Domingo, E.; Escarmís, C. Evolutionary transition toward defective RNAs that are infectious by complementation. *J. Virol.* **2004**, *78*, 11678–85, doi:10.1128/JVI.78.21.11678-11685.2004.

5. Ojosnegros, S.; García-Arriaza, J.; Escarmís, C.; Manrubia, S. C.; Perales, C.; Arias, A.; Mateu, M. G.; Domingo, E. Viral Genome Segmentation Can Result from a Trade-Off between Genetic Content and Particle Stability. *PLoS Genet.* **2011**, *7*, e1001344, doi:10.1371/journal.pgen.1001344.

6. McDonald, S. M.; Nelson, M. I.; Turner, P. E.; Patton, J. T. Reassortment in segmented RNA viruses: mechanisms and outcomes. *Nat. Rev. Microbiol.* **2016**, *14*, 448–60,

doi:10.1038/nrmicro.2016.46.

7. Chao, L. Evolution of sex in RNA viruses. *J. Theor. Biol.* **1988**, *133*, 99–112, doi:10.1016/S0022-5193(88)80027-4.

8. Sicard, A.; Michalakis, Y.; Gutiérrez, S.; Blanc, S. The Strange Lifestyle of Multipartite Viruses. *PLOS Pathog.* **2016**, *12*, e1005819, doi:10.1371/journal.ppat.1005819.

9. Sicard, A.; Yvon, M.; Timchenko, T.; Gronenborn, B.; Michalakis, Y.; Gutierrez, S.; Blanc, S. Gene copy number is differentially regulated in a multipartite virus. *Nat. Commun.* **2013**, *4*, doi:10.1038/ncomms3248.

10. Wu, B.; Zwart, M. P.; Sánchez-Navarro, J. A.; Elena, S. F. Within-host Evolution of Segments Ratio for the Tripartite Genome of Alfalfa Mosaic Virus. *Sci. Rep.* **2017**, *7*, doi:10.1038/s41598-017-05335-8.

11. Torrance, L.; Lukhovitskaya, N. I.; Schepetilnikov, M. V.; Cowan, G. H.; Ziegler, A.; Savenkov, E. I. Unusual long-distance movement strategies of Potato mop-top virus RNAs in Nicotiana benthamiana. *Mol. plant-microbe Interact.* **2009**, *22*, 381–390, doi:10.1094/MPMI-22-4-0381.

12. Gilmer, D.; Ratti, C.; ICTV Report Consortium ICTV Virus Taxonomy Profile: Benyviridae. *J. Gen. Virol.* **2017**, *98*, 1571–1572, doi:10.1099/jgv.0.000864.

13. Peltier, C.; Hleibieh, K.; Thiel, H.; Klein, E.; Bragard, C.; Gimer, D. Molecular Biology of the Beet necrotic yellow vein virus. *Plant Viruses* **2008**, *2*, 14–24.

14. Taylor, S. C.; Laperriere, G.; Germain, H. Droplet Digital PCR versus qPCR for gene expression analysis with low abundant targets: from variable nonsense to publication quality data. *Sci. Rep.* **2017**, *7*, 2409, doi:10.1038/s41598-017-02217-x.

15. Pinheiro, L. B.; Coleman, V. A.; Hindson, C. M.; Herrmann, J.; Hindson, B. J.; Bhat, S.; Emslie, K. R. Evaluation of a droplet digital polymerase chain reaction format for DNA copy number quantification. *Anal. Chem.* **2012**, *84*, 1003–1011, doi:10.1021/ac202578x.

16. Zhao, Y.; Xia, Q.; Yin, Y.; Wang, Z. Comparison of Droplet Digital PCR and Quantitative PCR Assays for Quantitative Detection of Xanthomonas citri Subsp. citri. *PLoS One* **2016**, *11*, e0159004, doi:10.1371/journal.pone.0159004.

17. Uchiyama, Y.; Nakashima, M.; Watanabe, S.; Miyajima, M.; Taguri, M.; Miyatake, S.; Miyake, N.; Saitsu, H.; Mishima, H.; Kinoshita, A.; Arai, H.; Yoshiura, K.; Matsumoto, N. Ultra–sensitive droplet digital PCR for detecting a low–prevalence somatic GNAQ mutation in Sturge–Weber syndrome. *Sci. Rep.* **2016**, *6*, 22985, doi:10.1038/srep22985.

18. Ziegler-Graff, V.; Bouzoubaa, S.; Jupin, I.; Guilley, H.; Jonard, G.; Richards, K. Biologically Active Transcripts of Beet Necrotic Yellow Vein Virus RNA-3 and RNA-4. *J. Gen. Virol.* **1988**, *69*, 2347–2357, doi:10.1099/0022-1317-69-9-2347.

19. Quillet, L.; Guilley, H.; Jonard, G.; Richards, K. In vitro synthesis of biologically active beet necrotic yellow vein virus RNA. *Virology* **1989**, *172*, 293–301.

20. Delbianco, A. Agroinoculation of Beet necrotic yellow vein virus cDNA clones results in plant systemic infection and efficient Polymyxa betae transmission. *Mol. Plant Pathol.* **2013**, *14*, 422–428, doi:10.1111/mpp.12018.

21. Laufer, M.; Mohammad, H.; Maiss, E.; Richert-Pöggeler, K.; Dall'Ara, M.; Ratti, C.; Gilmer, D.; Liebe, S.; Varrelmann, M. Biological properties of Beet soil-borne mosaic virus and Beet necrotic yellow vein virus cDNA clones produced by isothermal in vitro recombination: Insights for reassortant appearance. *Virology* **2018**, *518*, 25–33, doi:10.1016/j.virol.2018.01.029.

22. Jupin, I.; Richards, K.; Jonard, G.; Guilley, H.; Pleij, C. W. Mapping sequences required for productive replication of beet necrotic yellow vein virus RNA 3. *Virology* **1990**, *178*, 273–80.

23. Lauber, E.; Guilley, H.; Tamada, T.; Richards, K. E.; Jonard, G. Vascular movement of beet necrotic yellow vein virus in Beta macrocarpa is probably dependent on an RNA 3 sequence domain rather than a gene product. *J. Gen. Virol.* **1998**, *79*, 385–393, doi:10.1099/0022-1317-79-2-385.

24. Elde, N. C.; Child, S. J.; Eickbush, M. T.; Kitzman, J. O.; Rogers, K. S.; Shendure, J.; Geballe, A. P.; Malik, H. S. Poxviruses Deploy Genomic Accordions to Adapt Rapidly against Host Antiviral Defenses. *Cell* **2012**, *150*, 831–841, doi:10.1016/j.cell.2012.05.049.

25. Duvaux, L.; Geissmann, Q.; Gharbi, K.; Zhou, J.-J.; Ferrari, J.; Smadja, C. M.; Butlin, R. K. Dynamics of Copy Number Variation in Host Races of the Pea Aphid. *Mol. Biol. Evol.* **2015**,

32, 63–80, doi:10.1093/molbev/msu266.

26. Sandegren, L.; Andersson, D. I. Bacterial gene amplification: implications for the evolution of antibiotic resistance. *Nat. Rev. Microbiol.* **2009**, *7*, 578–588, doi:10.1038/nrmicro2174.

27. San Millan, A.; Santos-Lopez, A.; Ortega-Huedo, R.; Bernabe-Balas, C.; Kennedy, S. P.; Gonzalez-Zorn, B. Small-plasmid-mediated antibiotic resistance is enhanced by increases in plasmid copy number and bacterial fitness. *Antimicrob. Agents Chemother.* **2015**, *59*, 3335–41, doi:10.1128/AAC.00235-15.

28. Chiba, S.; Miyanishi, M.; Andika, I. B.; Kondo, H.; Tamada, T. Identification of amino acids of the beet necrotic yellow vein virus p25 protein required for induction of the resistance response in leaves of Beta vulgaris plants. *J. Gen. Virol.* **2008**, *89*, 1314–1323, doi:10.1099/vir.0.83624-0.

29. Thiel, H.; Hleibieh, K.; Gilmer, D.; Varrelmann, M. The P25 pathogenicity factor of Beet necrotic yellow vein virus targets the sugar beet 26S proteasome involved in the induction of a hypersensitive resistance response via interaction with an F-box protein. *Mol. Plant-Microbe Interact.* **2012**, *25*, 1058–1072.

30. Gilmer, D. Molecular Biology and Replication of Beet Necrotic Yellow Vein Virus. In *Rhizomania*; Springer International Publishing: Cham, 2016; pp. 85–107.

31. Peltier, C.; Klein, E.; Hleibieh, K.; D'Alonzo, M.; Hammann, P.; Bouzoubaa, S.; Ratti, C.; Gilmer, D. Beet necrotic yellow vein virus subgenomic RNA3 is a cleavage product leading to stable non-coding RNA required for long-distance movement. *J. Gen. Virol.* **2012**, *93*, 1093–1102, doi:10.1099/vir.0.039685-0.

32. Canova, A. Appunti di patologia della barbabietola. *Inf. Fitopatol.* **1959**, *9*, 390–396.

33. Dall'Ara, M.; Ratti, C.; Bouzoubaa, S.; Gilmer, D. Ins and Outs of Multipartite Positive-Strand RNA Plant Viruses: Packaging versus Systemic Spread. *Viruses* **2016**, *8*, 228, doi:10.3390/v8080228.

Chapter II

BNYVV genome integrity within infected cells

1. Introduction: a link between viral movement and multipartitism

Described as obligate intracellular pathogens, viruses require, always and without any exception, to enter and replicate within an infected cell. The way viruses propagate from one cell to another seems to be dependent on the type of infected multicellular host and on the virus itself. Animal viruses spread by two distinct but not exclusive models (Figure 1), both requiring the capsid formation and expulsion from the cell after budding, exocytosis or cell lysis. Dissemination of viral particles in the extracellular space allows the long distance spread of the virus in the infected host and an easier transmission to new hosts [1]. Besides dissemination, cell to cell transmission takes place when viral particles are retained on the outside surface of the plasma membrane (PM) and their passage in new cells is promoted by existing or *de novo* formed cell contacts. Neurotropic viruses take advantage of the microtubule-mediated transport to spread from one neuron to another through synaptic connections [2]. Instead, retroviruses induce uninfected cells to forms virological synapses or filopodial bridges allowing a stable link with the infected cells [3,4]. T cells that usually don't engage prolonged interaction to each other, could be physically connected by membrane nanotubes to allow *human immunodeficiency virus* type 1 (HIV-1) to be transferred from infected to uninfected cells in a receptor-dependent manner and with a cell surface movement [5]. However, in some rare cases the virus can move cell to cell within vesicles thought cytoplasmic connections such as bridging conduits that allow HIV-1 trafficking between macrophages following the endoplasmatic reticulum (ER) and Golgi network [6]. It has been proposed that *Influenza A virus* (IAV) uses similar intercellular connections to transport viral ribonucleoprotein complexes (vRNPs) that contain polymerase as infectious viral machinery rather than virions [7].

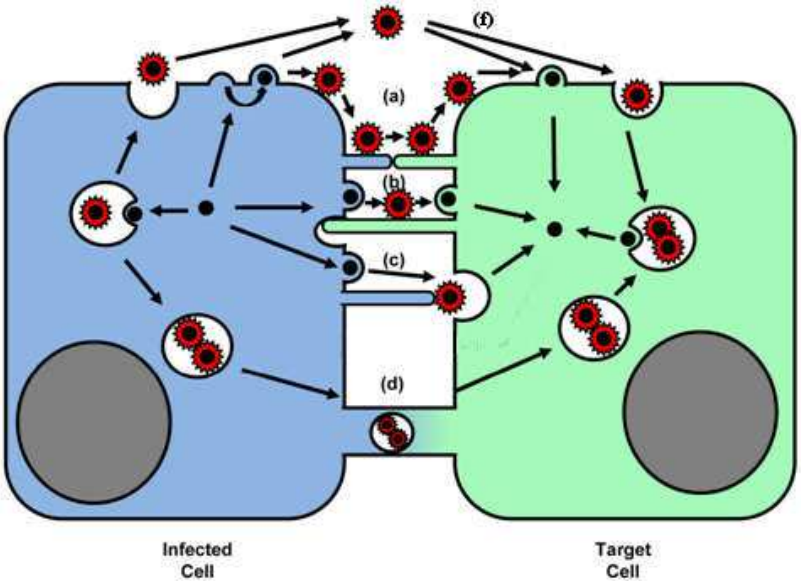

Figure 1 Schematic representation of viral movement in animal hosts requiring as prerequisite virion formation: virus can move as free particles released in extracellular matrix **(f)** or exploiting existing **(a)** or de novo formed intercellular communication for cell to cell transmission **(b, c, d)**. Retrovirus can remain associated with the surface of the infected cell and spread thanks long filopodial bridges that connect target to donor cells **(b)**; *Vaccinia virus* polymerizes actin to propel itself from infected to target cell [8] **(c)**. Lastly, in some rare circumstance, animal viruses can induce the formation of cytoplasmic connections that are used as conduits for the transfer of virion enveloped by vesicles **(d)**. Figure is adapted from Zhong et al. [1]

If animal viruses rarely promote cytoplasmic connections formation, it appears a prerequisite for phytoviruses. Indeed, the main morphological feature of plant tissues is the cell holding and delimitation within rigid and thick cell wall that render the direct access to the PM surface impossible for macromolecules and viruses. Phytoviruses must be retained in the inner side of the PM (symplast) to be replicated and to spread cell to cell. Plants possess intercellular junctions, namely plasmodesmata (Pds) that directly interconnect the cytoplasms of adjacent cells. This provides a whole-body macromolecular transport network called symplastic continuity [9]. Functionally comparable to animal cell gap junction, the simplest form of Pd is composed essentially by membrane and spaces [10] that form a linear channel delimited by PM and containing an axial membranous tubule called desmotubule, derived from the ER union. The region between desmotubule and PM is called cytoplasmic sleeve and presents structurally organized cytoskeleton components, together with other structural and non-structural proteins required for trafficking functions [11]. Soluble environments (cytoplasmic sleeve and ER lumen) and membrane

environments (PM and ER) are both exploited as paths for molecular trafficking. This trafficking is controlled by Pd size exclusion limit (SEL), which is regulated by the highly dynamic callose (β-1.3-glucan) deposition in the cell wall. This callose deposition surrounds and constricts the neck region of the pore [11]. Aimed to defines the standard SEL, experimental studies demonstrate that GFP (26kDa), 2XGFP (52kDa) and, less efficiently, 3XGFP (78kDa) soluble proteins can diffuse through most tissues of the plants especially in early stage of embryogenesis [12]. However, with tissue development, branches and cavities formation modifies Pd permeabilities and creates symplastic domains with different types of connectivity between cells. This restricts GFP diffusion in younger sink tissues and makes the protein movement between vascular boundaries difficult [13]. To use Pd as gates for viral cell to cell movement within the symplast, phytoviruses have to increase SEL thanks the production of viral movement proteins (MPs) that adjust Pd structure to let virions or vRNP complexes transport, allowing the propagation of the infection [11]. This symplastic route is maintained even during the long-distance movement of macromolecules and therefore viral entities. Once gained the companion cells (CCs), viral entities are loaded in the sieve element (SE) conduits of source tissues, passively transported within the source-to-sink flow of photoassimilates and then unloaded into sink tissues [14].

With some rare exceptions (Bidensoviruses [15] and *Guaico Culex virus* infecting silkworm mosquitoes [16], respectively) multipartite viruses mostly infect plants and fungi. They represent about 30% - 40% of phytovirus genera and families [17]. Such viral strategy could be explained by the virus retention in the symplastic continuity, rather than virions expulsion and entry from one cell to another. The separated genomic components would then act as one unique genome segregated all along the interconnected cells. If such a situation exists, there is still now answer on the way it is accomplished. The results presented in this chapter suggest that for BNYVV, as it is modelized to date[18], an uncoordinated trafficking of viral genomic material through Pds does not guarantee the complete set of genomic segments in each infected cell. Indeed, the differential accumulation of

each BNYVV RNA measured within the infected tissues drastically increases both the multiplicity of infection (MOI) and the biological cost, in terms of viral load, required to preserve BNYVV genomic integrity. This lead to the formulation of two opposed hypotheses illustrated in figure 2:

1. BNYVV segments may not necessarily be present "all together" in every infected cell. The RNA replication and stabilization are therefore ensured by the exchange of viral proteins through the symplastic continuity.

2. A specific mechanism guarantees the coordinated movement of each segment as infective collective units.

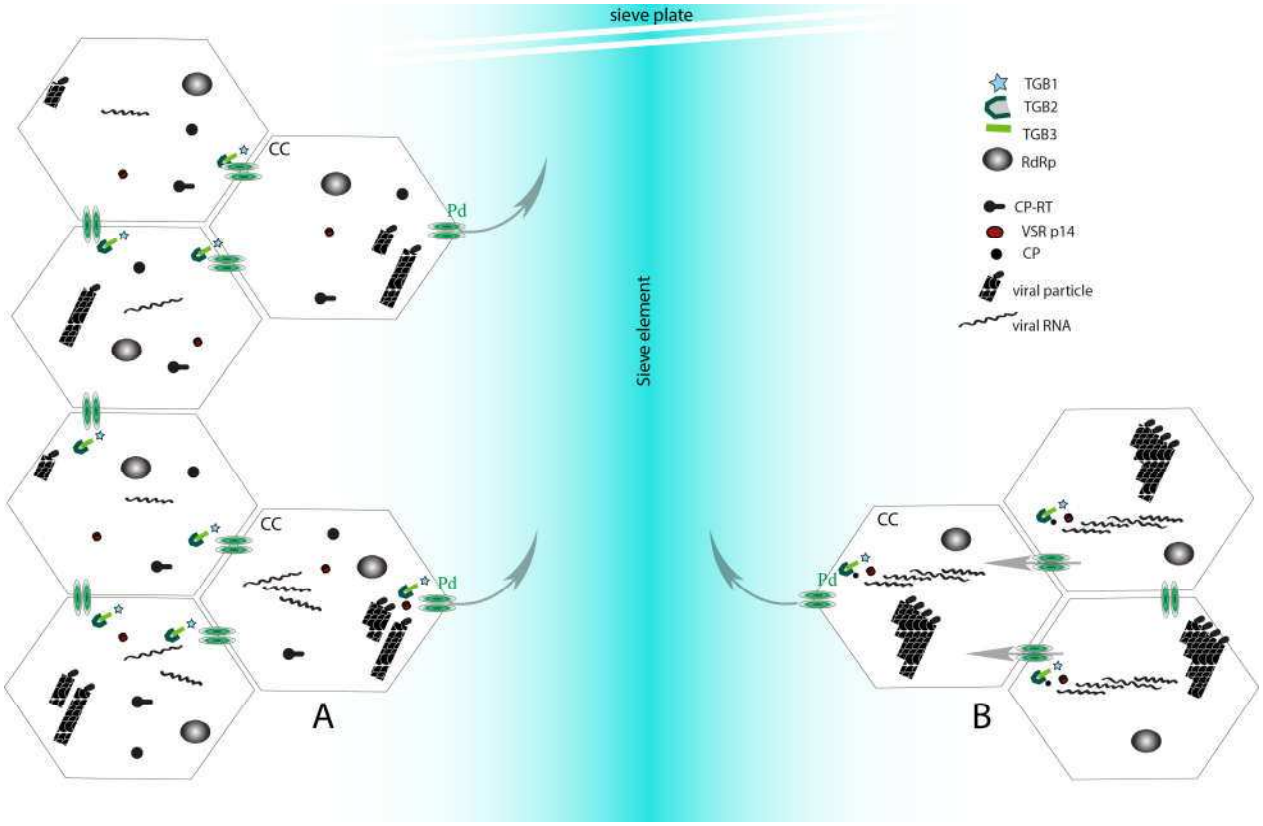

Figure 2 Simplified representation of the two hypotheses formulated for BNYVV genomic preservation during plant colonization. In panel A genomic segments, as particles or free RNAs, are distributed randomly in neighbored cells. Replication and stabilization of the four vRNAs are ensured by the free symplastic trafficking of house-keeping viral factors such as replicase (RdRp), coat protein (CP), coat protein-readthrough (CP-RT), viral suppressor of RNA silencing (VSR) and TGB proteins involved in the SEL increasing and in the free diffusion of high molecular weight proteins through plasmodesmata (Pd). In this model Sieve elements (Blue shaded) are considered as reservoir of viral RNAs and particles stochastically loaded from companion cells (CC). In panel B collective units keep together the different genomic elements and permit their co-presence in each infected cell and their coordinated movement through Pds and Sieve elements. Collective mobile units are here represented as both vRNP complexes and particle aggregates. Figure is adapted from Dall'Ara et al. [19]

As it has been demonstrated performing leaf rub-inoculation of GFP tagged viruses in permissive host, BNYVV is able to move cell to cell and long distance infecting all plant tissues, demonstrating an extensive tissue tropism [20]. For this reason, to gain experimental data to favor one or the other hypothesis, I choose to characterize the viral content of individual cells that have been infected after long distance movement of BNYVV. To perform such analyses, I isolated cells from systemically infected tissues and searched for the presence of viral RNA species. Therefore, I had to develop a multiplex RT-qPCR protocol on single protoplast isolated from mesophyll of systemically infected *Spinacia oleracea* with the aim to test the co-presence of the four genomic BNYVV RNAs within each infected cell.

2. Preparation of *S. oleracea* protoplast and fixation

In the present work, the optimized protocol for individual protoplast isolation and selection from mesophyll BNYVV infected *S. oleracea* leaves does not require specialized expertise or instrumentation and reduces vRNA cross contamination. Indeed, viral titer per cell can be in general extremely high [21] and cross contamination of genomic material between infected cells is an eventuality that has be taken into consideration to avoid the generation of false positives by RT-qPCR.

Young spinach seedlings (cv. Viking), with two true leaves, were infected by sap mechanical inoculation, using, as source of inoculum, frozen leaf tissues of systemically BNYVV-infected *S. oleracea* plants. Inoculated plants were grown in the green house at 24/20°C and 16/8h (days/night) and 4 week later an equal amount of young leaves from symptomatic (infected) and healthy (non inoculated plants), were mixed together for protoplast preparation. Four grams of sterilized and scarified leaf lamina were treated to isolate protoplasts according to Veidt et al. protocol [22] revised in the maceration step. In particular, after overnight maceration at 24°C under dark condition, in a medium containing Mannitol 0.6M, MES 5mM, $CaCl_2$ 10mM, Macerozyme R10

0,4% and Cellulase R10 0,7%, protoplasts were collected by two passages of low centrifugation (88 RCF), suspended in MMC buffer (Mannitol 0.6M, MES 5mM, $CaCl_2$ 10mM) and adjusted to a concentration of 1 cell/10µl before 15 min incubation step in fixing solution (MMC buffer, glutaraldehyde 0.5%). After two washing steps, protoplasts were decontaminated from viral particles or RNAs retained on the cell external surface by 10 min incubation in MMC buffer, containing Trypsin 0.1%, RNAse A 0.025% and $MgCl_2$ 50mM. Trypsin and RNAse A were then removed from the cell suspension by three washing steps and protoplast concentration was adjusted to 1 cell/10µl in MMC.

3. Individual protoplast isolation and triplex RT-qPCR

Single protoplast isolations for the RT-qPCR based analysis was perform by free hand pipetting under light microscope: 100 µl of protoplast suspension was placed on glass slides and, under magnification of 40X, individual cells were collected by pipetting volumes of 4µl. Sampling accuracy was increased by the use of acrylamide gel tips (ART 20 GEL, Barrier Tip) and by controlling the protoplast shape, under 80X microscope magnification, after selection and loading in new glass slides. Selected and checked protoplasts or MMC buffer depleted from protoplast (as negative control) were then loaded in PCR tube and used as template for a triplex RT-qPCR reaction targeting two different BNYVV RNAs and Rubisco Large subunit (RbcL). In each tube 16µl of the following RT-qPCR mixture were added:

- 10µl Promega GoTaq® Probe qPCR Master Mix (2X)
- 0.5µl Promega M-MLV RT (4 unit/µl)
- 0.5µl RNA1 or RNA3 Forward primer (20µM)
- 0.5µl RNA1 or RNA3 Reverse primer (20µM)
- 0.5µl RNA1 or RNA3 FAM probe (4µM)
- 0.5µl RNA2 or RNA4 Forward primer (20µM)

- 0.5µl RNA2 or RNA4 Reverse primer (20µM)
- 0.5µl RNA2 or RNA4 HEX probe (4µM)
- 0.5µl RbcL Forward primer (20µM)
- 0.5µl RbcL Reverse primer (20µM)
- 0.5µl TWEEN 20 (8%)

Primers and probes sequences as well as amplicon sizes are given in table 4 (annexes).

Tubes were vigorously vortexed and briefly centrifuged before RT-qPCR reactions described in Table 1.

Step	Cycles	Temperature	Time
Reverse transcription	1	42° C	30 min
Polymerase activation	1	90° C	10 min
Denaturation	45	90° C	30 s
Annealing/Extension		60° C	1 min

Table 1 RT-PCR cycling parameters

The RT-qPCR of BNYVV RNAs was followed in Real-Time using TaqMan probes with different fluorophores (FAM and HEX) while the presence of the endogenous control RbcL was confirmed after amplification (end-point) in agarose gel (Figure 3). Four different reactions were performed to detect the presence of RNA1 with RNA2 (RNA1/RNA2), RNA2 with RNA3 (RNA2/RNA3), RNA1 with RNA4 (RNA1/RNA4) and RNA3 with RNA4 (RNA3/RNA4) (Figure 3). To discriminate the background from real amplification signals, for each reaction, threshold lines of different targets were set manually above the base line derived from the delta Rn against PCR cycle plot. Basically, two population of curves occurred in each reaction distinguishing positive from negative samples. To produce a reference pattern for collected protoplasts analyses, 500 ng of total RNAs extracted from *S. oleracea* infected tissues (qualitative positive control) was used (Figure 3). Fourteen up to sixteen protoplasts have been tested for each of the four reactions described above and the presence of each RNA target has been evaluated using Ct values as qualitative data (Table 2

and 3). The percentages of BNYVV positive protoplasts were ~ 50% for RNA1/RNA2 and for RNA2/RNA3, ~31% for RNA1/RNA4 and 42% for RNA3/RNA4 reactions. Such results are in agreement with the initial mixing of infected and not infected tissues during the protoplast preparation. Furthermore, infected protoplasts (determined by RT-qPCR analyses) have been associated with a co-amplification of the analyzed BNYVV RNAs with an exception for RNA4 that has been sometimes found without its co-analyzed genomic RNAs. Since RNA1 is always co-detected with RNA2 and RNA2 is co-detected with RNA3, I determined that RNA4 has been found alone with an incidence of 20% (Table 2 samples 42 & 52). For all co-amplification, the endogenous control RbcL was confirmed and no amplification was observed in the absence of cell.

Sample	Detector	Target	Ct	Sample	Detector	Target	Ct
1	FAM	RNA1	Undet.	**17**	FAM	RNA3	**30.61**
	HEX	RNA2	Undet.		HEX	RNA2	**31.72**
2	FAM	RNA1	Undet.	**18**	FAM	RNA3	**36.88**
	HEX	RNA2	Undet.		HEX	RNA2	**42.83**
3	FAM	RNA1	Undet.	**19**	FAM	RNA3	Undet.
	HEX	RNA2	Undet.		HEX	RNA2	Undet.
4	FAM	RNA1	Undet.	**20**	FAM	RNA3	Undet.
	HEX	RNA2	Undet.		HEX	RNA2	Undet.
5	FAM	RNA1	**30.9**	**21**	FAM	RNA3	Undet.
	HEX	RNA2	**32.28**		HEX	RNA2	Undet.
6	FAM	RNA1	**36.06**	**22**	FAM	RNA3	Undet.
	HEX	RNA2	**42.62**		HEX	RNA2	Undet.
7	FAM	RNA1	**30.88**	**23**	FAM	RNA3	Undet.
	HEX	RNA2	**33.02**		HEX	RNA2	Undet.
8	FAM	RNA1	**33.87**	**24**	FAM	RNA3	Undet.
	HEX	RNA2	**38.16**		HEX	RNA2	Undet.
9	FAM	RNA1	**31.49**	**25**	FAM	RNA3	**31.22**
	HEX	RNA2	**34.01**		HEX	RNA2	**31.74**
10	FAM	RNA1	Undet.	**26**	FAM	RNA3	**31.00**
	HEX	RNA2	Undet.		HEX	RNA2	**33.92**
11	FAM	RNA1	**32.00**	**27**	FAM	RNA3	**37.73**
	HEX	RNA2	**33.09**		HEX	RNA2	**43.6**
12	FAM	RNA1	Undet.	**28**	FAM	RNA3	**29.55**
	HEX	RNA2	Undet.		HEX	RNA2	**31.04**
13	FAM	RNA1	**35.04**	**29**	FAM	RNA3	**32.83**
	HEX	RNA2	**39.35**		HEX	RNA2	**35.4**
14	FAM	RNA1	Undet.	**30**	FAM	RNA3	Undet.
	HEX	RNA2	Undet.		HEX	RNA2	Undet.

15	FAM	RNA1	**33.48**	**31**	FAM	RNA3	Undet.
	HEX	RNA2	**36.5**		HEX	RNA2	Undet.
16	FAM	RNA1	Undet.	**32**	FAM	RNA3	**32.08**
	HEX	RNA2	Undet.		HEX	RNA2	**34.2**

Table 2 Real time Cts for RNA1/RNA2 and RNA2/RNA3 reactions

Sample	Detector	Target	Ct	Sample	Detector	Target	Ct
33	FAM	RNA1	Undet.	**49**	FAM	RNA3	**38.47**
	HEX	RNA4	Undet.		HEX	RNA4	**31.89**
34	FAM	RNA1	**33.21**	**50**	FAM	RNA3	Undet.
	HEX	RNA4	**33.74**		HEX	RNA4	Undet.
35	FAM	RNA1	**30.76**	**51**	FAM	RNA3	Undet.
	HEX	RNA4	**30.39**		HEX	RNA4	Undet.
36	FAM	RNA1	Undet.	**52**	FAM	RNA3	**Undet.**
	HEX	RNA4	Undet.		HEX	RNA4	**42.16**
37	FAM	RNA1	Undet.	**53**	FAM	RNA3	Undet.
	HEX	RNA4	Undet.		HEX	RNA4	Undet.
38	FAM	RNA1	Undet.	**54**	FAM	RNA3	Undet.
	HEX	RNA4	Undet.		HEX	RNA4	Undet.
39	FAM	RNA1	Undet.	**55**	FAM	RNA3	**34.78**
	HEX	RNA4	Undet.		HEX	RNA4	**34.04**
40	FAM	RNA1	**41.13**	**56**	FAM	RNA3	Undet.
	HEX	RNA4	**38.53**		HEX	RNA4	Undet.
41	FAM	RNA1	Undet.	**57**	FAM	RNA3	**36.49**
	HEX	RNA4	Undet.		HEX	RNA4	**38.15**
42	FAM	RNA1	**Undet.**	**58**	FAM	RNA3	Undet.
	HEX	RNA4	**35.14**		HEX	RNA4	Undet.
43	FAM	RNA1	Undet.	**59**	FAM	RNA3	Undet.
	HEX	RNA4	Undet.		HEX	RNA4	Undet.
44	FAM	RNA1	**40.87**	**60**	FAM	RNA3	**29.68**
	HEX	RNA4	**37.32**		HEX	RNA4	**30.69**
45	FAM	RNA1	Undet.				
	HEX	RNA4	Undet.				
46	FAM	RNA1	Undet.				
	HEX	RNA4	Undet.				
47	FAM	RNA1	Undet.				
	HEX	RNA4	Undet.				
48	FAM	RNA1	Undet.				
	HEX	RNA4	Undet.				

Table 3 Real time Cts for RNA1/RNA4 and RNA3/RNA4 reactions

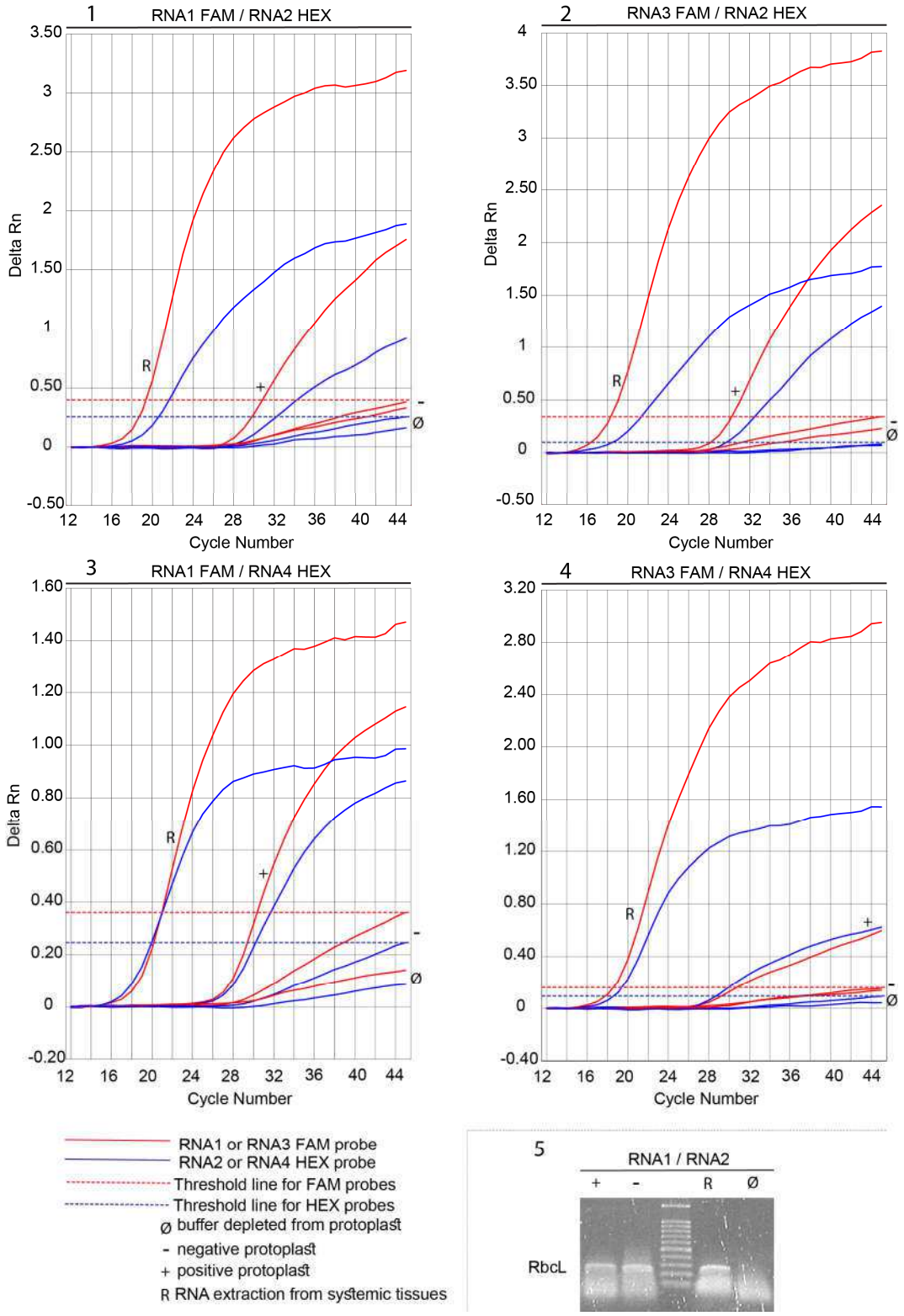

Figure 3 Profile examples of the co-detection of genomic BNYVV RNA pairs in isolated protoplasts. Real-Time PCR plots (**1, 2, 3, 4**) represent target amplification in the four different reactions: co-amplification of RNA1/RNA2 (**1**), RNA2/RNA3 (**2**), RNA1/RNA4 (**3**) and RNA3/RNA4 (**4**). The amplification issued from positive control is present in each plot (**R**), positive protoplast (+), negative protoplast (-) and of MMC buffer depleted from protoplast (**Ø**) (negative control). Dashed lines set above negative control signals indicate threshold for FAM and HEX signals. End-point reactions are loaded in agarose gel to verify RT-PCR amplification of RbcL endogenous control (**5**).

4. Discussion

S. oleracea is a permissive host that allows BNYVV systemic infection even in the absence of RNA3 and RNA4 [23]. The obtained results demonstrate that the virus maintains its genomic integrity in each infected cell even if the dispensability of ancillary RNAs could led to the conclusion that the virus is prone to lose one of its unnecessary RNAs during its spread from cell to cell in the host. On the one hand RNA1 and RNA2 are intrinsically coupled, since the expression of the TGB and VSR proteins depend on the production of subgenomic RNA2 by the RNA1-encoded replicase; on the other hand RNA3 and RNA4 can be lost in systemic tissues where there appear unessential, as described for BNYVV laboratory isolates on *Chenopodium quinoa*, *Tetragonia expansa* and *Nicotiana benthamiana* [24–26]. However, this was mainly explained as an effect of deletions compromising the RNA abilities to be replicated rather than spontaneous segregation of defective BNYVV genomes. From the results obtained in this study, we can conclude that in every RNA1 and RNA2 infected cells both RNA3 and RNA4 are present. This confirms the necessity for BNYVV to lower the MOI deriving from its genomic formula favoring cell entry of the genomic segments as collective infective units. In such scenario, the "significant" incidence of RNA4 segregating alone can be interpreted as a result of its relative abundance. In leaves of *S. oleracea*, RNA4 was found with a relative frequency average value of 0.65 (Chapter 1) meaning that its spread from the infected cell appears more stochastical than regulated. However, in roots of the same analyzed plants, relative frequency value lowers of 0.37 (approximately), suggesting the requirement of a coordinated movement for this abundant RNA4 species.

Moreover, the particular biology of BNYVV reinforces the hypothesis of having the full set of genomic RNAs in each infected cell. Indeed, to naturally extend the infection in new hosts the virus is transmitted by the soil-borne protozoa vector *Polymyxa betae*: avirulifer zoospores transfer their cytoplasmic content into the rootlets infected cells. The multinucleate sporangial plasmodium form

matures into zoosporangium and eventually in sporosori [27]. Cytoplasmic sharing between infected host and spore occurs at the level of a single infected cell that consequently must possess all genomic set of particles.

If on the one hand BNYVV genomic integrity within infected cells suggests the formation of mobile collective infective units, on the other hand further experiments are required to directly demonstrate their existence. Sieve elements are plant conduits where viruses rapidly move long distance but do not replicate. For this reason vascular elements should be particularly enriched with mobile BNYVV entities. A non-invasive extraction from such tissues could provide the material for mobile BNYVV entity characterization. Nanofluidic technology as digital droplets (dd)RT-PCR can be used to demonstrate the existence of viral entities that transport the complete set of BNYVV genomic RNAs. Similarly to a Real-Time multiplex reaction on single protoplasts, the phloem exudate partitioning in 1 nl droplets allows to link the co-detection of different genomic targets in the same reaction event to their association in a molecular complex. Furthermore, comparing results obtained from protocols of one-step and two-step ddRT-PCR reaction it will possible to calculate the genomic formula characterizing such complexes (Figure 4).

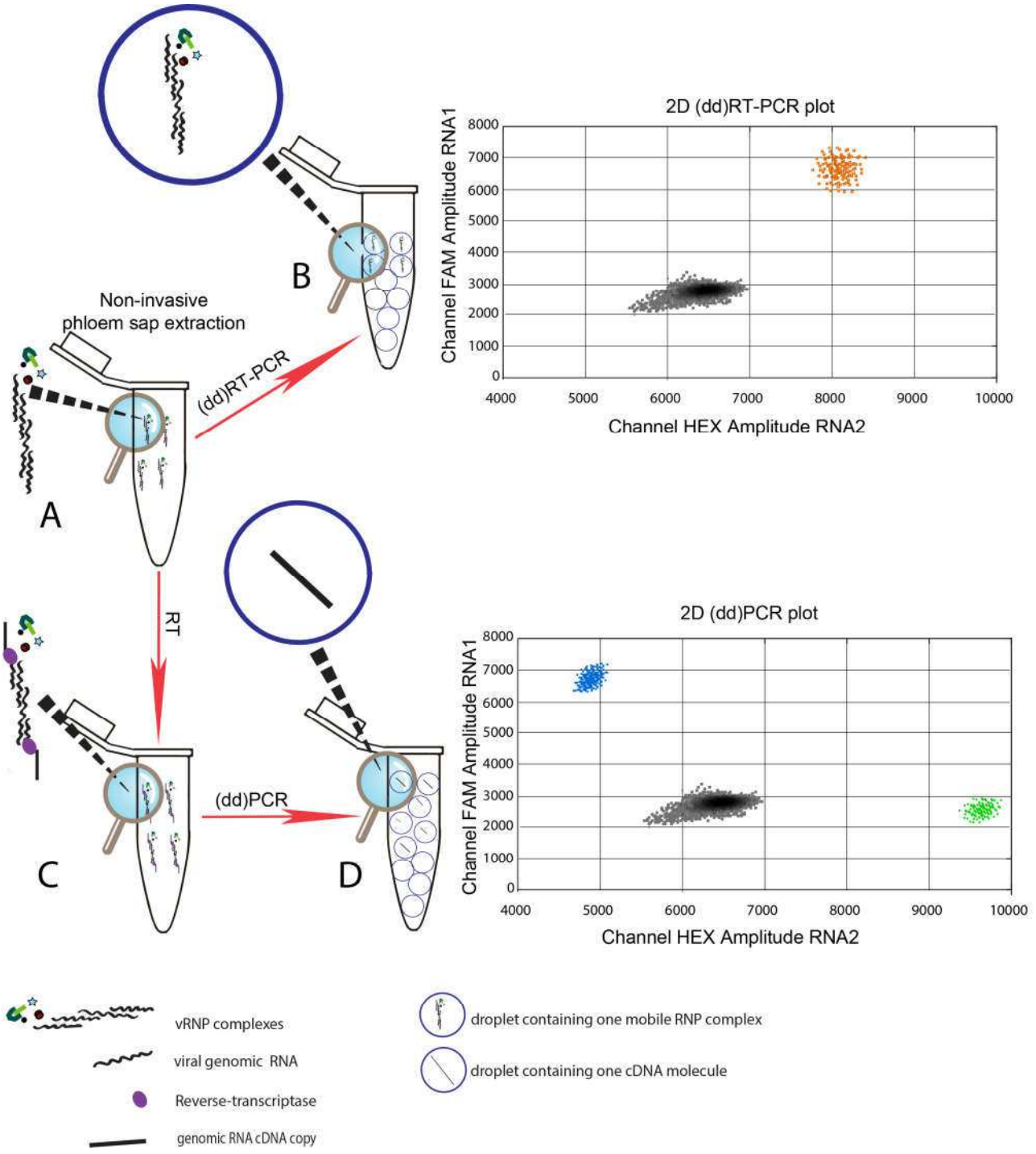

Figure 4 Simplified representation of the work flow to demonstrate the existence of viral entities that transport the complete set of BNYVV genomic RNAs. From phloem sap extraction enriched of BNYVV mobile collective units (**A**), here represent as vRNP complexes, both ddRT-PCR one step (**B**) and duplex dual step (**C** & **D**) will be performed. With ddRT-PCR one step, after partitioning, vRNP complexes are singularly segregated in droplets (**B**). As result of the end-point amplification, represented in the two dimension HEX and FAM amplitude plot, each positive droplet will have signals deriving from both probes (here RNA1-FAM and RNA2-HEX). Contrarily, with a step of reverse-transcription prior to partitioning (**C**), single cDNA copies of genomic RNAs will segregate in droplets (**D**). If phloem sap extraction was diluted properly, as result of ddPCR amplification FAM and HEX signals will not merge. The copy number of the two RNAs calculated in dual step ddRT-PCR divided by the number of co-amplifications in one step ddRT-PCR will give the genomic RNAs composition and ratio of the BNYVV mobile infective units.

5. References

1. Zhong, P.; Agosto, L. M.; Munro, J. B.; Mothes, W. Cell-to-cell transmission of viruses. *Curr. Opin. Virol.* **2013**, *3*, 44–50, doi:10.1016/j.coviro.2012.11.004.

2. Smith, G. A.; Gross, S. P.; Enquist, L. W. Herpesviruses use bidirectional fast-axonal transport to spread in sensory neurons. *Proc. Natl. Acad. Sci.* **2001**, *98*, 3466–3470.

3. Sherer, N. M.; Lehmann, M. J.; Jimenez-Soto, L. F.; Horensavitz, C.; Pypaert, M.; Mothes, W. Retroviruses can establish filopodial bridges for efficient cell-to-cell transmission. *Nat. Cell Biol.* **2007**, *9*, 310–315, doi:10.1038/ncb1544.

4. Sherer, N. M.; Jin, J.; Mothes, W. Directional Spread of Surface-Associated Retroviruses Regulated by Differential Virus-Cell Interactions. *J. Virol.* **2010**, *84*, 3248–3258, doi:10.1128/JVI.02155-09.

5. Sowinski, S.; Jolly, C.; Berninghausen, O.; Purbhoo, M. A.; Chauveau, A.; Köhler, K.; Oddos, S.; Eissmann, P.; Brodsky, F. M.; Hopkins, C.; Önfelt, B.; Sattentau, Q.; Davis, D. M. Membrane nanotubes physically connect T cells over long distances presenting a novel route for HIV-1 transmission. *Nat. Cell Biol.* **2008**, *10*, 211, doi:10.1038/ncb1682.

6. Kadiu, I.; Gendelman, H. E. Macrophage Bridging Conduit Trafficking of HIV-1 Through the Endoplasmic Reticulum and Golgi Network. *J. Proteome Res.* **2011**, *10*, 3225–3238, doi:10.1021/pr200262q.

7. Roberts, K. L.; Manicassamy, B.; Lamb, R. A. Influenza A Virus Uses Intercellular Connections To Spread to Neighboring Cells. *J. Virol.* **2014**, *89*, 1537–1549, doi:10.1128/JVI.03306-14.

8. Frischknecht, F.; Way, M. Surfing pathogens and the lessons learned for actin polymerization. *Trends Cell Biol.* **2001**, *11*, 30–38, doi:10.1016/S0962-8924(00)01871-7.

9. Ueki, S.; Citovsky, V. To Gate, or Not to Gate: Regulatory Mechanisms for Intercellular Protein Transport and Virus Movement in Plants. *Mol. Plant* **2011**, *4*, 782–793, doi:10.1093/mp/ssr060.

10. Zambryski, P. Plasmodesmata. *Curr. Biol.* **2008**, *18*, R324–R325.

11. Niehl, A.; Heinlein, M. Cellular pathways for viral transport through plasmodesmata. *Protoplasma* **2011**, *248*, 75–99, doi:10.1007/s00709-010-0246-1.

12. Kim, I.; Kobayashi, K.; Cho, E.; Zambryski, P. C. Subdomains for transport via plasmodesmata corresponding to the apical-basal axis are established during Arabidopsis embryogenesis. *Proc. Natl. Acad. Sci. U. S. A.* **2005**, *102*, 11945–50, doi:10.1073/pnas.0505622102.

13. Oparka, K. J.; Roberts, A. G.; Boevink, P.; Cruz, S. S.; Roberts, I.; Pradel, K. S.; Imlau, A.; Kotlizky, G.; Sauer, N.; Epel, B. Simple, but Not Branched, Plasmodesmata Allow the Nonspecific Trafficking of Proteins in Developing Tobacco Leaves. *Cell* **1999**, *97*, 743–754, doi:10.1016/S0092-8674(00)80786-2.

14. Hipper, C.; Brault, V.; Ziegler-Graff, V.; Revers, F. Viral and Cellular Factors Involved in Phloem Transport of Plant Viruses. *Front. Plant Sci.* **2013**, *4*, doi:10.3389/fpls.2013.00154.

15. Hayakawa, T.; Kojima, K.; Nonaka, K.; Nakagaki, M.; Sahara, K.; Asano, S. I.; Iizuka, T.; Bando, H. Analysis of proteins encoded in the bipartite genome of a new type of parvo-like virus isolated from silkworm - Structural protein with DNA polymerase motif. *Virus Res.* **2000**, *66*, 101–108, doi:10.1016/S0168-1702(99)00129-X.

16. Ladner, J. T.; Wiley, M. R.; Beitzel, B.; Auguste, A. J.; Dupuis, A. P.; Lindquist, M. E.; Sibley, S. D.; Kota, K. P.; Fetterer, D.; Eastwood, G.; Kimmel, D.; Prieto, K.; Guzman, H.; Aliota, M. T.; Reyes, D.; Brueggemann, E. E.; St. John, L.; Hyeroba, D.; Lauck, M.; Friedrich, T. C.; O'Connor, D. H.; Gestole, M. C.; Cazares, L. H.; Popov, V. L.; Castro-Llanos, F.; Kochel, T. J.; Kenny, T.; White, B.; Ward, M. D.; Loaiza, J. R.; Goldberg, T. L.; Weaver, S. C.; Kramer, L. D.; Tesh, R. B.; Palacios, G. A Multicomponent Animal Virus Isolated from Mosquitoes. *Cell Host Microbe* **2016**, *20*, 357–367, doi:10.1016/j.chom.2016.07.011.

17. Sicard, A.; Michalakis, Y.; Gutiérrez, S.; Blanc, S. The Strange Lifestyle of Multipartite Viruses. *PLOS Pathog.* **2016**, *12*, e1005819, doi:10.1371/journal.ppat.1005819.

18. Verchot-Lubicz, J.; Torrance, L.; Solovyev, A. G.; Morozov, S. Y.; Jackson, A. O.; Gilmer, D. Varied movement strategies employed by triple gene block-encoding viruses. *Mol. plant-microbe Interact.* **2010**, *23*, 1231–1247, doi:10.1094/MPMI-04-10-0086.

19. Dall'Ara, M.; Ratti, C.; Bouzoubaa, S.; Gilmer, D. Ins and Outs of Multipartite Positive-Strand RNA Plant Viruses: Packaging versus Systemic Spread. *Viruses* **2016**, *8*, 228, doi:10.3390/v8080228.

20. Tamada, T.; Kondo, H.; Bouzoubaa, S. Pattern of systemic movement of soil-borne plant viruses: evidence obtained from GFP-tagged Beet necrotic yellow vein virus. *Proc. Ninth Symp. Int. Work. Gr. Plant Viruses with Fungal Vectors, Obihiro, Hokkaido, Japan, 19-22 August 2013* 2013, 11–14.

21. Yvon, M.; Monsion, B.; Martin, J.-F.; Gutiérrez, S.; Blanc, S. PCR-based amplification and analysis of specific viral sequences from individual plant cells. *J. Virol. Methods* **2009**, *159*, 303–307, doi:10.1016/J.JVIROMET.2009.04.016.

22. Veidt, I.; Bouzoubaa, S. E.; Leiser, R. M.; Ziegler-Graff, V.; Guilley, H.; Richards, K.; Jonard, G. Synthesis of full-length transcripts of beet western yellows virus RNA: messenger properties and biological activity in protoplasts. *Virology* **1992**, *186*, 192–200.

23. Lauber, E.; Guilley, H.; Tamada, T.; Richards, K. E.; Jonard, G. Vascular movement of beet necrotic yellow vein virus in Beta macrocarpa is probably dependent on an RNA 3 sequence domain rather than a gene product. *J. Gen. Virol.* **1998**, *79*, 385–393, doi:10.1099/0022-1317-79-2-385.

24. Kuuszala, M.; Ziegler-Graff, V.; Bouzoubaa, S.; Richards, K.; Putz, C.; Guilley, H.; Jonard, G. Beet necrotic yellow vein virus: different isolates are serologically similar but differ in RNA composition. *Ann. Appl. Biol.* **1986**, *109*, 155–162, doi:10.1111/j.1744-7348.1986.tb03194.x.

25. Tamada, T.; Shirako, Y.; Abe, H.; Saito, M.; Kiguchi, T.; Harada, T. Production and pathogenicity of isolates of beet necrotic yellow vein virus with different numbers of RNA components. *J. Gen. Virol.* **1989**, *70*, 3399–3409.

26. Wang, Y.; Fan, H.; Wang, X.-B.; Li, M.; Han, C.; Li, D.; Yu, J. Detection and characterization of spontaneous internal deletion mutants of Beet Necrotic yellow vein virus RNA3 from systemic host Nicotiana benthamiana. *Virol J* **2011**, *8*, 335.

27. Peltier, C.; Hleibieh, K.; Thiel, H.; Klein, E.; Bragard, C.; Gimer, D. Molecular Biology of the Beet necrotic yellow vein virus. *Plant Viruses* **2008**, *2*, 14–24.

5. Annexes

Primers	Taq-man TAMRA probes	Amplicon lenght
BNYVV1 F(TGGTTTCACAAGGAGATGTCGTT) BNYVV1 R (TCTGCACAATCAAAGGCATCA)	FAM-TTTTGGACATAGCACGTGTGGAAAACGATA	78
BNYVV2 F(TGGACCCGGGATAAATTTGA) BNYVV2 R(CGGGTGGACTGGTTCTACCTT)	HEX-ACCGGTTCAAATTACCATGGACACCTGTT	72
BNYVV3 F(ATATGTGAGGACGCTAGCCTGTT) BNYVV3 R(TGAAACGATGGAGTCACTATGCTT)	FAM-CTGACCGACCAAATCCAAGCGAGCTTAAT	118
BNYVV4 F(TCCTCCTTTGATACGTCATGAAGA) BNYVV4 4R(CAATGGGCCAATCTCAATCC)	HEX-TGATTGTACTGCTAGGATGGTGCA	75
RbcL F(GGTAACGTATTTGGGTTCAAAGC) RbcL R(CATCTTTGGTAAAATCAAGTCCACC)		244

Table 4 Primers, probes ad relative amplicons used for triplex RT-qPCR

Chapter III

A specific heterologous RNA/RNA interaction is involved in the BNYVV infectivity

1. Introduction

Maintenance of genome integrity to prevent loss of genetic information is a vital requisite for viruses as well as for any kind of organism. If genomic corruption by recombination events, inaccurate replication, attack by nucleases or other host modifying enzymes [1] are excluded, monopartite viruses fulfill easily the "one genome one infectious unit" paradigm [2] since their genome is constituted by one unique codifying unit. Conversely, segmented and multipartite viruses have to developed strategies to bring the different genomic entities together in collective units especially during the transmission from one cell to another within the same host or between hosts [3]. Such strategies are well described for segmented virus and are finalized to assure in each mature virion the complete set of genomic segment. The tripartite dsRNA genome of phage φ6 is packaged through a NTP dependent mechanism involving the controlled and sequential recognition of Small (S), Medium (M) and Large (L) different plus strand transcripts by preformed dodecahedral pro-capsid particle or inner core [4,5] (Figure 1). The inner core recognizes each different segments from their specific 5' end packaging domains. Furthermore, sequential recognition depends on conformational changes that take place whenever previous type of ssRNA has been packaged [4,5]. After packaging of the last (L) ssRNA, The inner core changes its conformation to allow minus strands syntheses [4,5]. From dodecahedral, the particles become spherical [4,5]. Specific recognition between viral proteins and genomic RNAs is not the sole determinant for packaging specificity of segmented virus. Recent studies demonstrate that for some segmented animal virus, belonging to *Reoviridae* and *Orthomyxoviridae* family, the specific and coordinated segment packaging is determined by RNA/RNA interaction networks [6–8]. Such model was deeply investigated for Influenza A virus (IAV) together with its important genetic reassortment processes [9]. IAV genome consists of eight single stranded negative sense RNAs (vRNAs) organized in individual ribonucleoprotein complexes (vRNPs) that show a conserved

tridimensional supramolecular organization inside the viral particle. This organization is characterized by the disposition of seven vRNPs around one central vRNP corresponding to vRNA1 (7+1 pattern) [7,10]. This supramolecular complex formation depends on a selective packaging mechanism implying direct RNA/RNA interactions [9]. The resulted network of interactions between viral RNAs appears to be strain specific and plays an important function in the regulation of genomic reassortment events. Only IAV strains with a compatible network of interaction can generate reassortant progenies [9] (Figure 2).

Genomic RNAs of multipartite viruses do not co-package in one mature virion but are segregated in different and independent particles [3]. Such aspect discriminate segmented and multipartite viruses that should have evolve alternative strategies to selective co-packaging in order to produce collective infectious units able to preserve genome integrity during the host colonization. The multipartite *Beet necrotic yellow vein virus* (BNYVV) spreads in the plant as RNP complexes that require TGB proteins for cell to cell movement and CP for its systemic infection [3,11,12]. Segment encapsidation appears dispensable for the long distance movement of the virus [3,13]. No BNYVV protein has been identified as able to specifically bind and discriminate one genomic RNA from another [14]. We expected BNYVV collective infection unit to depend on network of RNA/RNA interaction that could insure the presence of at least one of each genomic RNAs [3]. This hypothesis recalls the demonstration of RNA-RNA interactions required for IAV segments packaging. My objective was to experimentally determine the existence of such RNA/RNA interactions between genomic RNA1 and RNA2, the minimal infectious unit of BNYVV. Indeed, within certain hosts, RNA1 and RNA2 are sufficient for the systemic infection of the plant. Thus, the minimal efficient RNP complex should involve RNA1 and RNA2 interaction. For this reason, the existence of specific heterologous interactions between these two RNAs has been evaluated as well as the implication for such interactions in the BNYVV viral cycle.

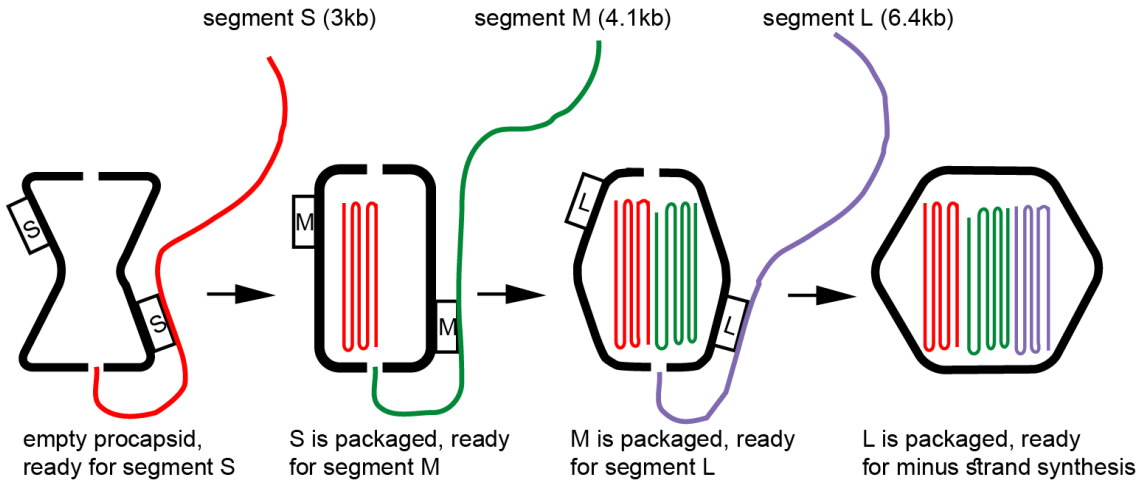

Figure 1. Packaging model proposed for the φ6 bacteriophage. The inner core interacts specifically with S segment. After S packaging, a M binding site appears on the inner core and similarly, after M packaging L binding site allows the entry of the largest segment When all three segment are packaged minus strand synthesis starts. (modified from Mindich [4]). This model could fit with a specific S entry bringing M segment and then L within the capsid thanks to RNA/RNA interactions.

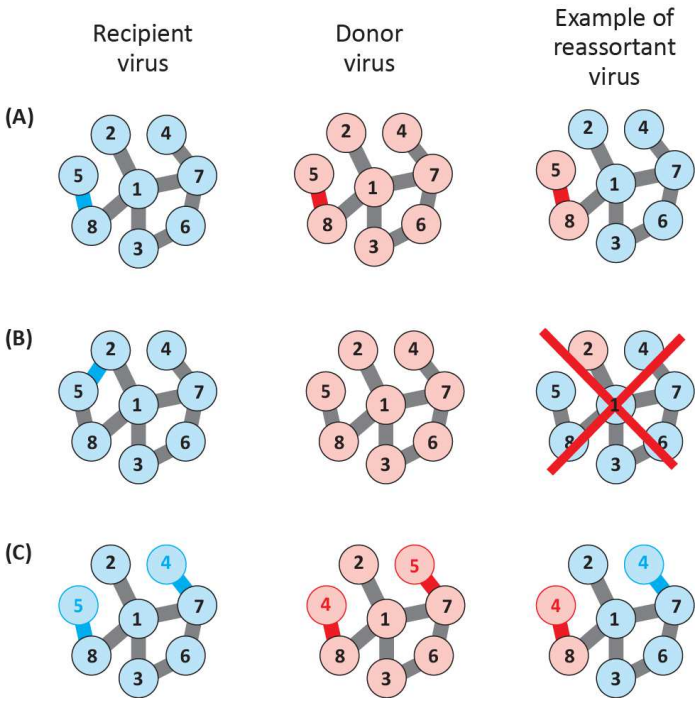

Figure 2 Model of IAV RNA/RNA interactions and its implications on genetic reassortment. (A) example of compatible exchanges of vRNAs: vRNA5 and vRNA8 interact through different (incompatible) sequences (blue and red lines) in the two parental viruses while vRNA1 and vRNA8 interaction is compatible. The two parental viruses have the same RNA/RNA network of interaction. Co-segregation of vRNA5 and vRNA8 from donor virus to recipient virus is possible and results in a new functional reassortant virus. (B) vRNA2 and vRNA5 interaction exists in the recipient virus but not in the donor virus. This might prevent the segregation vRNA2 from donor to recipient virus. (C) In recipient virus vRNA8 interacts with vRNA1 and with vRNA5 while in donor virus vRNA8 interacts with vRNA1 and vRNA4. Segregation of vRNA8 together with vRNA4 from donor virus to recipient virus is possible but lead to the formation of a defective virus for vRNA5 (modified from Gerber et al. [9]).

2. Material and methods

2.1 Plasmids for Electro Mobility Shift Assay (EMSA)

RNA1b, RNA1c, RNA1d, RNA1e and RNA2d partial cDNA clones (Table 1) have been obtained by cloning of PCR products, integrating T7 RNA polymerase promoter, into pUC19-based vectors. PCR reactions have been conducted using Phusion High-Fidelity PCR Master Mix (Thermo Fisher Scientific), BNYVV (B type) RNA1 (pB15) and RNA2 (pB214) full length cDNA clones [12] as templates and DNA oligonucleotides primers described in Table 2. Amplicons have been cloned into pUC19 using *Eco*RI and *Hin*dIII restriction sites, after digestion and ligation by, respectively, FastDigest restriction and T4 DNA Ligase enzymes (Thermo Fisher scientific). Recombinant plasmids have been linearized by *Hin*dIII restriction enzyme before *in vitro* transcription. All enzymatic reactions have been carried out according to manufacturer's protocol.

Partial clones	First nucleotide	Last nucleotide	Restriction site for linearization
RNA1a	1	1424	*Age*I
RNA1b	1367	2455	*Hin*dIII
RNA1c	2455	3801	*Hin*dIII
RNA1d	3655	4748	*Hin*dIII
RNA1e	4748	6746	*Hin*dIII
RNA2a	1	2715	*Sal*I
RNA2b	1	1113	*Mlu*I
RNA2c	1	668	*Nco*I
RNA2d	1155	2789	*Hin*dIII
RNA2e	1155	2065	*Pst*I

Table 1 List of partial cDNA clones used to produce *in vitro* transcripts for EMSA. The first and the last nucleotide of BNYVV sequence produced is indicated for each clone as well as the restriction enzyme used for linearization before run-off transcription.

RNA1a, RNA2b, RNA2c and RNA2e clones derives from previously reported plasmids whose sequences, downstream T7 promoter, have been shortened by linearization using alternative restriction enzymes. In particular, RNA1a has been produced from pB15 linearized with *Age*I. RNA2a, RNA2b and RNA2c have been produced using the partial cDNA clone pB218 [15] linearized with *Sal*I, *Mlu*I and *Nco*I restriction enzymes, respectively. RNA2e derives from RNA2d.

Plasmid was digested with *Pst*I followed by an exonuclease digestion of 3' end protrusion by T4 DNA polymerase (Thermo Fisher Scientific). All enzymatic reactions were carried out according manufacturer's protocol.

Clone	Primer pair	Sequence
RNA1b	***Eco*RI T7 RNA1 1367 F**	TT GAATTC TAATACGACTCACTATAGGG $_{1367}$GTGAAG ATGTTGGTTAC
	***Hin*dIII RNA1 2566 R**	AA AAGCTT $_{2566}$CCGCCCCGCACTCTAC
RNA1c	***Eco*RI T7 RNA1 2455 F**	TT GAATTC TAATACGACTCACTATAGGG $_{2455}$CCTGCTGACACTTTAC
	***Hin*dIII RNA1 3801 R**	AA AAGCTT $_{3801}$CCCAAGGTACATCCCAAC
RNA1d	***Eco*RI T7 RNA1 3655 F**	TT GAATTC TAATACGACTCACTATAGGG $_{3655}$CTGGTAGCTTTATCTCG
	***Hin*dIII RNA1 4783 R**	TT AAGCTT $_{4783}$CAGTCTTTCCCCCTGCC
RNA1e	***Eco*RI T7 RNA1 4748 F**	TT GAATTC TAATACGACTCACTATAGGG $_{4748}$ACGATGATTTTGTC
	***Hin*dIII RNA1 6746 R**	GCC AAGCTT TTTTTTTTTTTTTTTTT $_{6746}$ATATCAATATACTGA
Rna2d	***Eco*RI T7 RNA2 1155 F**	TT GAATTC TAATACGACTCACTATAGGG $_{1155}$TGTTAGTTTGGGAACC
	***Hin*dIII RNA2 2789 R**	TT AAGCTT $_{2789}$TAACCCTTGCGCCGGATC

Table 2 Primers used for RNA1 and RNA2 partial cDNA cloning into pUC19

2.2 Native or partially denaturating EMSA of *in vitro* co-transcribed transcripts

Couples of linearized plasmid templates were co-transcribed *in vitro* at 37°C for 3 h, using RiboMAX™ Large Scale RNA Production System-T7 (Promega) according to the following protocol:

- 0.5 µl linearized plasmid 1 (250 ng)
- 0.5 µl linearized plasmid 2 (250 ng)
- 2 µl Buffer 5X
- 3 µl rNTP (100 µM each)
- 0.25 µl RNase inhibitor (40U/µl) (RNasin Promega)
- 0.5 µl DTT (100 mM)
- 1 µl T7 RNA polymerase (20U/µl)
- 2.25 µl DNase/RNase free water

DNA templates were then removed adding 1µl of RQ1 RNase-Free DNase (1U/µl) (Promega) and incubating the reaction for 30 min at 37°C. Two µL of blue loading solution (50% glycerol, bromophenol blue) were added to the transcription reaction products prior analysis on 0.8% native (TBM: Tris 25 mM; boric acid 22.25 mM; $MgCl_2$ 50 µM; Ethidium bromide 0.5 µg/ml) or partially denaturating Mg^{2+}-chelating (TBE: Tris 45 mM; boric acid 45mM; EDTA 1.25 mM; Ethidium

bromide 0.5 µg/ml) agarose gel electrophoresis conducted at 150 V for 4 h at 4°C. After imaging the gel under UV exposure, RNAs were transfered from agarose gels to Hybond-NX membranes overnight by capillarity in 20X SSC buffer. RNAs were UV cross-linked and membranes were pre-hybridized at 60°C for at least one hour in Perfect Hyb PlusTM hybridization buffer (Sigma-Aldrich). Hybridizations with ^{32}P labeled ODNs were carried out overnight at 42°C. Membranes were washed for 15 min at 50°C in 2XSSC 2% SDS buffer. Transfer of the γ-phosphate from ^{32}P γ labeled ATP to the 5'-OH of ODN probes (10-30 pmol) (Table 3) was performed by T4 Polynucleotide Kinase according to manufacturer's protocol (Thermo Fisher Scientific). Unincorporated radiolabeled ATP was removed by gel filtration using G-25 Sepharose colums. Radiolabeled RNAs and related band-shifts were detected by autoradiography.

RNA	ODN	Sequence
RNA1	3739 R	$_{3739}$TGCCTTTCAAAACAGCACC
RNA2	334 R	$_{334}$GTCAGTCCAACCCGAGCCC
RNA2	B3	$_{188}$TGTGACATATCCTTCCATGT
RNA2	F3	$_{646}$ATTTATCCCGGGTCCACATT

Table 3 Complementary ODNs used to probe RNA1 and RNA2 partial clones in EMSAs

2.3 Site directed mutagenesis of BNYVV full length cDNA clones

Site directed mutagenesis of full length RNA1 and RNA2 cDNA clones have been carried out using primer listed in table 4 using the one step quick change strategy described by Liu et al.[16].

RNA	Primer pair	Sequence
RNA1	Mut RNA1 F	$_{4353}$GTCCGGTGACAACAGTAAGAAACC
	Mut RNA1 R	$_{4376}$GGTTTCTTACTGTTGTCACCGGAC
RNA2	Mut RNA2 F	GG$_1$AAATTCTAACTGTTGTCACCATTG
	Mut RNA2 R	$_{38}$GGTGAAATTCTATTCAATGGTGACAACAGT

Table 4 ODNs used for site directed mutagenesis of RNA1 and RNA2 cDNA clones. Point mutations are underlined.

Briefly, PCR reactions have been conducted using Phusion High-Fidelity PCR Master Mix (Thermo Fisher Scientific) and pB15 or pB214 plasmids as templates. *In vivo* methylated templates were removed by *Dpn*I digestion (FastDigest Thermo Fisher Scientific) and amplicons were purified by phenol/chloroform extraction and NaCl/EtOH precipitation. All enzymatic reactions have been

carried out according to manufacturer's protocol. Purified PCR products have been used to transform Sure2 (RNA1 mut) and MC1022 (RNA2 mut) (Stratagene) electro-competent *Escherichia coli* cells.

2.4 Construction of RNA5 derived replicons carrying RNA1 or RNA2 interaction domains

RNA5 derived replicons (Rep5) [17] carrying RNA1 and RNA2 interaction domains in their natural context (Rep5 RNA1 I.D. and Rep5 RNA2 I.D.), have been used to conduct *in vivo* experiments with the aim to disrupt RNA1/RNA2 interactions. The first 400 nts of pB214 or the mutagenized clone as well as the RNA1 interaction domain (present between nts 4,143 and 4,520 of pB15) and the mutagenized version have been amplified by PCR using Phusion High-Fidelity PCR Master Mix (Thermo Fisher Scientific) and primers, flanked with *Bam*HI (Table 5). *Bam*HI-digested amplicons were introduced into *Bgl*II linearized Rep5-cDNA clone and ligated using their compatible cohesive ends. After transformation, insert orientation was verified by PCR. Prior to *in vitro* transcription, replicons Rep5 RNA1 I.D, Rep5 RNA1 I.D. mut, Rep5 RNA2 I.D and Rep5 RNA2 I.D. mut were linearized by *Hin*d III digestion..

RNA	ODN	Sequence
RNA1	RNA1 *Bam*HI 4143 F	AA GGATCC $_{4143}$GTCTCCATCAACTTGG
RNA1	RNA1 *Bam*HI 4520 R	AA GGATCC $_{4520}$CACGATTGCAAGCTC
RNA2	RNA2 *Bam*HI I 1 F	AA GGATCC $_{1}$AAATTCTAACTATTATCTCC
RNA2	RNA2 *Bam*HI 1mut F	AA GGATCC $_{1}$AAATTCTAACTGTTGTCACC
RNA2	RNA2 *Bam*HI 400 R	AA GGATCC $_{400}$ACACAAGTGCACCATAC

Table 5 ODNs used for the obtention of RNA5-derived cDNA replicons carrying RNA1 or RNA2 interaction domains. RNA2 point mutations are underlined

2.5 *In vitro* transcription, infection of *Chenopodium quinoa* protoplasts or plants and Northern blotting (high molecular weight RNAs)

Linearized full-length Benyviridae clones pB15, pB214, RNA1 mut, RNA2 mut, *Beet soil-borne mosaic virus* (BSBMV) RNA2 [18] as well as linearized Rep5 replicons carrying wild type or mutated BNYVV RNA1 or RNA2 interaction domains, served for *in vitro* run-off transcription as

previously described [12,17,18]. Electroporation of *C. quinoa* protoplasts and mechanical infection of *C. quinoa* plants have been conducted as previously described [19,20]. Viral RNAs have been extracted using "polysome buffer" protocol [21] while Northern blot RNA analyses have been conducted as previously described [11,22,23].

3. Results

3.1 EMSAs of *in vitro* co-transcription of partial RNA1 and RNA2 cDNA clones

In vitro co-transcription of RNA1 and RNA2 full length or partial T7 cDNA clones has been followed by electrophoresis into native and Mg^{2+}-chelating agarose gels. Homo and hetero RNA duplexes have been observed both by ethidium bromide staining and hybridization using specific radiolabeled ODN probes after RNA transfer. In the described conditions no significant band-shift has been observed with full length RNA1 and RNA2 (data not shown) probably due to an absence of cellular or viral factors that could help and stabilized RNA/RNA interactions in the natural context. The use of RNA1d and RNA2a partial clones (Figure 3 (A)) highlighted one important hetero duplex retrieved as well in semi-denaturing conditions where Mg^{2+}-stabilization of RNA structures is reduced (Figure 3 (1, I, 2, II)). Such interaction appears specific since no band shift was observed when Luciferase mRNA was co-transcribed with RNA2a (data not shown). Interestingly, using specific probes, I also evidenced RNA1c and RNA1e homo-dimerization indicating that BNYVV RNAs self-interact. If the biological significance of such homo-interaction has been not investigated in this chapter, it could suggest that BNYVV RNP supramolecular assembly can involve more than one genomic RNA molecule of the same species, rendering the stoichiometry determination difficult. The complete sequences of RNA1 and the domain of RNA2 ranging from its 5' to last residue preceding the first nucleotide of subgenomic RNA2 have been

tested. This follows our proposed model of supramolecular assembly of genomic RNAs where shorter RNA species should not compete.

EMSA of products obtained co-transcribing RNA1d with partial sequences of RNA2a (RNA2b, RNA2c, RNA2d and RNA2e) (Figure 4 (A)) reveals that the RNA2 domain involved in the RNA1d/RNA2a interaction is located within its first 668 nts (Figure 4 (1 , 2)). Interestingly, two RNA2 self-interaction domains, located within the first 668 and between nucleotides 1155 and 2065, have been detected. In particular, RNA2e self-interaction does not appear as an alternative to an hetero-dimer formation since both complexes are present after co-transcription of RNA1d/RNA2c.

To localize more precisely the region involved in the RNA1d/RNA2c interaction, we introduced into the co-transcription mixes five complementary ODNs (10 pmol each). These ODNs represent putative competitors covering the first 668 bases of RNA2 (table 6). In these condition, no RNA/RNA interaction was detected in the presence of A1 - A5 ODNs mixes, covering the first 116 nucleotides (Figure 5 (1, 2)). Finally, using single ODN (A1 to A5) as competitor, the RNA2 interaction domain has been localized within the first 20 nts. Indeed, the use of ODN A1 alone prevent RNA1d/RNA2b hetero-dimer formation (Figure 6 (2, 3)).

In order to identify the domain of RNA1d sequence putatively able to interact with the first 20 nts of RNA2, the IntaRNA program (Freiburg RNA Tools) has been used for *in silico* analysis [24,25]. A maximum score has been found and corresponds to a 17 nts long sequence located in the coding region of RNA1, between nucleotides 4357 and 4373. This suspected RNA1/RNA2 interaction consists therefore in Watson-Crick base pairing of 17 nucleotides with a bulge due to two unpaired bases (Figure 7 panel I). BLAST analyses revealed a high conservation of both motifs within BNYVV RNA1 and RNA2 published sequences of different strains: 100% nucleotide conservation was found for RNA2 whereas one nucleotide mismatch exist for a RNA1 isolate that results in a A-

U to G-U base pair substitution in the extended duplex dimer. However, one Japanese isolate (GenBank accession number: KX665536.1) presents a supplemental mismatch in the RNA1 domain sequence and no compensatory sequence was found in this isolate RNA2 domain.

Synonymous and compensatory mutations based on *three nucleotide changes* (Figure 7, panel I) were designed on ODNs and EMSA experiments. For this purpose, I used competitor oligonucleotides covering interactions domains and carrying or not the indicated mutations. Competitor ODNs A1, G1 and H1 were able to prevent the RNA1/RNA2 interactions as seen for A1 ODN previously (Figure 6). However, ODN A1 mut and H1 mut, were not able to disrupt the interaction between wild type RNAs (Figure 7, panel II) (Table6).

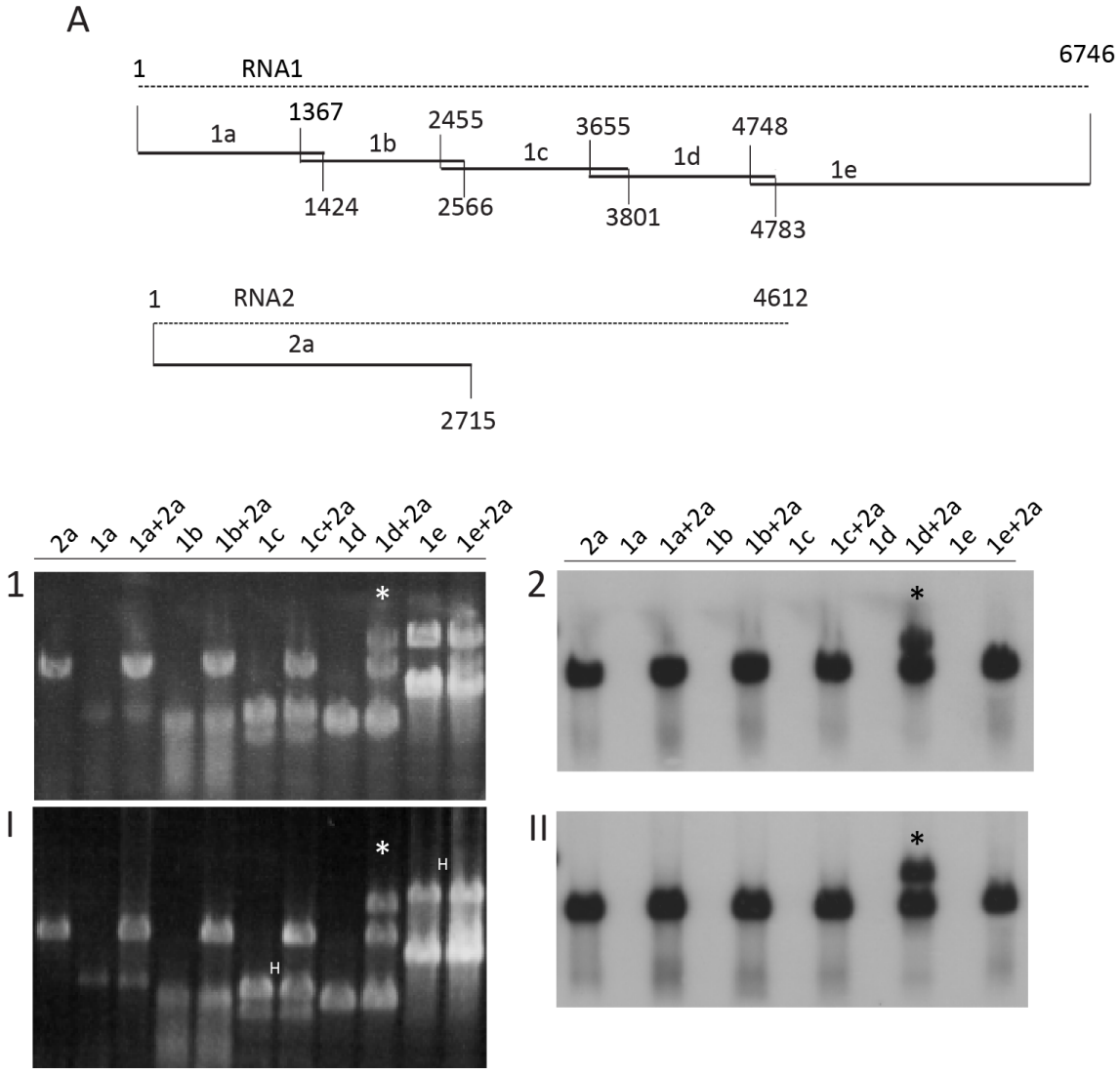

Figure 3 EMSA I: (A) representation of the sequences covered by RNA1a, b, c, d, e and RNA2a partial clones used for qualitative analysis of RNA/RNA interaction by native agarose gel (1) or semi-denaturing TBE agarose gel (I). To improve the resolution, RNAs were transferred onto membranes (2 and II) and RNA2 revealed using radio-labeled ODNs 334R (Table 3). Asterisks indicate hetero-dimer formations while H indicates RNA self interaction.

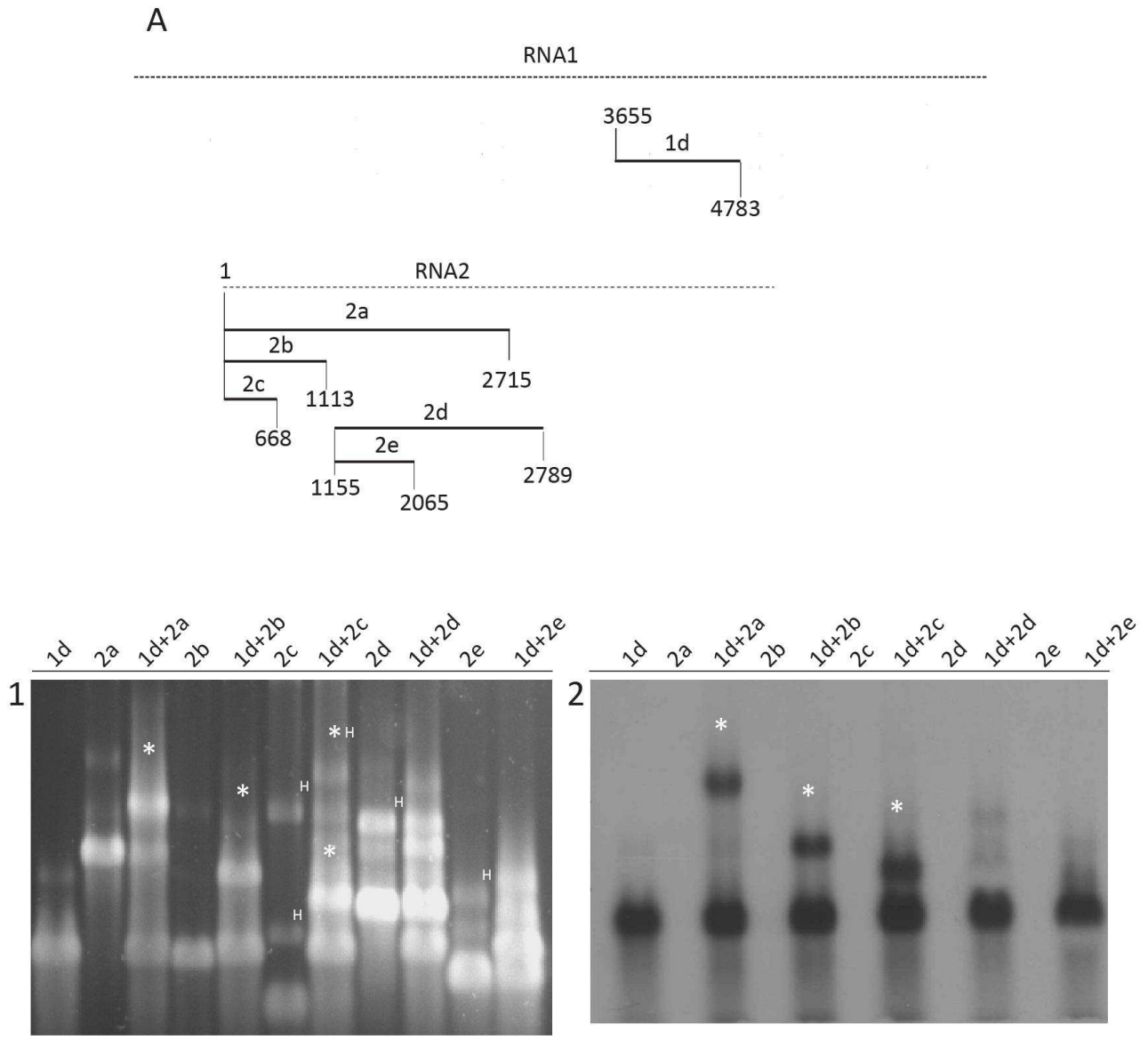

Figure 4 EMSA II: (A) representation of the sequences covered by RNA1d and RNA2a, b, c, d, e partial clones used for RNA/RNA interaction analyses. TBE agarose gel reveals several band-shifts (1) caused by hetero-dimer formation marked with asterisks and homo-multimers marked with H letter; (2) RNAs were transferred onto membranes and RNA1 revealed using radio-labeled ODNs 3739 R (Table 3).

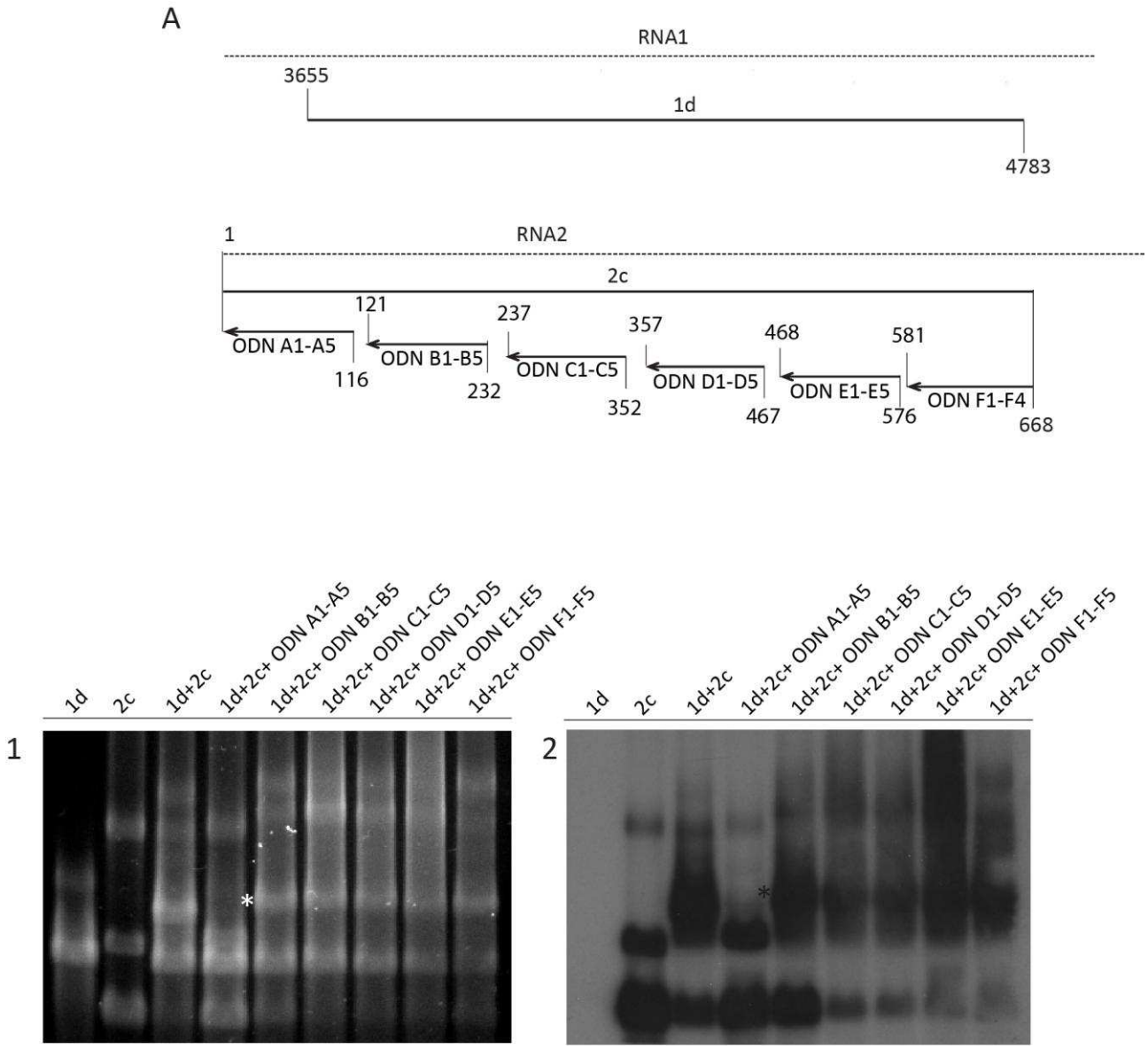

Figure 5 EMSA III: (A) representation of the sequences covered by RNA1d and RNA2c partial clones and six sets of five ODNs (ODN A1-A5, B1-B5, C1-C5, D1-D5, E1-E5, F1-F4 detailed in Table 6). These ODN are complementary to the first 668 nts of RNA2. The interference of ODN on RNA1d/RNA2c interaction has been analysed in TBE gel (1). ODN set able to disrupt the interaction are highlighted by Asterisks. Northern blot (2) analysis has been performed using radio-labeled ODNs (B3 and F3) complementary to RNA2 (Table3).

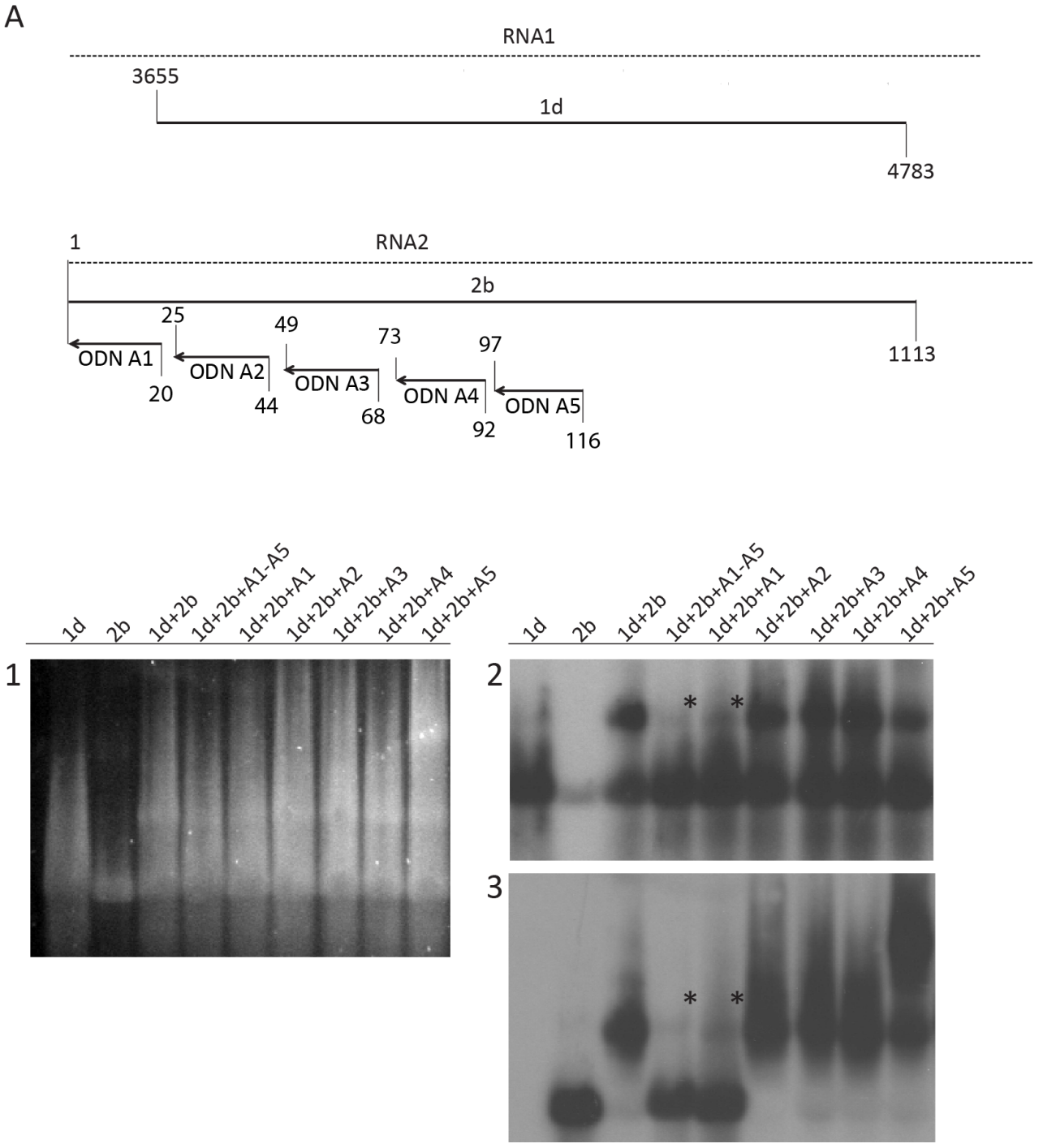

Figure 6 EMSA IV: (A) representation of the sequences covered by RNA1d , RNA2b and ODNs complementary to the first 116 nts of RNA2. RNAs from TBE gel (1) were northern blotted and RNA1d revealed using radio-labeled ODN 3739R (2) while RNA2 positions revealed using radio-labeled ODN 334R (3). Asterisks indicate the disruption of RNA1d/RNA2b hetero-duplex.

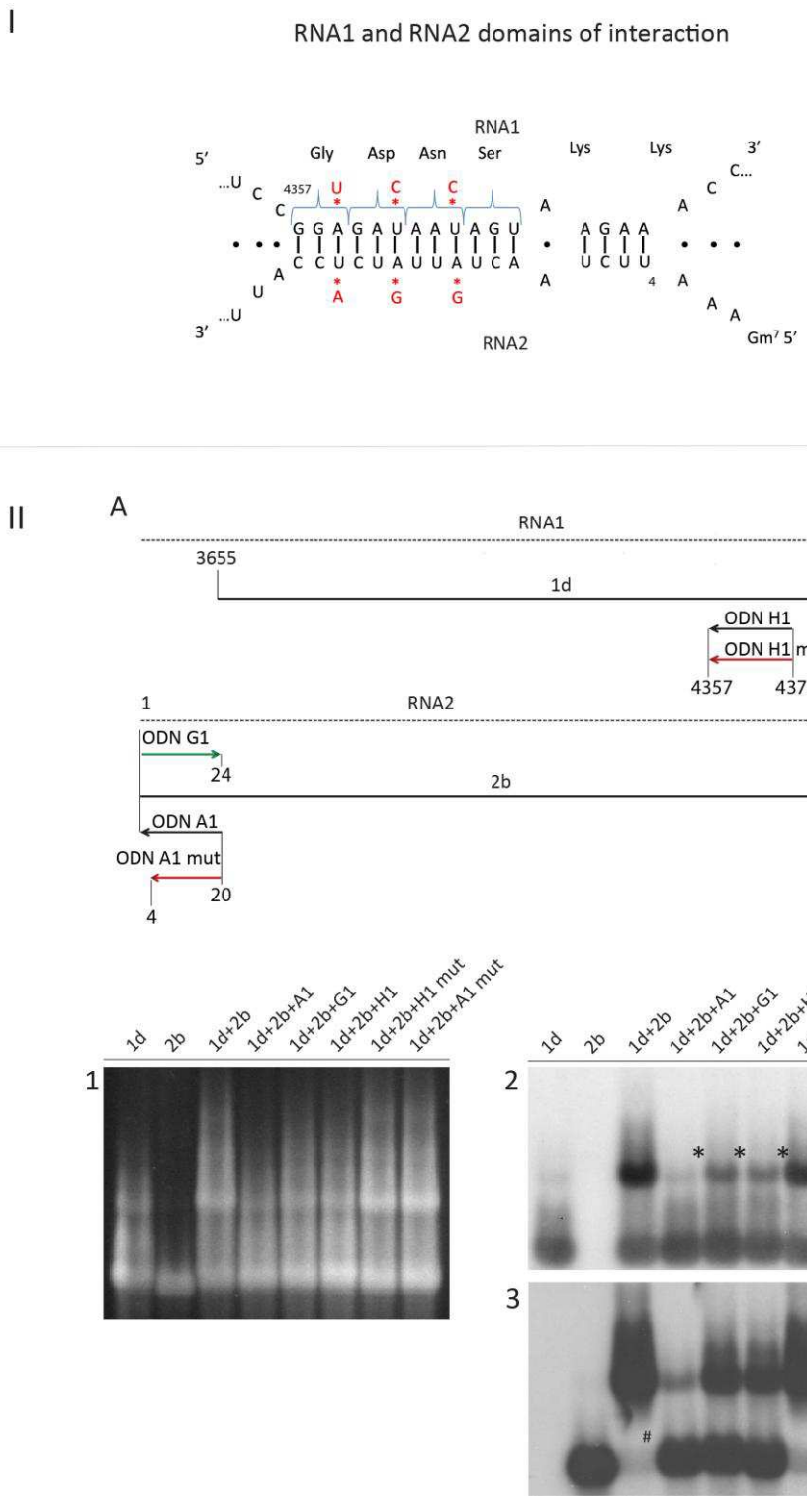

Figure 7 (I) RNA1 and RNA2 interaction domains is characterized by 17 nucleotides base pairing with a bulge due to two unpaired bases (A·A). Bases in red correspond to RNA1 synonymous mutation introduced and compensatory mutations on RNA2 to maintain the interaction. (II) EMSA V: panel A represents the sequences covered by RNA1d , RNA2b and ODNs complementary to both putative interaction domains (A1,H1) and carrying the designed mutations (A1 mut and H1 mut). The capacity to disrupt RNA1d/RNA2b interaction has been also evaluated with ODN G1 (corresponding to the first 24 nts of RNA2, table 6). TBE gel (1) has been blotted in to membrane and RNA1d revealed with radiolabeled ODN 3739R (2) while RNA2b position revealed with ODN 334R (3). Asterisks indicate disruption of RNA1d/RNA2b hetero-duplex and hashtags indicate depletion of RNA2b monomer form.

RNA2	**A1**	$_{20}$GGAGATAATAGTTAGAATTT$_{1}$	**RNA2**	**D1**	$_{376}$GTGTCTGTGGAAAACGGGTC$_{357}$
RNA2	**A2**	$_{44}$ACAGACGGTGAAATTCTATT$_{25}$	**RNA2**	**D2**	$_{400}$ACACAAGTGCACCATACATA$_{381}$
RNA2	**A3**	$_{68}$GCCCCCAGAACAAAATAAGA$_{49}$	**RNA2**	**D3**	$_{424}$CTGGGTCAGACAGATTAACA$_{405}$
RNA2	**A4**	$_{92}$TAAAGTAGGGCCCTGAATAA$_{73}$	**RNA2**	**D4**	$_{448}$CCTTAGTCATTATCAACGCA$_{429}$
RNA2	**A5**	$_{116}$CTACTTATTACTCGCACCTA$_{97}$	**RNA2**	**D5**	$_{467}$GAATCAGTTAAAGTATTT A$_{449}$
RNA2	**B1**	$_{140}$GTACTATCTTCTTCTGGACG$_{121}$	**RNA2**	**E1**	$_{484}$CATTATCTGCTAACCCT$_{468}$
RNA2	**B2**	$_{164}$TATCTACCTTCACTCGACAT$_{145}$	**RNA2**	**E2**	$_{504}$TCTACGTACATTAGCAGATG$_{485}$
RNA2	**B3**	$_{188}$TGTGACATATCCTTCCATGT$_{169}$	**RNA2**	**E3**	$_{528}$AGCTTTATTTCCAGACACCA$_{509}$
RNA2	**B4**	$_{212}$CATCGATCGGTCATAAACTT$_{193}$	**RNA2**	**E4**	$_{552}$ACCAGCAGTTTTACCGGATG$_{533}$
RNA2	**B5**	$_{232}$CGACGTCCGAAACACG$_{217}$	**RNA2**	**E5**	$_{576}$CGTATAAGCAGAGTTCTCAT$_{557}$
RNA2	**C1**	$_{256}$CATGCGATTGTTTAATAACA$_{237}$	**RNA2**	**F1**	$_{600}$TAAACCAGCAAGACTGACAG$_{581}$
RNA2	**C2**	$_{280}$TCGCAGCCTTGGACAAGTCC$_{261}$	**RNA2**	**F2**	$_{622}$CTTCAAGCCTAAGAGCTT$_{605}$
RNA2	**C3**	$_{304}$AAGCAGTTTTAATTATAGAT$_{285}$	**RNA2**	**F3**	$_{646}$ATTTATCCCGGGTCCACATT$_{627}$
RNA2	**C4**	$_{328}$ACCAACCCGAGCCTAATCCT$_{309}$	**RNA2**	**F4**	$_{668}$GGTAATTTGAACCGGTCC$_{651}$
RNA2	**C5**	$_{352}$GAGACACAAAAGGATTACTG$_{333}$	**RNA2**	**G1$_{(sense)}$**	$_{1}$AAATTCTAACTATTATCTCCATTG$_{24}$
RNA2	**A1$_{mut}$**	$_{20}$GGTGACAACAGTTAGAA$_{4}$	**RNA1**	**H1**	$_{4373}$TTCTTACTATTATCTCC$_{4357}$
RNA2	**I2$_{(sense)}$**	$_{113}$GTAGCCGCCGTCCAGAAGAAG$_{133}$	**RNA1**	**H1$_{mut}$**	$_{4373}$TTCTTACTGTTGTCACC$_{4357}$
			RNA1	**I1**	$_{1421}$ACCTCGAACAAATGCAACC1$_{403}$

Table 6 ODNs used as competitors in EMSAs and in *C. quinoa* protoplast experiments

3.2 *In vivo* experiment of RNA1/RNA2 interaction disruption by interfering of competitive RNA5 derived replicons.

RNA5 derived replicons (Rep5 [22]) carrying interactions domains have been used to evaluate a putative interference with RNA1/RNA2 interaction assembly (Figure 8, A) . These replicons contain a 400 nts sequence of RNA1 or RNA2 encompassing the wild type or mutated interaction domain. Protoplasts were infected with RNA1 and RNA2 (Helper strain) supplemented or not with Rep5 constructions. Viral RNAs were analyzed 40 hpi. The presence of the Rep5 or Rep5 containing the wt or mutated RNA1 interaction domain (Rep5 RNA1 I.D., Rep5 RNA1 I.D. mut) did not interfere with the viral replication machinery, guaranteeing an intracellular accumulation of viral RNAs. However, when Rep5 contained the interaction domain of RNA2 (Rep5 RNA2 ID), no viral accumulation was observed, indicating a defective interfering effect (DI) of the domain used [26]. Such DI effect is partially alleviated with a mutated interaction domain provided by Rep5 (Figure 8, B). Experiments on *C. quinoa* leaves confirmed these results as no local lesion appeared on leaves inoculated with BN12 supplemented with Rep5 RNA2 I.D. However, the capacity of the

virus to form loci of infection was partially restored when Rep5 carried RNA2 mutated domain (Figure 8, B). Finally, Rep5 containing the RNA1 domain (wt or mutated) did not interfered on the infection as indicated by the high number of local lesions formed in the inoculated leaves (Figure 8, B). Molecular analysis of viral RNA accumulations confirmed the absence of RNA1 and 2 accumulation in the presence of Rep5RNA2 I.D. as observed in *C. quinoa* protoplasts. Interestingly, when the mutated version of the Rep5RNA2 I.D. was added to the inoculum, few lesions appeared (Figure 8, C) and their viral RNA content was similar to that observed on BN12 or BN12+ Rep5 inoculum of control (Figure 8, D).

3.3 *In vivo* experiment of RNA1/RNA2 interaction disruption by interfering of competitive ODNs

To discriminate between a DI effect of the Rep5 RNA2 I.D. and an effect of the RNA/RNA interaction, the replication RNA1 and RNA2 was evaluated on *C. quinoa* protoplasts inoculated in the presence or absence of ODN G1 (Table 6), complementary to the interaction domain of RNA1. Since RNA/DNA duplex can trigger cellular RNAse H activity, ODNs complementary to other regions of RNA1 (I1) and to minus strand of RNA2 (I2) have been chosen as controls (Figure 9, A). When the concentration of ODN targeting RNA1 was 15 times higher to the concentration of genomic RNAs, a significant reduction of viral RNA accumulation was detected by Northern blot (Figure 9, B). However, the same behavior has been observed in the negative control when the ratio between ODNs and genomic RNAs was 50:1 probably due to a cytoplasmic RNAse H activity.

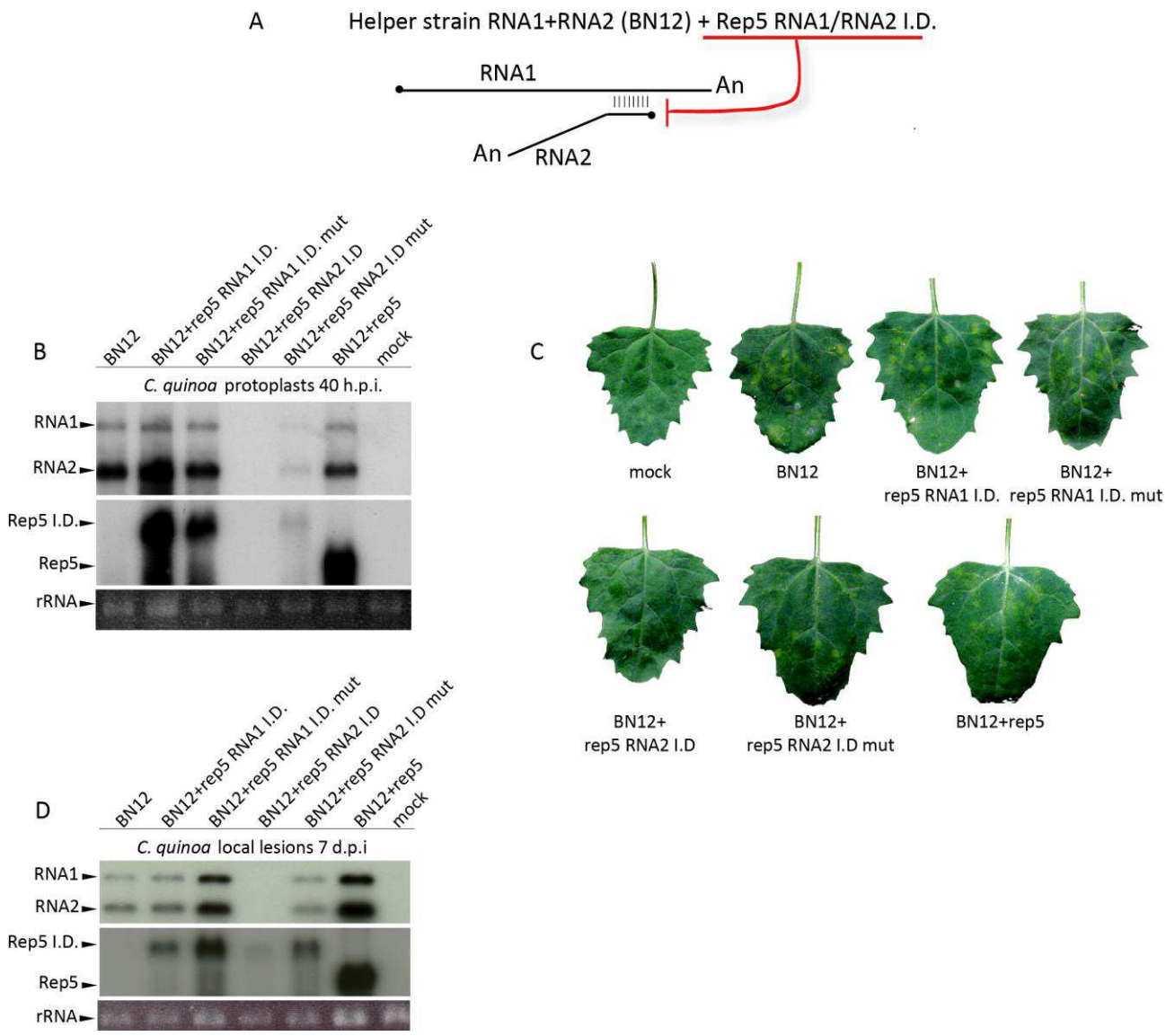

Figure 8 Disruption of RNA1/RNA2 interaction by competitive RNA5 derived replicons. Schematic representation of experimental strategy (A): Rep5 carrying or not an RNA1 or RNA2 interaction domain have been supplemented to RNA1 and RNA2 (BN12) for *C. quinoa* protoplast transfection or mechanical leaf inoculations. Northern blots (B) of vRNAs extracted from protoplast 40 hpi or (D) from leaf local lesions 7 dpi. RNA loads are visualized by Ribosomal RNAs (rRNA) staining. Number of leaf local lesions varies with the inoculum (C): comparable number of local lesions were obtained with BN12 alone or supplemented with Rep5 replicon containing or not wild type or mutated Rep5 RNA1 I.D. No local lesion was observed in leaves when rep5 RNA2 I.D. was added to the BN12 helper strain and few foci of infections were found on leaves inoculated with BN12+rep5 RNA2 I.D.mut.

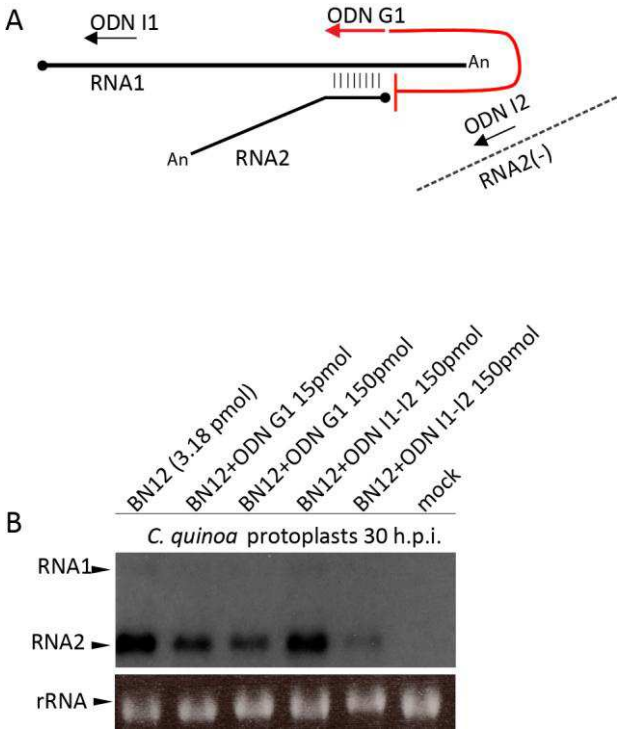

Figure 9 Disruption RNA1/RNA2 interaction with competitive ODNs. Schematic representation of experimental strategy (A): ODN G1 corresponding to the first 24 nts of RNA2 and complementary to RNA1 domain of interaction was used to disrupt RNA1/RNA2 interaction in *C. quinoa* protoplasts. ODNs complementary to other regions of RNA1 (I1) and to minus strand of RNA2 (I2) were chosen as negative controls. Northern blot of vRNAs 30 h.p.i. (B) evidence a significant reduction of viral RNA accumulation when ODN G1 is present even at low concentration (15 pmol). A similar behavior has been observed for the negative control when ratio between ODNs and genomic RNAs were 50:1. rRNAs staining served for RNA loading.

3.4 *In vivo* experiment of disrupted and restored RNA1/RNA2 interaction by synonymous and compensatory mutations

Synonymous and compensatory mutations were introduced within the 17 nts interacting sequences of RNA1 and RNA2 infectious T7 cDNA clones with the aim to prevent and/or restore RNA base pairing *in planta* and validate the biological significance of the RNA/RNA interaction identified. Vitality tests for the mutated genomic RNAs, RNA1 mut and RNA2 mut, were performed in *C. quinoa* plants to evaluate the essential functions of replication, cell to cell movement, and RNA silencing suppression.. Wild type RNA1 (WT) + RNA2 MUT (BN1 WT+BN2 mut) and RNA1 MUT + RNA2 MUT (BN1 mut+BN2 mut) combinations did not allow the formation of local lesion on *C. quinoa* leaves probably due to the 5' promoter disruption on RNA2 MUT. However, RNA1

MUT + RNA2 WT (BN1 mut+BN2 WT) combination allowed the replication and cell to cell movement of the virus, however we observed a dramatic decrease of local lesions number when compared to wild type combination (BN12) (Figure 8). BNYVV and *Beet soil borne mosaic virus* (BSBMV) are distinct but closely related species belonging to the *Benyvirus* genus within the *Benyviridae* family [27] and possess the same genomic organization. Under laboratory conditions genomic RNA exchanges between RNA1 and RNA2 of BNYVV and BSBMV result in functional chimeric viruses [23]. Using bioinformatics comparisons, we evidenced that RNA1 domain of interaction identified in BNYVV is not present on BSBMV RNA1, suggesting that an alternative network of RNA1/RNA2 interaction is established for BSBMV and for Benyviridae reassortants [11]. For this reason we used such opportunity to compare the behavior of BNYVV RNA1 WT + BSBMV RNA2 (BN1BS2) and BNYVV RNA1 MUT + BSBMV RNA2 (BN1 mut+ BS2) chimeras. In *C. quinoa*, numbers of local lesions were similar, demonstrating that the mutations introduced in BNYVV RNA1 were not affecting the replication and viral progression of the chimeras. In BNYVV context, the mutation affected the viral behavior on leaves, suggesting that indeed this RNA-1/RNA-2 interaction is orchestrating a regulatory network.

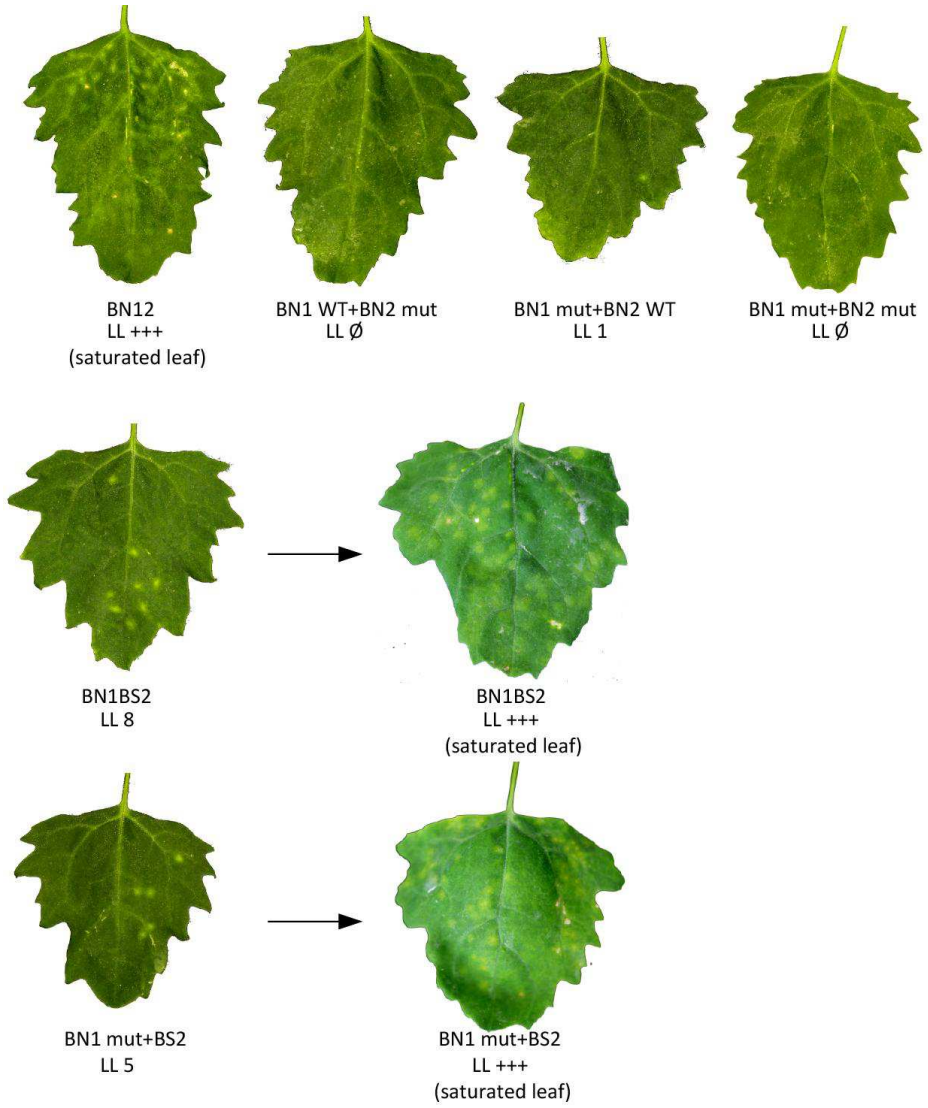

Figure 10 Disruption and restoration of RNA1/RNA2 interaction by synonymous and compensatory mutations. Number of local lesions (LL) in *C. quinoa* leaves 7 dpi of the following RNA combination: BN12, BN1 WT+BN2 mut, BN1 mut +BN2 WT, BN1 mut +BN2 mut, BN1BS2 and BN1 mut +BS2. Black arrows indicate three-fold increase of BSBMV RNA2 quantity in the inoculum

4. Discussion

The existence of interaction between BNYVV RNA1 and RNA2 has been confirmed *in silico* and *in vitro*. Such interaction involves two domains of 17 nts located in highly conserved region of RNA1 (sequence codifying the polymerase) and RNA2 (5' end UTR). No additional interaction domains have been evidenced, we suppose they exist but may be unavailable for interaction because

of their engagement in the formation of alternative structures under experimental conditions. Exposition of certain domains of interaction could be dependent by the presence of viral or cellular factor as regulators of riboswitches. It has been proposed, for example, that *human immunodeficiency virus 1* (HIV-1) leader sequence can adopt two alternative conformations that differ in the presentation of the dimerization initiation site (DIS hairpin) and consequently in its ability to dimerize *in vitro* [28]. Furthermore the presence of viral factor as the nucleocapsid protein enhance, in trans, HIV-1 efficiency to dimerize [29].

Biological significance of BNYVV RNA1/RNA2 interaction has been tested following two different experimental strategies: interfering the formation of RNA1 and RNA2 hetero-complexes using competitor replicon or ODNs and disrupting and restoring RNA1/RNA2 interaction by the introduction of synonymous and compensatory mutations in RNA1 and RNA2 interaction domains. First strategy demonstrates that Rep5 RNA2 D.I. as well as G1 ODN can significantly reduce viral replication rate. However, the mechanism of this interference is still to be verified since we can only attribute to the replicon a defective interfering activity and to G1 ODN the ability to trigger cytosolic RNase H for the RNA1 degradation. The use of oligoribonucleotide instead of ODN can be resolutive to understand if the effect on replication rate should be attributed to a competition between G1 and RNA2 for the interaction with RNA1 rather than to the triggering of RNAse H activity.

Second strategies evidenced that disruption of RNA1 interaction domain by synonymous mutation, leads the virus to strongly decrease its infectivity in *C. quinoa* leaves. In BN1BS2 chimerical context, however, the mutation effect disappears demonstrating that loss of function due to synonymous mutation is completed restored. For this reason we can affirm that RNA1 mut provides an efficient replicase machinery and the dramatic infectivity reduction in *C. quinoa* leaves is related to the disruption of RNA1mut/RNA2 WT interaction that could have an effect on the coordination

of viral replication or, instead on the regulation of cell to cell movement. Experiments on *C. quinoa* protoplast are necessary to validate one or the other hypothesis and sequence analysis of viral population from *C. quinoa* lesions will help to determine if selection and establishment of a *de novo* alternative network interaction between RNA1mut and RNA2WT can overcome the mutation on the RNA1 interaction domain.

An alternative network of interaction should already exist in BN1BS2 chimera and its identification can provide new insights in the regulation of genomic reassortment between Benyviridaes. BNYVV and BSBMV are distinct but closely related species possessing the same host range, vector and genome organization [23]. BNYVV and BSBMV share large areas of infection in the USA and they are frequently present in the same field infecting the same plant. Under laboratory conditions cognate RNA exchanges results in a functional chimeric virus, however, no natural chimeric forms have been described so far in field conditions [23]. The best fitness of parental RNA combination is therefore explained as the selection of the optimal RNA/RNA network interaction that permits, in the natural context, an easier RNA/ RNA recognition for the formation of mobile infective units.

Another way to demonstrate the occurrence of RNA/RNA interaction during the viral spread in the host is to produce an additional RNA able to move at long distance using an artificial RNA/RNA interaction with one of BNYVV genomic RNAs. For this purpose, BNYVV RNA3 derived replicon (Rep3) [30], unable to move long distance [31], and RNA2 eGFP fusion construct [32] should be used in an experiment of gain of function: Rep3 carrying 17 nucleotides long sequences and complementary to eGFP sequence should be tested together with the combination RNA1 + RNA2 eGFP in systemic infection of *Spinacia oleracea*. Occurring of Rep3 systemic spread, together with eGFP tagged helper strain, should represent a fine demonstration of the crucial role that RNA/RNA interaction play in the BNYVV viral movement.

5. References

1. Barr, J. N.; Fearns, R. How RNA viruses maintain their genome integrity. *J. Gen. Virol.* **2010**, *91*, 1373–1387, doi:10.1099/vir.0.020818-0.

2. Sanjuán, R. Collective Infectious Units in Viruses. *Trends Microbiol.* **2017**, *25*, 402–412, doi:10.1016/j.tim.2017.02.003.

3. Dall'Ara, M.; Ratti, C.; Bouzoubaa, S.; Gilmer, D. Ins and Outs of Multipartite Positive-Strand RNA Plant Viruses: Packaging versus Systemic Spread. *Viruses* **2016**, *8*, 228, doi:10.3390/v8080228.

4. Mindich, L. Packaging, replication and recombination of the segmented genomes of bacteriophage Φ6 and its relatives. *Virus Res.* **2004**, *101*, 83–92, doi:10.1016/J.VIRUSRES.2003.12.008.

5. Huiskonen, J. T.; de Haas, F.; Bubeck, D.; Bamford, D. H.; Fuller, S. D.; Butcher, S. J. Structure of the Bacteriophage φ6 Nucleocapsid Suggests a Mechanism for Sequential RNA Packaging. *Structure* **2006**, *14*, 1039–1048, doi:10.1016/j.str.2006.03.018.

6. Fournier, E.; Moules, V.; Essere, B.; Paillart, J.-C.; Sirbat, J.-D.; Cavalier, A.; Rolland, J.-P.; Thomas, D.; Lina, B.; Isel, C.; Marquet, R. Interaction network linking the human H3N2 influenza A virus genomic RNA segments. *Vaccine* **2012**, *30*, 7359–7367, doi:10.1016/j.vaccine.2012.09.079.

7. Gavazzi, C.; Isel, C.; Fournier, E.; Moules, V.; Cavalier, A.; Thomas, D.; Lina, B.; Marquet, R. An in vitro network of intermolecular interactions between viral RNA segments of an avian H5N2 influenza A virus: comparison with a human H3N2 virus. *Nucleic Acids Res.* **2013**, *41*, 1241–1254, doi:10.1093/nar/gks1181.

8. Fajardo Jr, T.; AlShaikhahmed, K.; Roy, P. Generation of infectious RNA complexes in Orbiviruses: RNA-RNA interactions of genomic segments. *Oncotarget* **2016**, *7*, 72559.

9. Gerber, M.; Isel, C.; Moules, V.; Marquet, R. Selective packaging of the influenza A genome and consequences for genetic reassortment. *Trends Microbiol.* **2014**, *22*, 446–455, doi:10.1016/j.tim.2014.04.001.

10. Fournier, E.; Moules, V.; Essere, B.; Paillart, J.-C.; Sirbat, J.-D.; Isel, C.; Cavalier, A.; Rolland, J.-P.; Thomas, D.; Lina, B.; Marquet, R. A supramolecular assembly formed by influenza A virus genomic RNA segments. *Nucleic Acids Res.* **2012**, *40*, 2197–2209, doi:10.1093/nar/gkr985.

11. Gilmer, D.; Bouzoubaa, S.; Hehn, A.; Guilley, H.; Richards, K.; Jonard, G. Efficient cell-to-cell movement of beet necrotic yellow vein virus requires 3′ proximal genes located on RNA 2. *Virology* **1992**, *189*, 40–47, doi:10.1016/0042-6822(92)90679-J.

12. Quillet, L.; Guilley, H.; Jonard, G.; Richards, K. In vitro synthesis of biologically active beet necrotic yellow vein virus RNA. *Virology* **1989**, *172*, 293–301.

13. Tamada, T.; Schmitt, C.; Saito, M.; Guilley, H.; Richards, K.; Jonard, G. High resolution analysis of the readthrough domain of beet necrotic yellow vein virus readthrough protein: a KTER motif is important for efficient transmission of the virus by Polymyxa betae. *J. Gen. Virol.* **1996**, *77*, 1359–1367.

14. Bleykasten-Grosshans, C.; Guilley, H.; Bouzoubaa, S.; Richards, K. E.; Jonard, G. Independent Expression of the First Two Triple Gene Block Proteins of Beet Necrotic Yellow Vein Virus Complements Virus Defective in the Corresponding Gene but Expression of the Third Protein Inhibits Viral Cell-to-Cell Movement. *Mol. Plant-Microbe Interact.* **1997**, *10*, 240–246, doi:10.1094/MPMI.1997.10.2.240.

15. Schmitt, C.; Balmori, E.; Jonard, G.; Richards, K. E.; Guilley, H. In vitro mutagenesis of biologically active transcripts of beet necrotic yellow vein virus RNA 2: evidence that a domain of the 75-kDa readthrough protein is important for efficient virus assembly. *Proc. Natl. Acad. Sci.* **1992**, *89*, 5715–5719.

16. Liu, H.; Naismith, J. H. An efficient one-step site-directed deletion, insertion, single and multiple-site plasmid mutagenesis protocol. *BMC Biotechnol.* **2008**, *8*, 91, doi:10.1186/1472-6750-8-91.

17. Schmidlin, L.; Link, D.; Mutterer, J. M.; Guilley, H.; Gilmer, D. Use of a Beet necrotic yellow vein virus RNA-5-derived replicon as a new tool for gene expression. *J. Gen. Virol.* **2005**, *86*, 463–467, doi:10.1099/vir.0.80720-0.

18. D'Alonzo, M. Reverse genetic studies of Benyvirus–Polymyxa betae molecular interaction:

Role of the RNA4-encoded protein in virus transmission, Université de Strasbourg: Strasbourg, 2011.

19. Veidt, I.; Bouzoubaa, S. E.; Leiser, R. M.; Ziegler-Graff, V.; Guilley, H.; Richards, K.; Jonard, G. Synthesis of full-length transcripts of beet western yellows virus RNA: messenger properties and biological activity in protoplasts. *Virology* **1992**, *186*, 192–200.

20. Guilley, H.; Bortolamiol, G.; Jonard, G.; Bouzoubaa, S.; Ziegler-Graff, V. Rapid screening of RNA silencing suppressors by using a recombinant virus derived from beet necrotic yellow vein virus. *J. Gen. Virol.* **2009**, *90*, 2536–2541, doi:10.1099/vir.0.011213-0.

21. Jupin, I.; Bouzoubaa, S.; Richards, K.; Jonard, G.; Guilley, H. Multiplication of beet necrotic yellow vein virus RNA 3 lacking a 3' poly(A) tail is accompanied by reappearance of the poly(A) tail and a novel short U-rich tract preceding it. *Virology* **1990**, *178*, 281–4.

22. Schmidlin, L.; Link, D.; Mutterer, J.; Guilley, H.; Gilmer, D. Use of a Beet necrotic yellow vein virus RNA-5-derived replicon as a new tool for gene expression. *J. Gen. Virol.* **2005**, *86*, 463–467, doi:10.1099/vir.0.80720-0.

23. Laufer, M.; Mohammad, H.; Maiss, E.; Richert-Pöggeler, K.; Dall'Ara, M.; Ratti, C.; Gilmer, D.; Liebe, S.; Varrelmann, M. Biological properties of Beet soil-borne mosaic virus and Beet necrotic yellow vein virus cDNA clones produced by isothermal in vitro recombination: Insights for reassortant appearance. *Virology* **2018**, *518*, 25–33, doi:10.1016/j.virol.2018.01.029.

24. Busch, A.; Richter, A. S.; Backofen, R. IntaRNA: efficient prediction of bacterial sRNA targets incorporating target site accessibility and seed regions. *Bioinformatics* **2008**, *24*, 2849–2856, doi:10.1093/bioinformatics/btn544.

25. Wright, P. R.; Georg, J.; Mann, M.; Sorescu, D. A.; Richter, A. S.; Lott, S.; Kleinkauf, R.; Hess, W. R.; Backofen, R. CopraRNA and IntaRNA: predicting small RNA targets, networks and interaction domains. *Nucleic Acids Res.* **2014**, *42*, W119–W123, doi:10.1093/nar/gku359.

26. Hehn, A.; Bouzoubaa, S.; Jonard, G.; Guilley, H.; Richards, K. E. Artificial defective interfering RNAs derived from RNA 2 of beet necrotic yellow vein virus. *Arch. Virol.* **1994**, *135*, 143–151.

27. Gilmer, D.; Ratti, C.; ICTV Report Consortium ICTV Virus Taxonomy Profile: Benyviridae. *J. Gen. Virol.* **2017**, *98*, 1571–1572, doi:10.1099/jgv.0.000864.